AD-A113 355 VON KARMAN INST FOR FLUID DYNAMICS RHODE-SAINT-GENESE--ETC F/G 13/1
THERMAL ENERGY STORAGE IN PHASE CHANGE MATERIAL.(U)
MAR 82 P WHITE, J BUCHLIN AFOSR-81-0119

UNCLASSIFIED EOARD-TR-82-8 NL

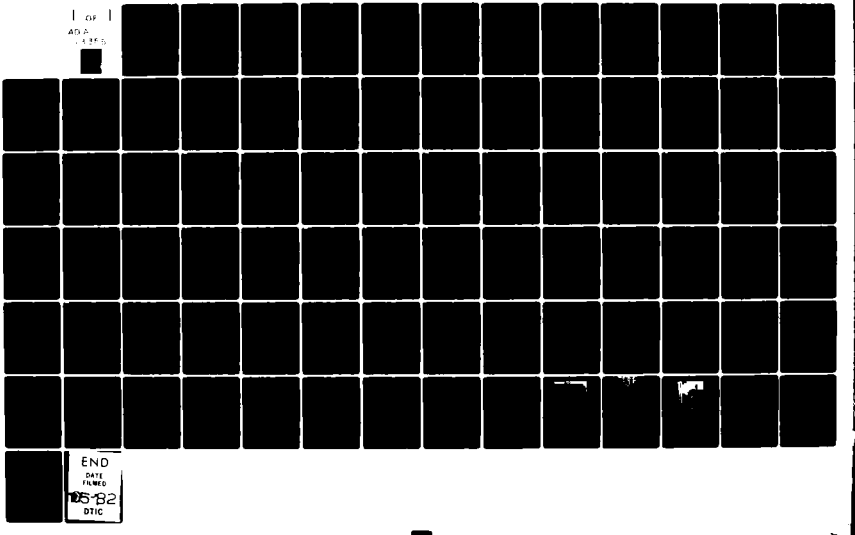

END
DATE FILMED
05-82
DTIC

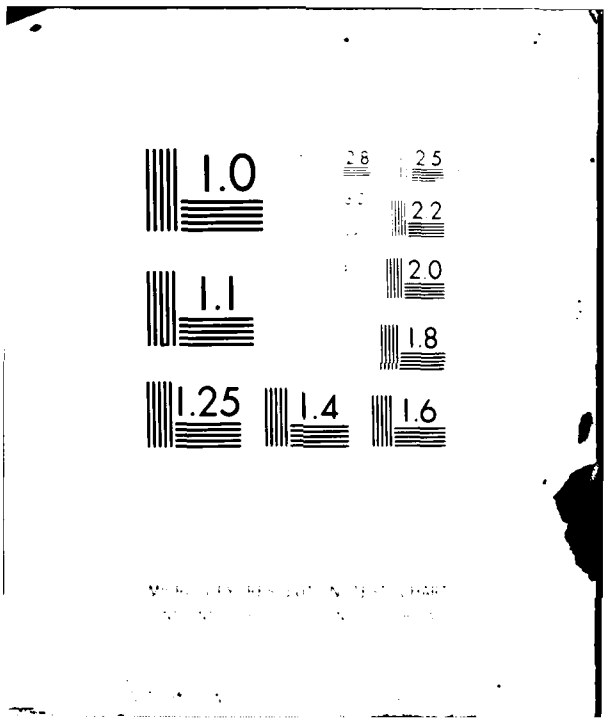
1.0
2.8
2.5
2.2
1.1
2.0
1.8
1.25
1.4
1.6

AD A113355

	READ INSTRUCTIONS BEFORE COMPLETING FORM
1. Report Number EOARD-TR-82-8	2. Govt Accession No. AD-A113
	3. Recipient's Catalog Number
4. Title (and Subtitle) Thermal energy storage in phase change material	5. Type of Report & Period Covered Final Scientific Report 1 Feb 81 - 31 Jan 82
	6. Performing Org. Report Number
7. Author(s) P. WHITE & J-M. BUCHLIN	8. Contract or Grant Number Grant AFOSR 81-0119
9. Performing Organization Name and Address von Karman Institute for Fluid Dynamics Chaussee de Waterloo, 72 B-1640 Rhode Saint Genèse, Belgium	10. Program Element, Project, Task Area & Work Unit Numbers P.E. 61102F Proj/Task 2301/D1 W.U. 120
11. Controlling Office Name and Address European Office of Aerospace Research and Development/LNT Box 14 FPO New York 09510	12. Report Date March 1982
	13. Number of Pages 81
14. Monitoring Agency Name and Address European Office of Aerospace Research and Development/LNT Box 14 FPO New York 09510	15.

16. & 17. Distribution Statement

Approved for public release; distribution unlimited.

18. Supplementary Notes

19. Key Words

Latent heat storage;Matrix heat exchanger;Solar energy application

20. Abstract

The present study deals with an experimental investigation of low temperature thermal storage based on macroencapsulation of Phase Change Material (PCM).
The storage performance capabilities of capsule bed, tube bank and tubular single-pass heat exchanger are compared. The tests are conducted on the VKI Solar Utility Network (SUN) which is a closed loop facility designed to study air heating systems.
An original data acquisition chain based on two conversing mircroprocessors is developed to carry out mass flow, pressure drop and temperature measurements. The experimental results are interpreted on the basis of comparison with numerical predictions and they allow to draw the following conclusions.
Each type of matrix has its own range of operation for practical application but from a heat transfer standpoint, the PCM capsule packing unit is strongly recommended. It is suggested to extend this investigation to the effect of Reynolds number to find optimum range for thermo-mechanical efficiency.

EOARD-TR-82-8

This report has been reviewed by the EOARD Information Office and is releasable to the National Technical Information Service (NTIS). At NTIS it will be releasable to the general public, including foreign nations.

This technical report has been reviewed and is approved for publication.

Winston K. Pendleton

WINSTON K. PENDLETON
Lt Colonel, USAF
Chief Scientist

Gordon L. Hermann

GORDON L. HERMANN
Lt Colonel, USAF
Deputy Commander

Accession For	
NTIS GRA&I	☒
DTIC TAB	☐
Unannounced	☐
Justification	
By	
Distribution/	
Availability Codes	
Dist	Avail and/or Special
A	

Acknowledgement

Thanks to the United States Air Force and the taxpayers of the United States for financing this year of study in Europe. I will strive to apply my training to the benefit of my country.

Table of Contents

I: Introduction

Imagine you have a greenhouse in Belgium. Here you have a natural solar collector that doesn't cost you anything, but you still spend thousands of dollars a year on heating fuel. What's more, and this is the really frustrating part, on the few beautiful days there are, you have to open windows to let out the hot air during the day, and then heat with oil during the night. You think this is crazy, which it is, and you decide to capture some of that heat you're letting out during the day, and use it at night.

So what do you do? There are several possibilities. You can put some rocks under your greenhouse, and then blow the hot air through during the day and blow cold air through the hot rocks during the night. Or you can fill old coke bottles with paraffin, or some other phase change material, and run the hot air through them. That way you have additional heat capacity in the same volume, due to the heat of fusion of the material. Also the storage will be at a more or less constant temperature, the temperature of fusion, while it is being loaded and unloaded with heat. Another thing you might do would be to put some plastic tubes under the greenhouse, put the phase change material in between the tubes, and then blow air through the tubes. The hot or cold air will then give or take up heat as it passes. Finally, you could put a phase change material in tubes, and blow the air through the tubes. There are other possibilities, and the different geometries and encapsulation methods are limited only by one's imagination.

What would be good to know is how to make a heat storage system that, over the lifetime of the greenhouse, will maximize the amount of money saved by acting, instead of continuing to throw out the heat captured during the day.

For the storage system you'd like to know how to get the most heat in and out in the shortest amount of time;

that will correspond to the minimum amount of electric energy needed for blowing the air. In fact for a storage system, one can name a criterion, a coefficient of performance, just like a heat pump has, which tells how much heat is saved for a given quantity of work, or pumping energy.

The goal of this report is to use the results of an experimental investigation three heat exchanger storage units, in order to decide which is best. the advantages and disadvantages of the encapsulation methods and geometries will be discussed; together with this, a theoretical model and its relation to the experimentally observed results will be presented.

II: Review of Literature

For his doctoral thesis at the von Karman Institute, Theunissen(8) has done a review of the state of the art in heat exchanger modeling and the chemical processes which are involved in heat-of-fusion storage systems. As the present work is complementary to the Theunissen thesis, a short review of some additional articles is presented here.

The world expert for phase change materials is Dr. Maria Telkes. She first suggested the idea of using Glauber's salts, paraffin, and eutectic salts for storing heat in the 1950's . In Solar Engineering (1) she notes in a review of the costs and benefits of various storage systems, that the people who work with phase change materials should be physical chemists, since many of the problems associated with these materials are chemical problems. Examples of this are the separation of the liquid from the solid in hydrated salts, and supercooling during the resolidification of the melted material. She also points out the need for attention to be paid to the method of encapsulation of the material.

In the Journal of Solar Engineering(2) a numerical simulation is presented which is similar to the one done in the present program. That is, the model consists of energy balances

both on the heat transfer fluid and on the solid phase, which receives the heat. In the trade publication, Solar Age (3,4) passive latent heat storage systems are discussed as are hybrid systems and the need for low-energy-consuming pumping.

In another article by Telkes(5), the need to consider systems which use electric resistance heating during off-peak utility periods, and the need to consider the encapsulation are discussed. Smith et al. (6) note that the limiting factor in heat exchanger performance of storage systems is the resistance to heat transfer in the solid phase. In modeling the microscopic phenomena of the phase change heat exchange, they stress the importance of natural convection in determining the shape of the melting front and in thus influencing the rate of heat transfer.

The heat transfer coefficient, h , models all the heat transfer from the fluid to the solid phase, or vice versa. This is always based on empirical correlations, and thus may be a dominant cause of error in any modeling of heat exchangers.

In this brief sample of the literature on the latent-heat storage subject, there are three problems which are continually mentioned. First, there is the need to model mathematically the performance of the heat storage unit. Second, there is the need to devise low-cost encapsulation methods. Finally there is the need to consider the pumping requirements for any heat exchanger, and to relate these to its thermal performance.

The goal of the present work is to address each of these three issues, based on the experimental program of the spring of 1981.

III: Theory

We have the first law of thermodynamics, which says that, for a given device,

Rate of heat going in + Rate of heat Production = Rate of heat going out

For the air going into a heat accumulator, one can consider the rate of heat going in to be:

$U_{int}A_3C_{p,air}T_{in}$ Convection of hot air in

The rate of heat going out equals

$\rho_{air}\ U_{int}A_3C_{p,air}T_{out}$ Convection of hot air out

$+\ h_1A_1(T_{air}(y)-T_{PCM}(y))$ Heat given to solid from air

$+\ h_2A_4(T_{air}(y)-T_{ambient}(y))$ Heat given to exterior through walls of storage unit

Where A_1 = Heat exchange surface area
A_2 = Accumulator cross-sectional area
A_3 = Accumulator interstitial area
A_4 = External surface area of acumulator

The rate of heat production, in the case of a machine degrading electrical or mechanical energy equals:

$$\rho_{air}\ V_{air}C_{p,air}dT_{air}/dt$$

If we put all these terms into an equation according to the first law of thermodynamics, we have:

$$\rho_{air}U_{int}A_3C_{p,air}T_{in} + \rho_{air}V_{air}C_{p,air}dT_{air}/dt=$$

$$\rho_{air}U_{int}A_3C_{p,air}T_{out}+ h_1A_1(T_{air}(y)-T_{PCM}(y))+h_2A_4(T_{air}(y)-T_{ambient}(y))$$

Now if we take this equation and divide all terms by the volume of the accumulator, we have (remembering that volume is equal to length times cross-sectional area):

$$\frac{\rho_{air} U_{int} A_3 C_{p,air} T_{in}}{A_2 L} - \frac{\rho_{air} U_{int} A_3 C_{p,air} T_{out}}{A_2 L} + \frac{\rho_{air} V_{air} C_{p,air} dT_{air}}{A_2 L \quad dt} =$$

$$\frac{h_1 A_1 (T_{air}(y) - T_{PCM}(y))}{A_2 L} + \frac{h_2 A_4 (T_{air}(y) - T_{ambient}(y))}{A_2 L}$$

From this equation, we let

$S_c = A_4 / A_2 L$

$\delta_s = A_3 / A_2$

$\varepsilon_v = V_{air} / A_2 L$

$a_s = A_1 / A_2 L$

h_1 = heat transfer coefficient between air and solid inside the heat accumulator

h_2 = heat transfer coefficient between air inside and outside of the heat accumulator

Rewriting the energy balance with the new notation, we have:

$$\frac{\rho_{air} U_{int} \varepsilon_s C_{p,air} (T_{in,air} - T_{out,air})}{L} + \varepsilon_v \rho_a C_{p,air} dT_{air}/dt =$$

$$h_1 a_s (T_{air}(y) - T_{PCM}(y)) + h_2 S_c (T_{air}(y) - T_{ambient}(y))$$

Letting the length of our accumulator become infinitesimal, we have:

$$-\rho_{air} U_{int} \varepsilon_s C_{p,air} dT_{air}/dy + \varepsilon_v \rho_{air} C_{p,air} dT_{air}/dt =$$

$$h_1 a_s (T_{air}(y) - T_{PCM}(y)) + h_2 S_c (T_{air}(y) - T_{ambient}(y))$$

or a complete statement for the energy balance on the air .

Similarly, we have an energy balance for the PCM, that is that all the heat it receives results from heat given up by the air:

$$\rho_{PCM} V_{PCM} C_{p,PCM} \, dT_{PCM}/dt = h_1 A_1 (T_{air}(y) - T_{PCM}(y))$$

Now we begin to make assumptions. First of all, let us say that the external losses and the accumulation of heat in the air are negligible when compared to the convection terms in the energy balance. The energy balance then becomes:

$$-\rho_{air} U_{int} \, s \, C_{p,air} \, dT_{air}/dy = h_1 a_s (T_{air}(y) - T_{PCM}(y))$$

together with the equation above it on this page.

The next assumption is that the T_{PCM} is constant with time and space, at the temperature of fusion of the PCM, while the fusion is occuring.

Thus we obtain:

$$\frac{dT_{air}(y)}{T_{air}(y) - T_{fusion}} = - \frac{h_1 a_s}{\rho_{air} U_{int} \varepsilon_s C_{p,air}} \, dy$$

Remembering the definitions of a_s and ε_s, we have:

$$\frac{dT_{air}(y)}{T_{air}(y) - T_{fusion}} = - \frac{h_1 A_1}{A_3 L \rho_{air} U_{int} C_{p,air}} \, dy$$

and we see that the multiplier of dy equals:

$$\frac{h_1 A_1}{\dot{m} \, C_{p,air} L}$$

where $\dot{m}$ is the air mass flow-rate.

Now integrating both sides of the energy balance, we have:

$$\int_{T_{in}}^{T_{air}(y)} \frac{dT_{air}(y)}{(T_{air}(y) - T_{fusion})} = -\frac{h_1 A_1}{\dot{m} C_{p,air} L} \int_0^y dy$$

which , evaluated, is:

$$\ln(T_{air}(y) - T_{fusion}) - \ln(T_{in} - T_{fusion}) = -\frac{h_1 A_1}{\dot{m} C_{p,air}} \frac{y}{L}$$

from which we arrive at:

$$\frac{T_{air}(y) - T_{fusion}}{T_{in} - T_{fusion}} = \exp(-St^* \, y/L)$$

where St^* is defined as $\dfrac{h_1 A_1}{\dot{m} C_{p,air}}$

Physically this dimensionless group the Stanton number gives us the ratio of the heat transfered in the heat accumulator to the heat convected through the accumulator.

From this derivation we can construct the following graph:

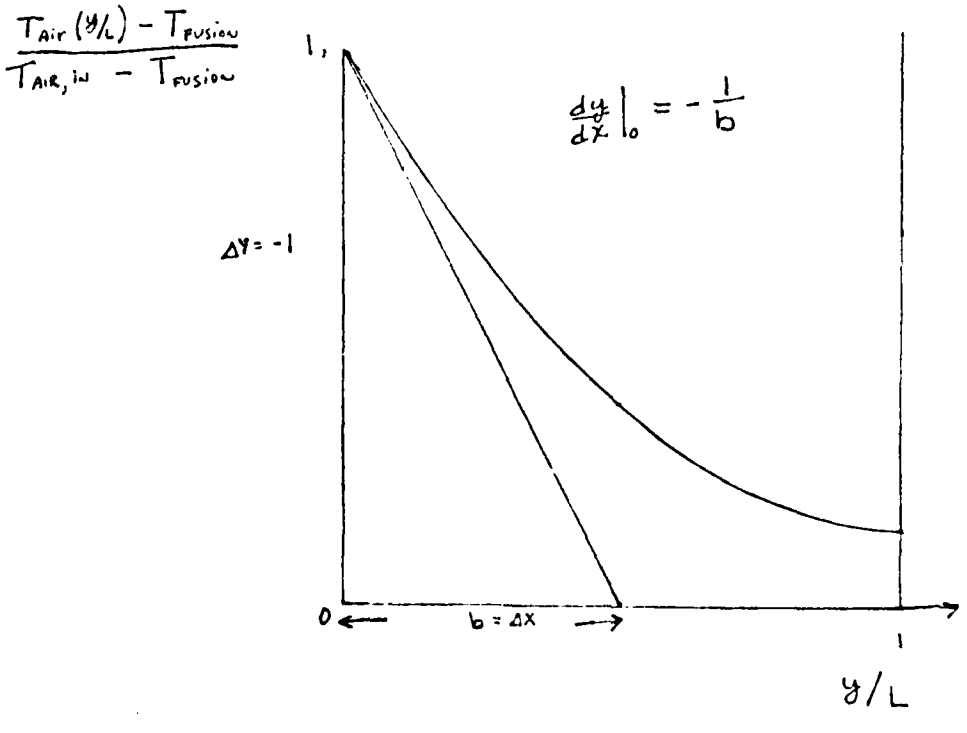

The slope of this graph at y=0 is simply:

$$\frac{d(\exp(-St^* y/L))}{d(y/L)} = -St^* = -\frac{1}{0}$$

Thus St^* can be deduced from the graph as $1/0$. Physically this means the number of times the reduced temperature decays by a factor of $1/e=0.37$ times its original value. Thus, for an accumulator with a St^* of 10, the value of the ordinate will be $(1/e)^{10}$ times its original value by the time the accumulator is completely traversed, while for a St^* of 2, the reduced temperature will decay by a factor of $(1/e)^2$ times its original value by the time the accumulator is traversed. The graph below illustrates the significance of this decay law.

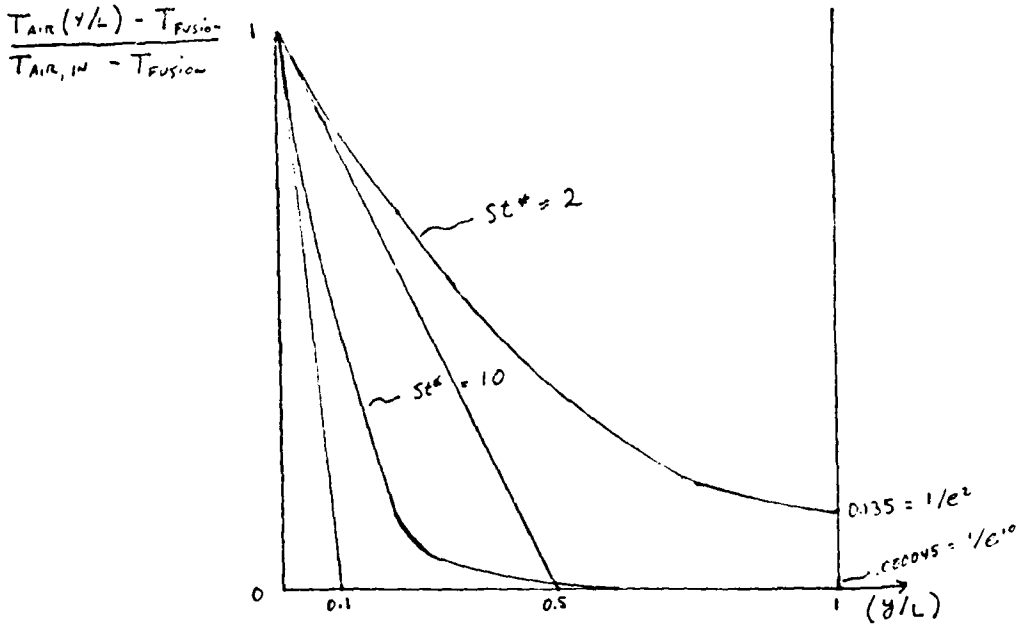

The higher the Stanton number is, the higher the heat transfer will be, and the higher the rate of reduction of air temperature will be as the accumulator is traversed. This has 2 important consequences. First, if one is interested in storing heat rapidly, one wants as large a temperature reduction as possible. Secondly, one must consider a closed loop solar heating system, including a solar collector and a heat storage unit. The higher the temperature going into

the collector is, the higher the temperature inside the collector will be. Therefore the heat losses of the collector will increase, and collector efficiency will decrease. It is thus of great interest to keep the air temperature going into the collector low. This is accomplished by having a storage unit which has a low outlet temperature, and a phase change storage with a high Stanton number achieves this result.

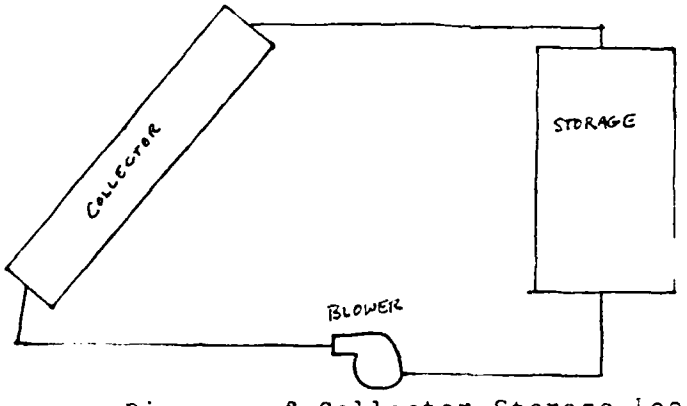

Diagram of Collector-Storage Loop

One may have noticed by now that not much has been said about h_1, the heat transfer coefficient. This is a problem which can be addressed only by means of empirical correlations. We know that originally, the Stanton number locally equals

$$h_1 / \rho_{air} C_{p,air} U_{int} =$$

$$h_1 D_p / k \times k / C_{p,air} \times / U_{int} D_p = Nu/PrRe$$

So it remains to find the Nusselt number by means of empirical correlations. For a packed bed, we have:

$$Nu = (1+1.5(1-\varepsilon_v))(2+.664 \quad 1+\left(\frac{.0557\, Re^{.3} Pr^{.67}}{1+2.44(Pr^{2/3}-1)Re^{-.1}}\right)^{?} \quad Pr^{1/3} Re^{1/2})$$

While for the tube cross flow,

$$Nu = .3\, Re^{.6}$$

and for the tube parallel flow, in the turbulent regime,

$$Nu = 0.22\, Pr^{.6} Re^{.8}$$

By rearranging the terms in the energy balance equations we arrive at the following:

$$dT_{air}/d(y/L) = h_1 A_1 / \rho_{air} C_{p,air} U_{int} A_2$$

$$dT_{PCM}/d\tau = \frac{h_1}{\rho_{air} C_{p,air} U_{int}} \frac{a_s L}{\varepsilon_s} \frac{\varepsilon_s}{1-\varepsilon_v} \frac{\rho_{air} C_{p,air}}{\rho_{PCM} C_{p,PCM}} (T_{air} - T_{PCM})$$

These 2 equations and their discretization form the subject of the work of Questois (9).

A brief summary of the numerical approach follows. We have a backward time, backward space discretization scheme:

$$dT/d\tau = T(i,j) - T(i-1,j)/\Delta\tau \qquad \text{for } i=1 \text{ to } n$$

$$dT/d(y/L) = T(i,j) - T(i,j-1)/\Delta(y/L) \quad \text{for } j=2 \text{ to } m$$

This is straightforward; the only part which requires a bit of thought is what to introduce as the heat capacity of the PCM when the fusion is occuring. The approach chosen is first to use a delta function, of finite width to express a "heat capacity of fusion". Normally this would be, with a precise fusion temperature;

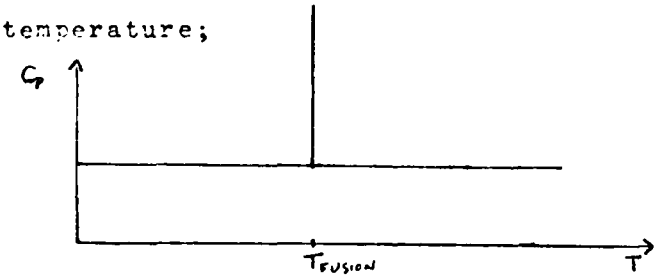

This is first modelled by having a finite-width spike centered on the fusion temperature;

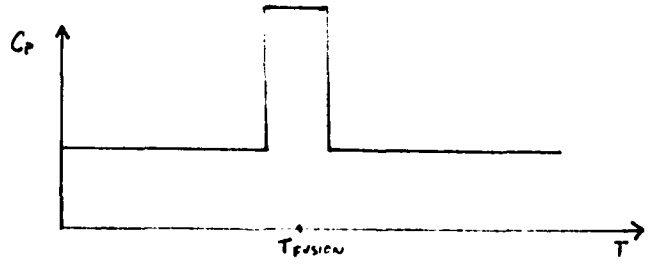

and then by a smoother distribution of heat capacity about the temperature of fusion, as shown on the top of the next page.

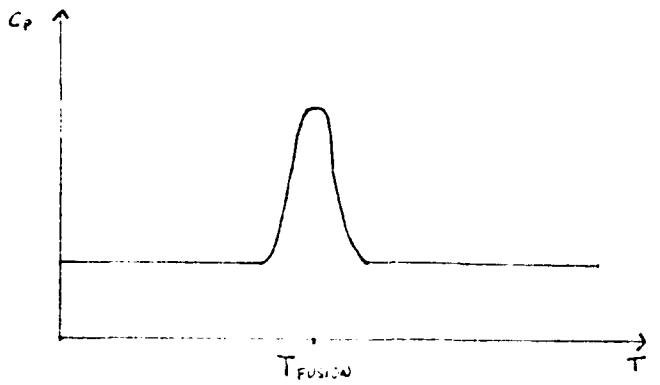

The simulation therefore increases the heat capacity of the PCM as the fusion temperature is approached, and the phenomenon of the temperature remaining constant during fusion is simulated.

IV: Comparison of Different Storage Systems

To compare the different methods of heat storage, it is important to consider: a water storage, a rock bed storage, a paraffin phase change storage, and a $CaCl_2 6H_2O$ system; all these systems are compared for air as the solar-heated fluid.

	Water	Rock bed	Paraffin	$CaCl_2 6H_2O$
First Costs	1. Pipes 2. Storage tank 3. Heat exchanger 4. Blower 5. Water pump 6. Ducting for air	1. Rocks 2. Air blower 3. Air ducts 4. Walls to hold rocks	1. Paraffin 2. Encapsulation 3. Ducting 4. Blower	1. $CaCl_2 6H_2O$ 2. Encapsulation 3. Ducting 4. Blower
Volume required	1. Water Volume 2. Heat Exchanger volume	1. Volume of rock bed	volume of PCM + Encapsulation	
Operation costs	In all cases, a function of the heat transfer coefficient, the pressure loss across the storage, and the volume flow rate of the air.			

From this qualitative evaluation we go to a quantitative comparison of volume requirements for different storage media given a set storage capacity of 500 megajoules, given a temperature change from 15°C to 35°C.

For water, C_p = 1 Kcal/KG-°C = 4.19 Kjoule/KG-°C
Thus the volume of water required should be:

$5 \times 10^8/(4.19 \times 10^3 \times 2 \times 10^1) = 5.97 \times 10^4$ KG = 59.7 M^3

For rocks, C_p = .9 Kjoule/KG-°C, = 2500 KG/M^3 and we will assume a void fraction of 0.4. One cubic meter of storage will then contain 0.6 M^3 of rock, or 1500 KG.
We then have:

$5 \times 10^8/(900 \times 20) = 2.8 \times 10^4$ KG

$2.8 \times 10^4/(1.5 \times 10^3) = 18.5$ M^3 of rock bed

For Paraffin, C_p = 2000 JOULE/KG-°C and we see that

$5 \times 10^8/(2000 \times 20) = 1.25 \times 10^4$ KG are required. Therefore the mass of paraffin required will be lower than that of water or rocks, but one must remember that encapsulation is required, which will have void space as well as volume itself.

For $CaCl_2 6H_2O$, the heat, sensible, of solid and liquid phases is 2000 Joule/KG-°C, the heat of fusion is 170000 joule/KG the temperature of fusion is 29°C , the solid density is 1.5 KG/Liter, and the liquid density is 1.4 KG/Liter. We have:

$5 \times 10^8/ (20°C \times 2000 + 170000) = 2.4 \times 10^3$ KG
$2.4 \times 10^3 / 1500 = 1.6$ M^3

As with paraffin, there is encapsulation and void space required but there is still a significant volume reduction over rocks or water.

Together with less volume, there is a smaller bed through which to pump the hot air from the solar collector, and this will result in lower blowing or pumping costs, since there is less pressure loss with the smaller accumulator.

V. Experimental System

As mentioned before, three heat accumulators, or three methods of encapsulation, were tested. The concepts are: tube cross flow, tube parallel flow, and a packed bed. These are diagrammed below.

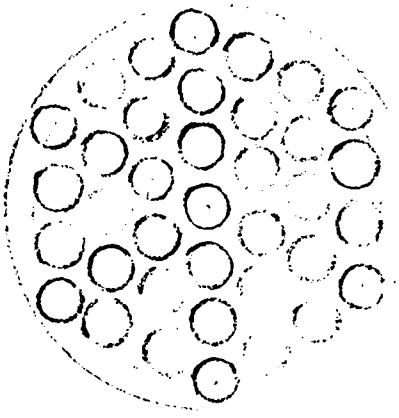

TOP VIEW

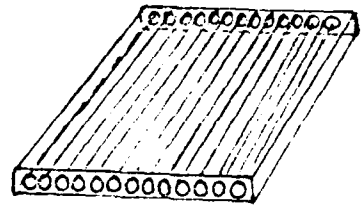

(SEE APPENDIX FOR PHOTOGRAPH)

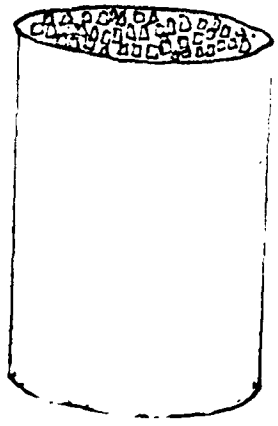

Tube Parallel Flow Tube Cross Flow Packed Bed

In addition to thermal characteristics, such as the stanton number, there are several other means by which the accumulators may be compared, as tabulated below:

	Tube Cross Flow	Packed Bed	Tube Parallel Flow
Heat exchange Surface area	18.1 M^2	14.3 M^2	5.9 M^2
Void fraction	0.58	0.4	0.35
$\frac{\text{Vol. PCM}}{\text{Vol. total}}$	0.26	0.5	0.6
$\frac{\text{Vol. encapsulation}}{\text{Vol. total}}$	0.17	0.11	0.03
Heat Capacity/M^3 (15°C to 35°C)	77 megajoule	154 megajoule	188 megajoule
Total Volume	333 Liters	175 Liters	210 Liters
Pressure drop	8 mm H_2O	1.5 mm H_2O	3 mm H_2O

From a first examination of these data for the three accumulators, one can see some obvious tradeoffs. For example the tube parallel flow, while having the highest heat capacity per unit volume, also has the least area for heat exchange. The volume of encapsulation is also low, which results in a low first cost, but this advantage is offset by the low heat exchange surface area, which results in higher operating costs due t. greater volumes of air being pumped for the given amount of heat transfer to take place.

Looking at the data for the three accumulators shows that the packed bed gives the best compromise between heat exchange surface area and volume of encapsulation material. Another factor, which must not be overlooked,is flow distribution. In the course of the experimental program , it was found that in the case of the tube cross flow and the tube parallel flow, all the air flow tended to go down one side of the storage unit due to an elbow and a broad angled diffuser just upstream of the storage unit. The packed bed, on the other hand had the advantage of evenly distributing the flow of air about itself.

VI: Measurement System

The measurement system consisted of two measurement chains. The more elaborate is the thermocouple temperature measurement chain. This starts with copper-constantan thermocouples, and is shown in the diagram below:

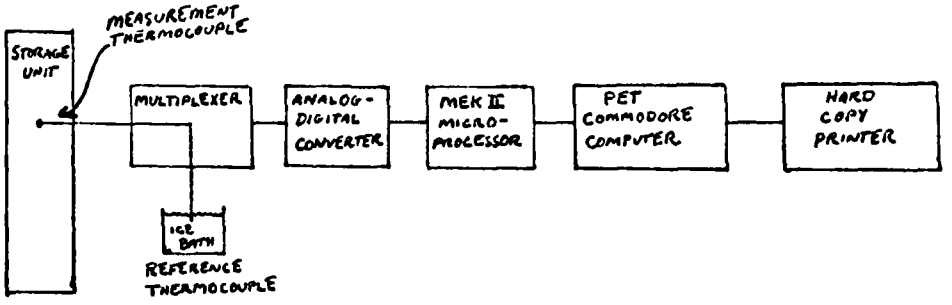

The Mek II microprocessor commands the system, and the multiplexer scans 48 channels of thermocouple measurements, which are then digitized by the analog-to-digital convertor.

The hexadecimal number , an average of 32 measurements taken sequentially in time, is transferred from the memory of the MekII microprocessor to the Pet Commodore computer. There a software program including the calibration curve for the thermocouples makes the final conversion from the millivolt reading of the Multiplexer to the temperature data which are required.

The second measurement chain is the flow measurement chain. This is simply an orifice plate flow-meter, with a water manometer used to measure the pressure drop across it. For this measurement, a previously obtained calibration curve was used to determine the air mass flow rate.

VII: Experimental Program and Results

The experimental program was designed to test 2 ideas. First of all, the validity of the numerical model needed to be established. Second, the assumptions going into the model needed to be tested. The most dangerous assumption is that the flow of heat into the accumulator is evenly distributed at each point in the cross-section perpendicular to the flow. It is a one-dimensional model. In each of the three accumulators tested, the accumulators were instrumented with thermocouples in the geometric center of the cross-section perpendicular to the flow, and at severalpoints along the length of the accumulators. This enabled a visualization of the evolution of the air and phase change material temperatures along the length of the bed. At three levels in the accumulators thermocouples were put at different points around the cross-section in order to test the uniformity of air and phase change material temperatures.

A resumé of the experiments done follows. The primary goal was to do one complet charge and one complete discharge of each of the three accumulators. This was achieved. A large amount of time went into instrumenting the accumulators, and then finding the "bugs" in the system and correcting them.

There were 14 tests altogether, which are tabulated on the next page, together with a list of other preparatory activities.

Test Number	Date	Title	Comments, Purpose
------	2/1/81-3/14/81		Preparation, calibration of thermocouples
1	3/14/81	Charge of Tube Cross Flow unit	First charge, complete system worked
2	3/19/81	"	Some leakage of liquid PCM occured; flow distribution problems
3	3/19/81	Discharge of TCF unit	Test terminated before complete resolidification had occured
4	3/19/81	Charge of TCF unit	Foam was added for better flow distribution in diffuser
5	3/24/81	Discharge of TCF unit	8-hour discharge, still not sufficient to totally resolidify
6	4/9/81	Charge of TCF unit	More liquid PCM leakage noticed; also leakage in ducting and dampers was discovered
7	4/10/81	Discharge of TCF unit	Complete discharge achieved; re-solidification in more than 15 hours
8	4/14/81	Charge of TCF unit	
------	4/14/81-5/12/81		a. Preparation of thermocouples for packed bed and tube parallel flow b. Resolution of air leakage problem c. Mixture of PCM for packed bed and tube parallel flow at Solvay chemical company d: Filling packed bed and tube parallel flow units with PCM
9	5/12/81	Charge of TCF unit	Sure of leak-proof air system; air flow measured downstream of accumulator, as well as upstream
10	5/13/81	Discharge of TCF unit	Problems with data acquisition during test
11	5/14/81	Charge of Packed bed	Some leakage of PCM
12	5/15/81	Discharge of Packed bed	No problems, complete discharge
13	5/19/81	Charge of Tube parallel flow unit	No PCM leakage, very long time required for PCM to melt
14	7/1/81	Tube parallel flow discharge	2 days required for experiment

Graphs of the experimental results follow: they are grouped in the three categories: tube cross flow, packed bed, and tube parallel flow.

A. Tube Cross Flow:

The tests on the tube cross flow unit served to give experience with the experimental apparatus, but due to the fact that there was marked leakage in the phase change material, they are not conclusive. Additional phase change material was not available, and developing a system for sealing the tubes at either end would have constituted a complete project in itself. The problem lay in degradation of the glue at either end of the tubes, where plastic caps were fixed.

In addition, since the air flow rate going into the accumulator was less than what was measured at the orifice plate upstream, due to air leaks in the damper system, the convective heat input was not known with sufficient precision to warrant a comparison with the numerical simulation. A comparison of the numerical results and the experimental results for Test number 1 showed that the phase change in the experiments proceeded much more slowly than the computer simulation predicted. This was because the mass flow rate which was used as input for the simulation was that which was measured at the orifice plate upstream of the accumulator, and did not take into account the air leakage which occured between the orifice plate and the accumulator.

These limitations not withstanding, some meaningful information can be drawn from the experiments on the tube cross flow unit. Graphs 1 and 2 show the evolutions of the air and phase change material temperatures. These have the characteristic plateau of fusion. Also as expected, the air temperature at each point is higher than the PCM temperature, until steady state, when the whole accumulator is at the influent air temperature, is reached. The time for reaching steady state, at 60°C, was 7 hours.

The other information that can be drawn regards the evenness of the flow distribution, and the thermal performance as repeated charges and discharges were performed. The second charge, as shown in graphs 3 and 4, shows already that the pretty plateaus

of the first charge are less flat than in the first test. Also the time for charging is about 4 hours, as versus 7 hours in Test 1. This should be due both to the fact that some PCM had already leaked, and the fact that the PCM may not have been completely solidified when the test was started. The second condition would mean that some of the latent heat of fusion remained in the bed at the test's start.

Graphs 5,6, and 7 address the question of air temperature distribution about the cross sections of the accumulator. These show that in each cross section, the temperature in the center of the tube on the side (curves 8,11, and 13) were higher than the temperatures at the 2 ends of the central tube. This can be attributed to a higher heat capacity of the greater amount of plastic at the ends of the tubes. This higher heat capacity will result in a lower rate of temperature increase for a given heat input. In addition the air flow rate should be somewhat higher at points 8,11, and 13 than at points 7,9,10,12,14, and 15, due to less resistance to the flow. The slightly higher flow rate would again result in a higher rate of temperature increase for the points exposed to the faster flow.

Graphs 8,9, and 10 from test number 4 show that the same pattern of temperature distributions about the cross-sections remains, even with the additon of foam to even out the flow going into the accumulator. Thus one can conclude that the addition of the foam resulted in additional pressure loss which was not justified by an improvement in thermal performance. Tests number 6 and 7 were made to see the temperature evolution during a complete discharge. Graphs 11, 12, and 13 show the inlet and outlet temperatures, their difference in time, and the integral of the temperature difference, respectively. The corresponding curves for the discharge are shown in graphs 14, 15, and 16. Graph 15 shows the phenomenon of supercooling appearing in the dip in the temperature difference and subsequent rise. Both graphs of the integrals of the temperature differences should be multiplied by the same mass flow rate to arrive at the amount of heat accumulated or discharged. Since the integral is not multiplied by $mC_{p,air}$ in either case, the numerical values

can be compared; we see that for the charge it is 5.11×10^5, whereas for the discharge it is 3.30×10^5. Thus one third of the heat must be lost through leakage. Graph 17 shows well how the PCM temperature follows the air temperature during the course of a charge of the storage unit, and Graph 18 shows the same same 3 curves for a discharge. Graphs 19, 20, and 21 show that the PCM temperatures are more or less constant about the cross-sections during the discharge.

The local phenomenon of supercooling can also be seen from these graphs. This is a decrease of the temperature below the fusion temperature, followed by a sharp rise to the fusion temperature as resolidification occurs, and then a decrease in temperature to that of the influent air. The supercooling poses problems for the latent-heat-of-fusion systems because: 1) All the heat is released in a short time when the chrystallization occurs, thus causing difficulties in controlling the solidification and 2) During the supercooling, air is being pumped at an expense in electric energy, for no benefit in thermal energy transfer.

Graph 1

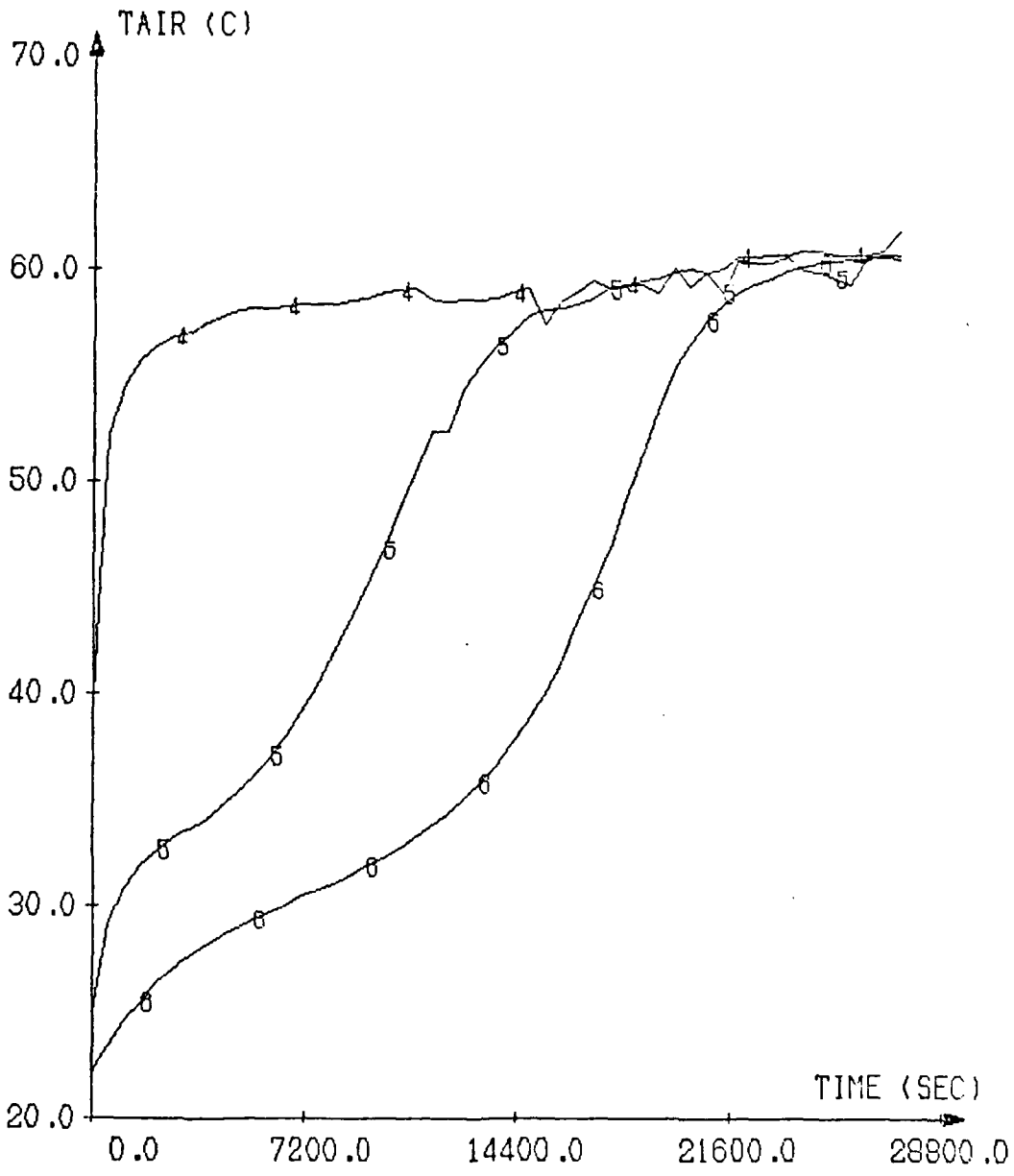

TEMPERATURE AS A FUNCTION OF TIME

AIR TEMPERATURE .TOP=4 .MIDDLE=5 .BOTTOM=6

DATE=3-14-81

MASS FLOW=0.05 KG/SEC

TUBE CROSS FLOW .CHARGING MODE .CACL2-6H20

THEUNISSEN P-H WHITE P ELMER J QUETSTROEY R

Graph 2

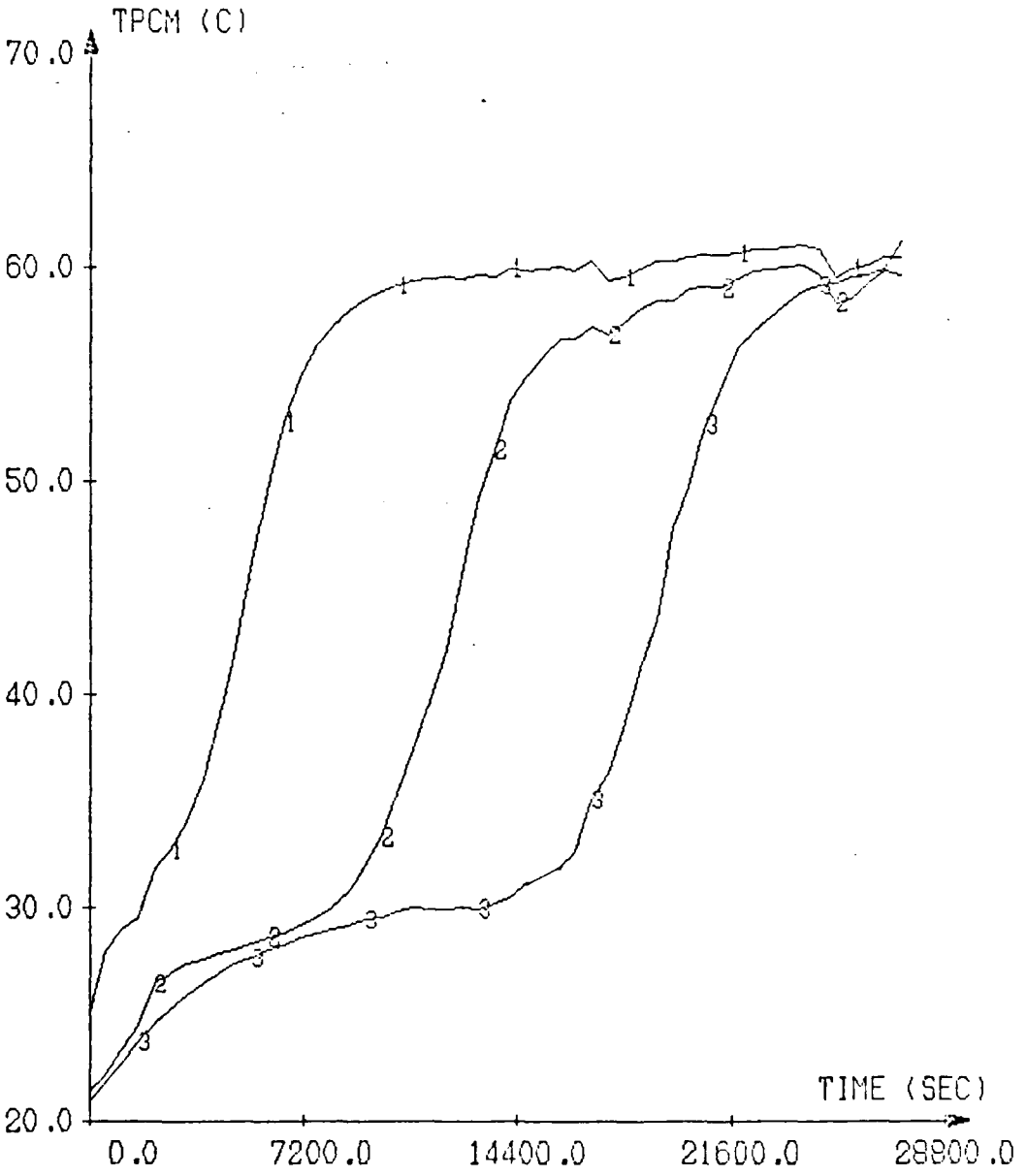

TEMPERATURE AS A FUNCTION OF TIME

PCM TEMPERATURE .TOP=1 .MIDDLE=2 .BOTTOM=3

DATE=3-14-81

MASS FLOW=0.05 KG/SEC

TUBE CROSS FLOW .CHARGING MODE .CACL2-6H2O

THEUNISSEN P-H WHITE P ELMER J QUETSTROEY R

Graph 3

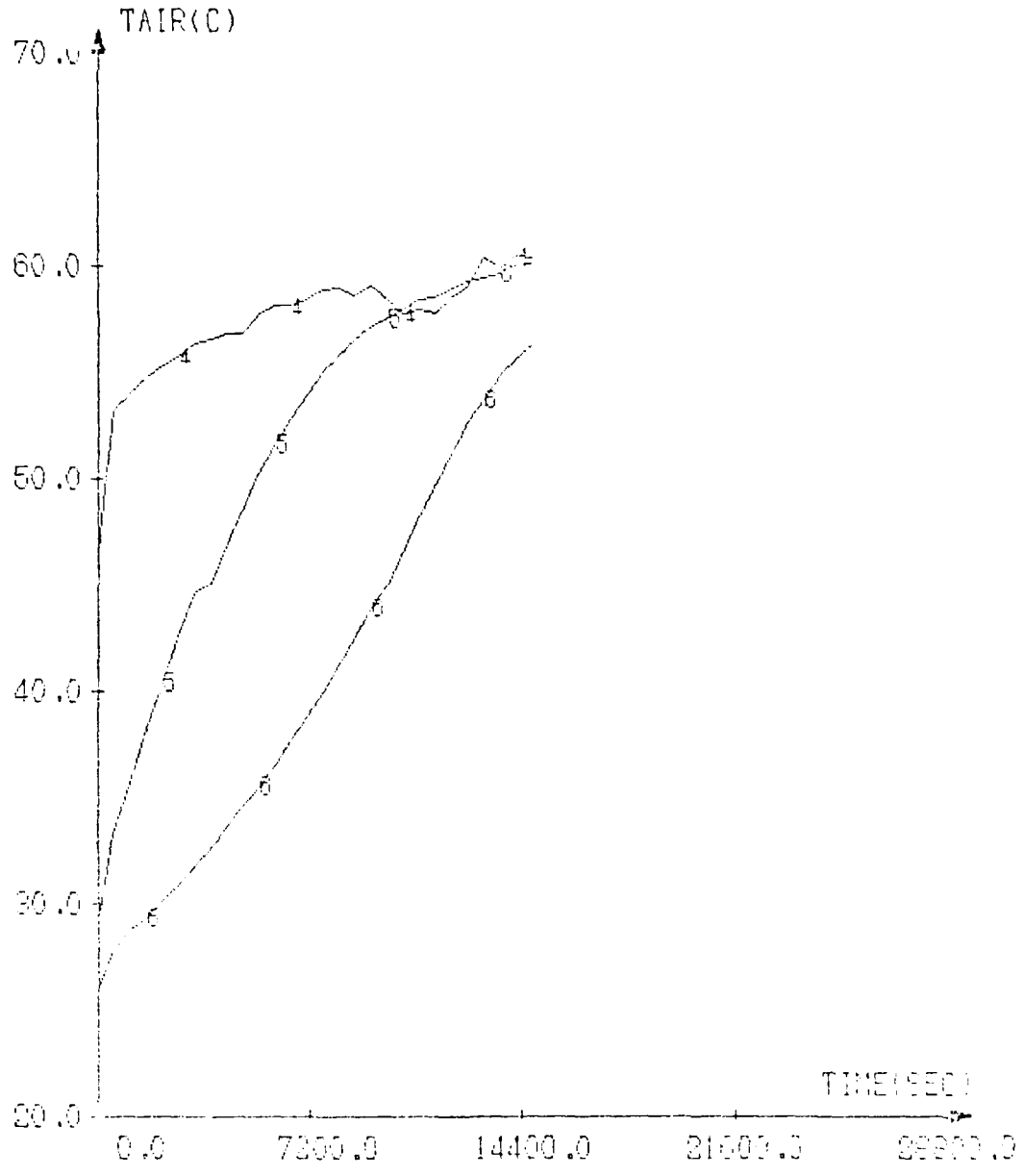

TEMPERATURE AS A FUNCTION OF TIME

AIR TEMPERATURE .TOP=4 .MIDDLE=5 .BOTTOM=6

DATE=3-19-81

MASS FLOW=.05 KG/SEC

TUBE CROSS FLOW. CHARGING MODE .CACLO-6H20

THERMISSEN P-H WHITE P ELMER J OMETSTROEY R

81 RECORD 9999 SEC 81/05/30 18.22.13 A10A350

Graph 4

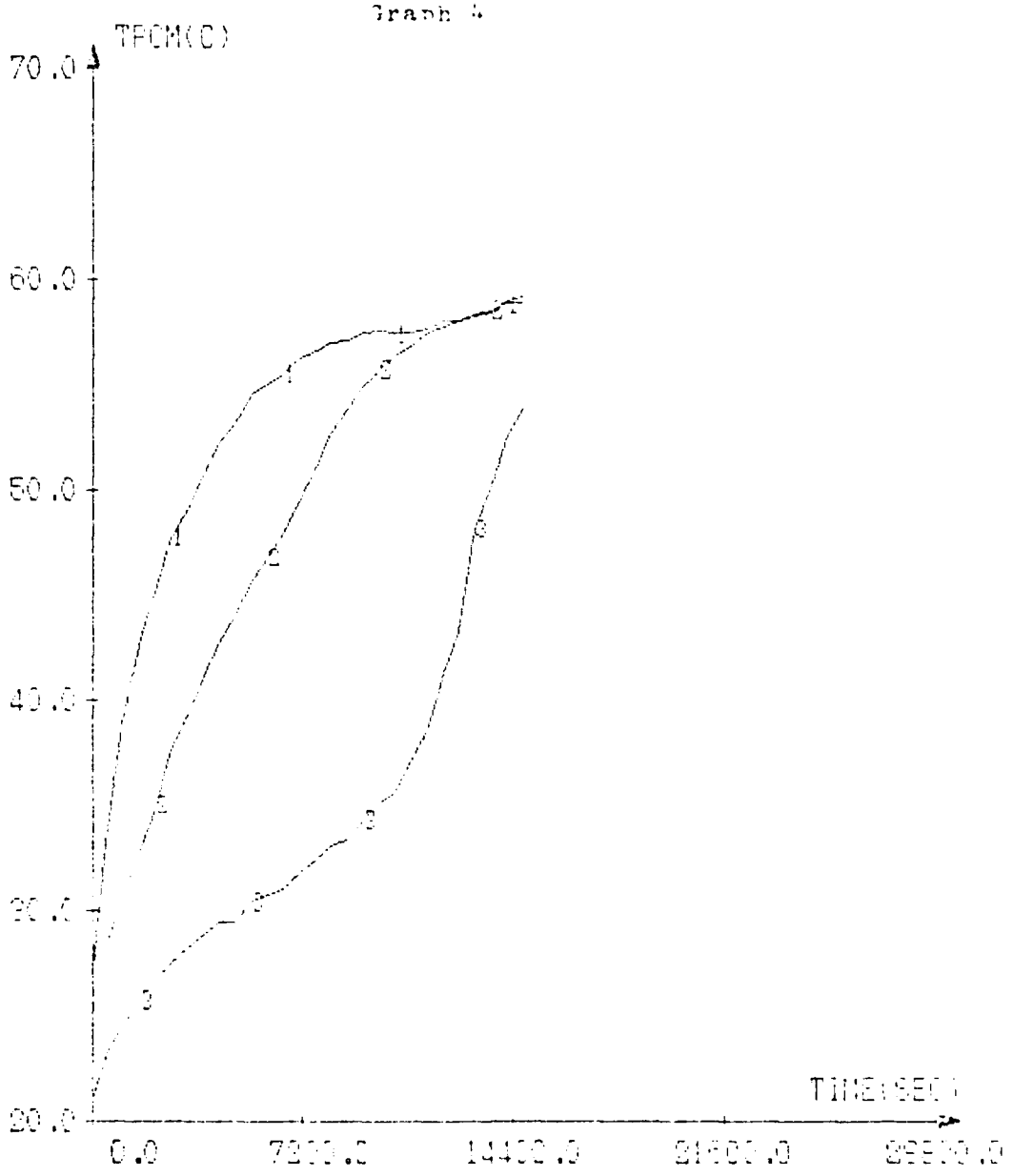

TEMPERATURE VS A FUNCTION OF TIME

PCM TEMPERATURE.TCF=16.NICOLE=2.COTTON=3

DATE=3-19-81

MASS FLOW=.05 KG/SEC

TUBE CROSS FLOW. CHARGING MOLE.CACL2-6H2O

Graph 5

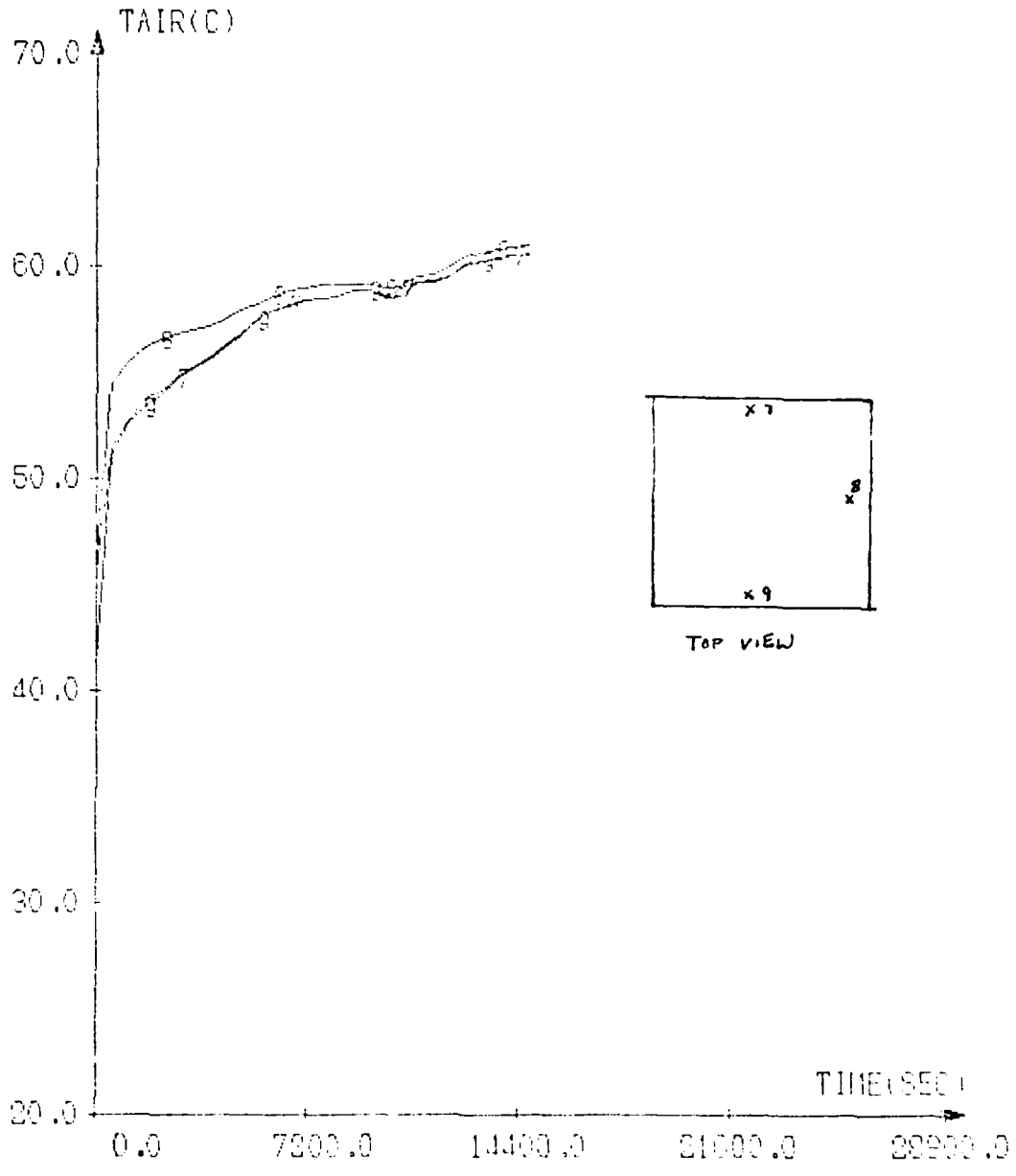

TEMPERATURE AS A FUNCTION OF TIME

AIR TEMPERATURE.DIFFERENT POINTS.TOP LEVEL

DATE=3-19-81

MASS FLOW=.05 KG/SEC

TUBE CROSS FLOW. CHARGING MODE.CACLB-6H30

THEUNISSEN P-H WHITE P ELMER J QUETSTROEY R

Graph 6

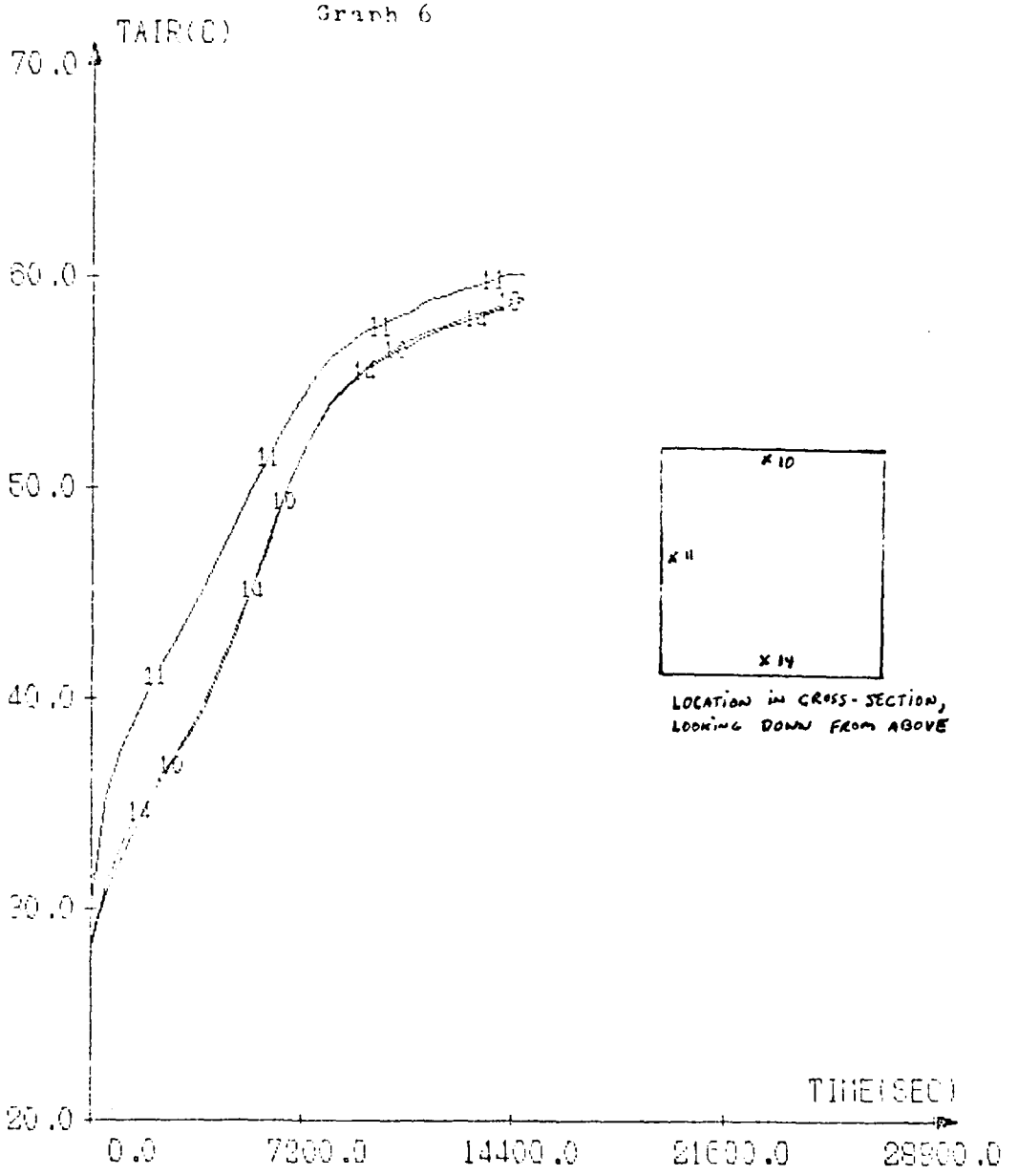

TEMPERATURE AS A FUNCTION OF TIME

AIR TEMPERATURE,DIFFERENT POINTS,MIDDLE LEVEL

DATE=3-19-81

MASS FLOW=.05 KG/SEC

TUBE CROSS FLOW, CHARGING MODE,CACL2-6H2O

THEUNISSEN P-H WHITE P ELMER J QUETSTADEY R

Graph 7

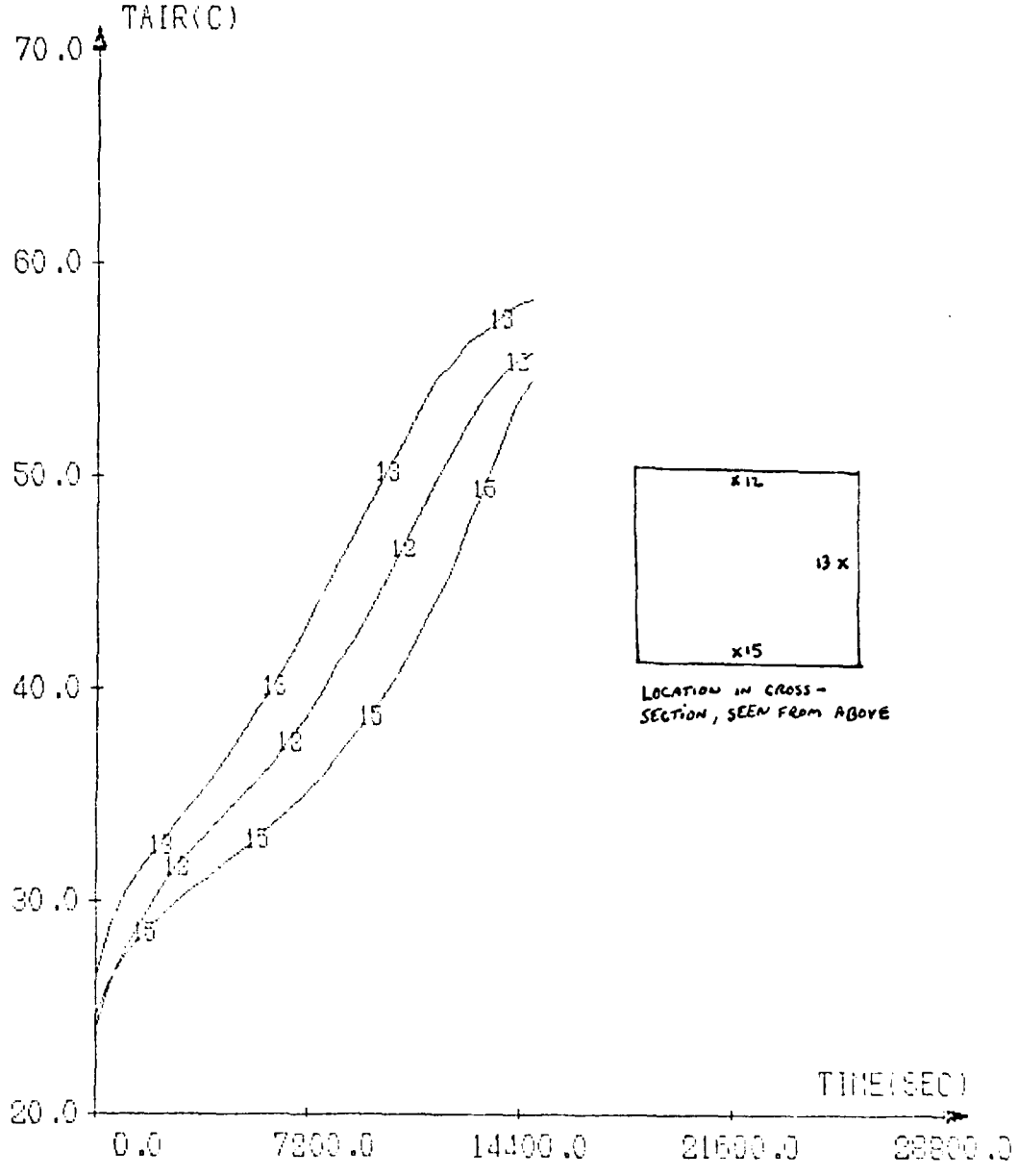

TEMPERATURE AS A FUNCTION OF TIME

AIR TEMPERATURE,DIFFERENT POINTS,BOTTOM LEVEL

DATE=3-19-81

MASS FLOW=.05 KG/SEC

TUBE CROSS FLOW, CHARGING MODE,CACLO-6H2O

THEUNISSEN P-H WHITE P ELMER J OUETSTROEY R

THEUNISSEN P-H WHITE P ELMER J QUETSTROEY R

Graph 8

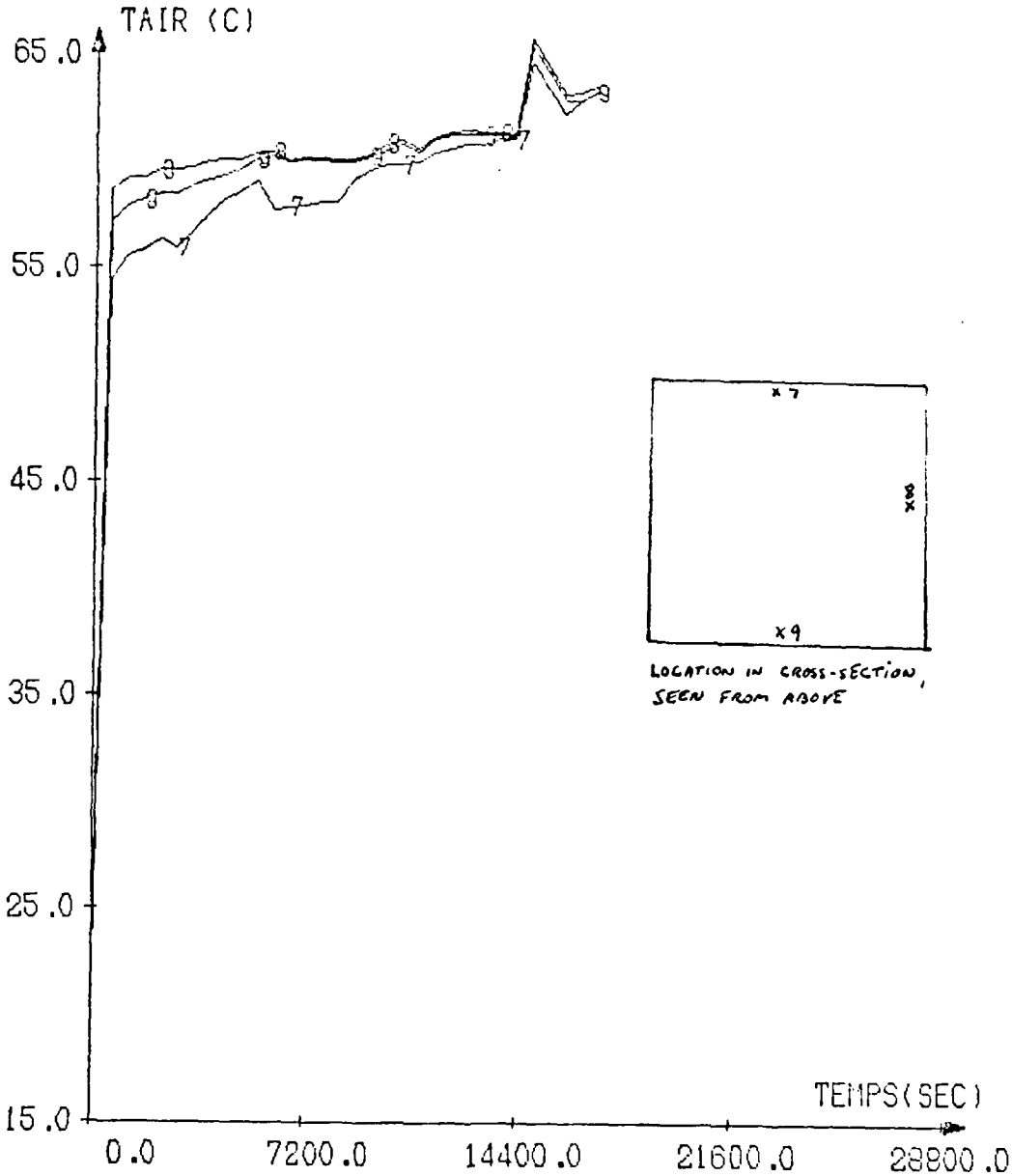

LOCATION IN CROSS-SECTION, SEEN FROM ABOVE

TEMPERATURE AS A FUNCTION OF TIME

AIR TEMPERATURE, DIFFERENT POINTS, INLET LEVEL

DATE 24-03-81

MASS FLOW .05 KG/SEC

TUBES CROSS FLOW, CHARGING MODE. CACL2 6H20

11.51.09 81/08/10 9999 SEC

THEUNISSEN P-H WHITE P ELMER J QUETSTROEY R

Graph 9

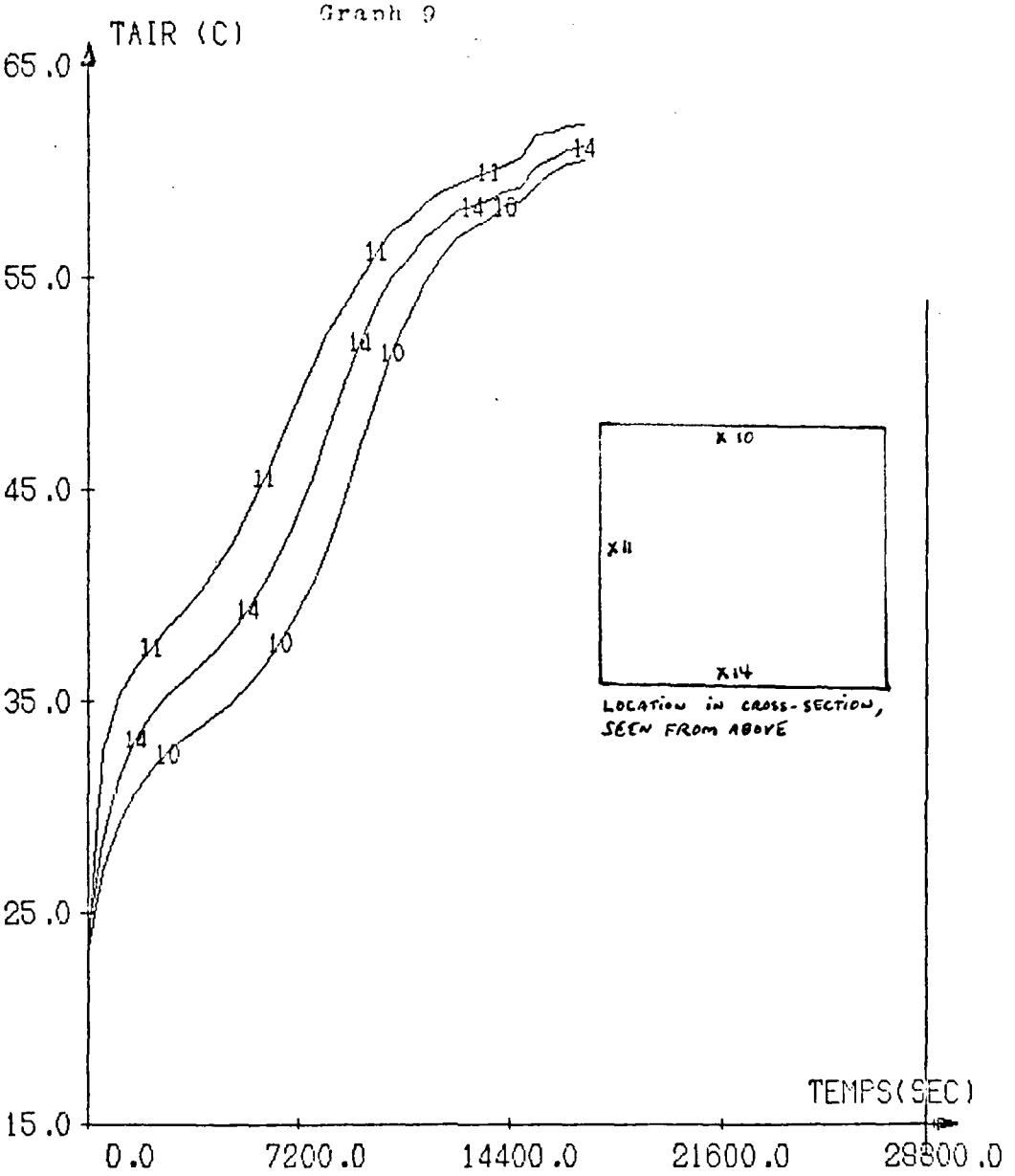

TEMPERATURE AS A FUNCTION OF TIME

AIR TEMPERATURE. DIFFERENT POINTS. MIDDLE LEVEL

DATE 24-03-81

MASS FLOW .05 KG/SEC

TUBES CROSS FLOW. CHARGING MODE. CACL2 6H20

THEUNISSEN P-H WHITE P ELMER J QUETSTROEY R

Graph 10

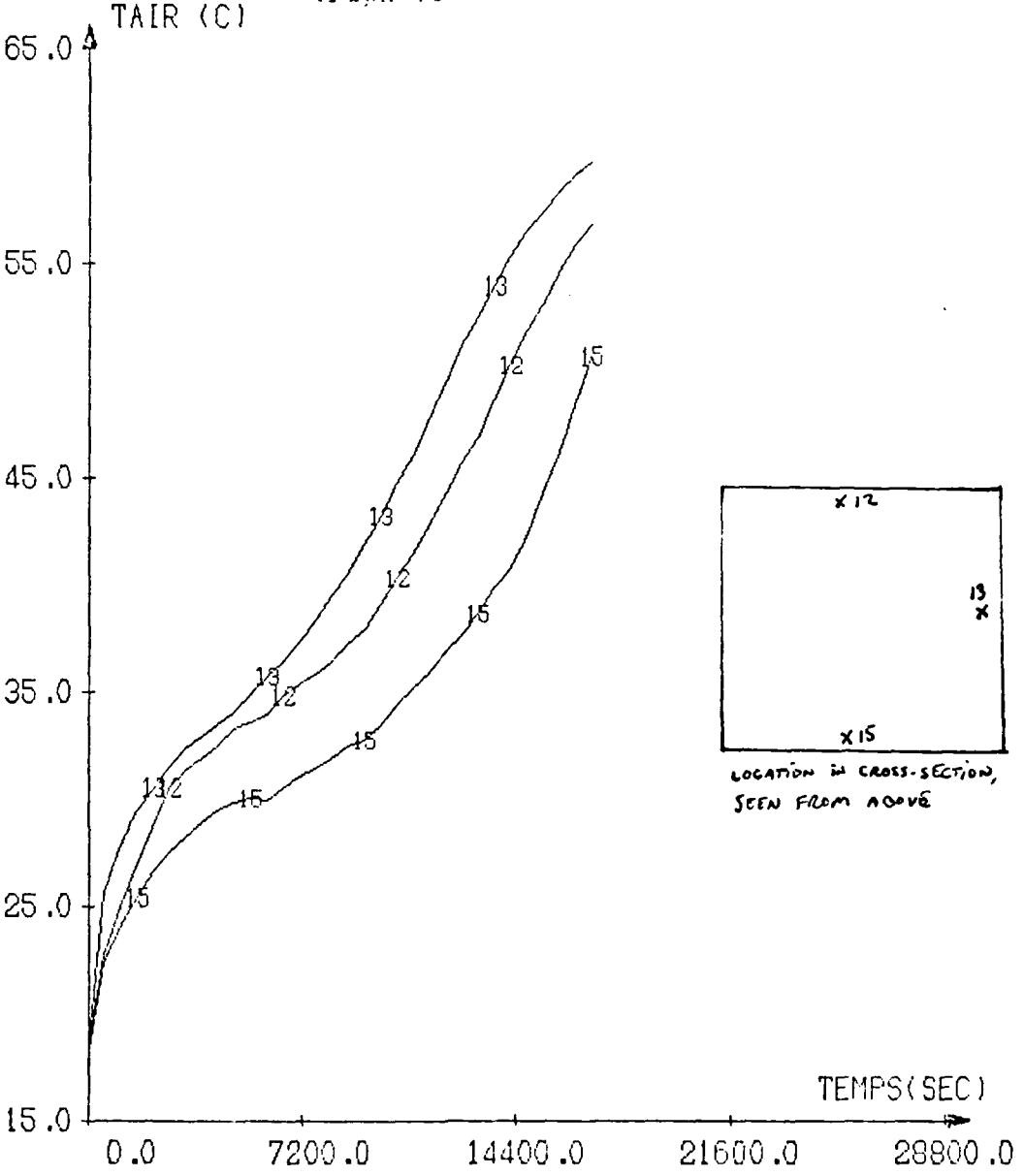

TEMPERATURE AS A FUNCTION OF TIME

AIR TEMPERATURE. DIFFERENT POINTS. OUTLET LEVEL

DATE 24-03-81

MASS FLOW .05 KG/SEC

TUBES CROSS FLOW. CHARGING MODE. CACL2 6H20

THEUNISSEN P-H WHITE P ELMER J OUETSTROEY R

Graph 11

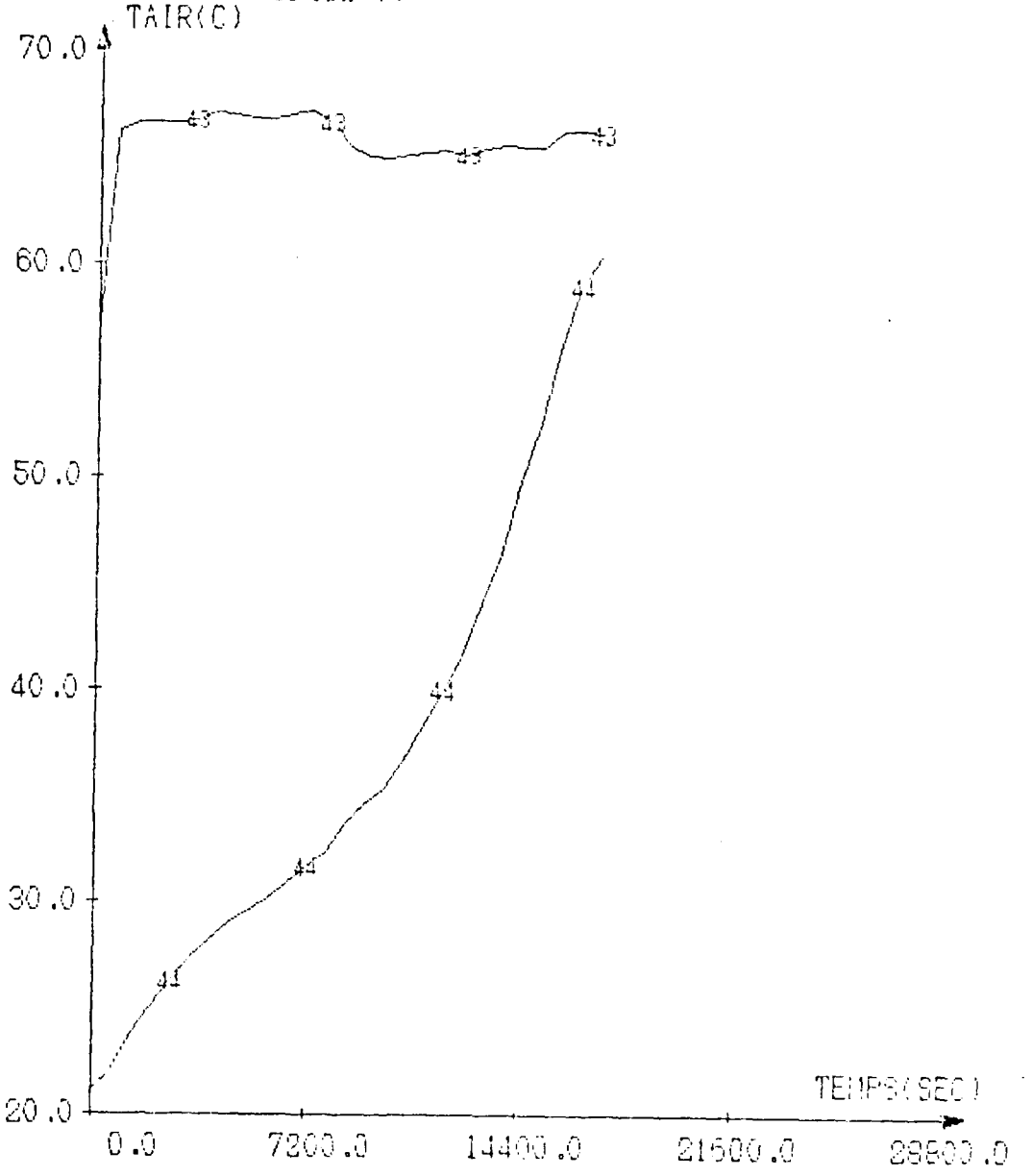

TEMPERATURE EN FONCTION DU TEMPS

AIR ENTREE(43) SORTIE(44)

DATE 9-04-81

DEBIT AIR .05 KG/SEC

TUBES CROSS FLOW CACL2-6H2O

THEUNISSEN P-H WHITE P ELMER J QUETSTROEY R

Graph 12

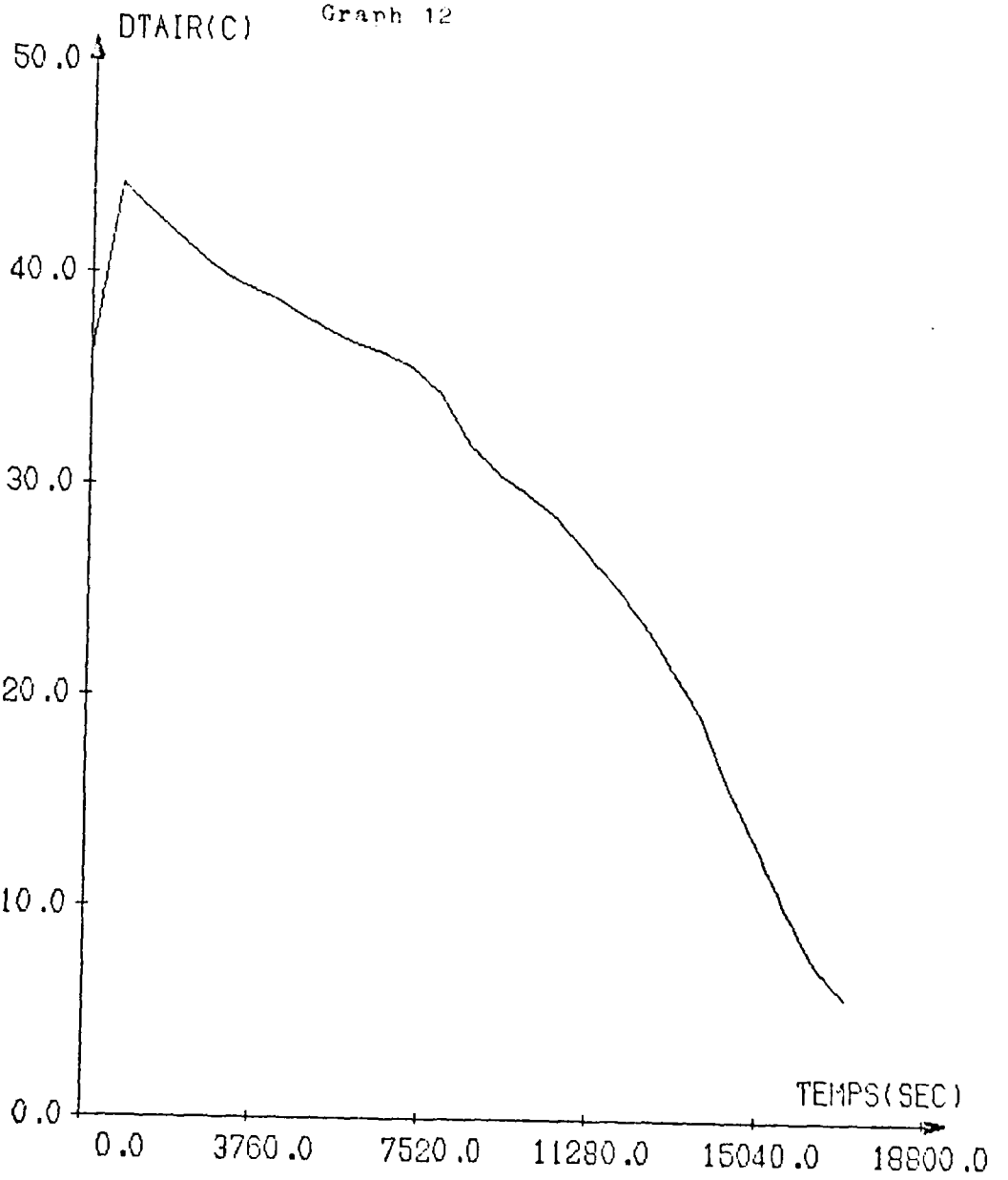

DIFFERENCE BETWEEN INLET AND OUTLET AIR
AIR TEMPERATURES (DTAIR)
DATE 9-04-81
MASS FLOW .05 KG/SEC
TUBES CROSS FLOW, CHARGING MODE. CACL2-6H2O

Graph 13

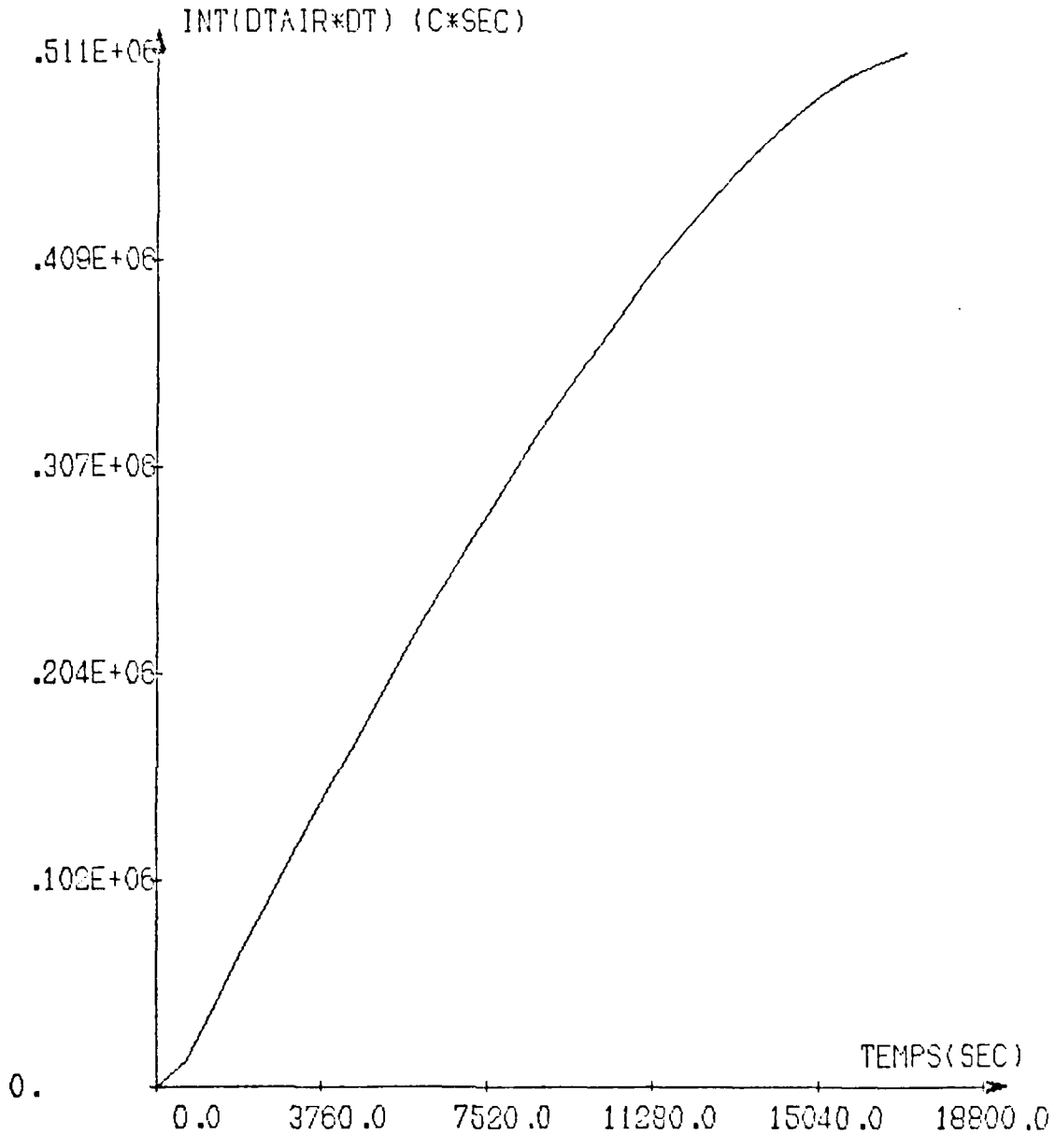

TIME INTEGRATION OF DIFFERENCE BETWEEN INLET ANU
OUTLET AIR TEMPERATURES (INT(DTAIR*DT)). VERSUS T
DATE 9-04-81
MASS FLOW .05 KG/SEC
TUBES CROSS FLOW. CHARGING MODE. CACL2-6H2O

THEUNISSEN P-H WHITE P ELMER J QUETSTROEY R

Graph 14

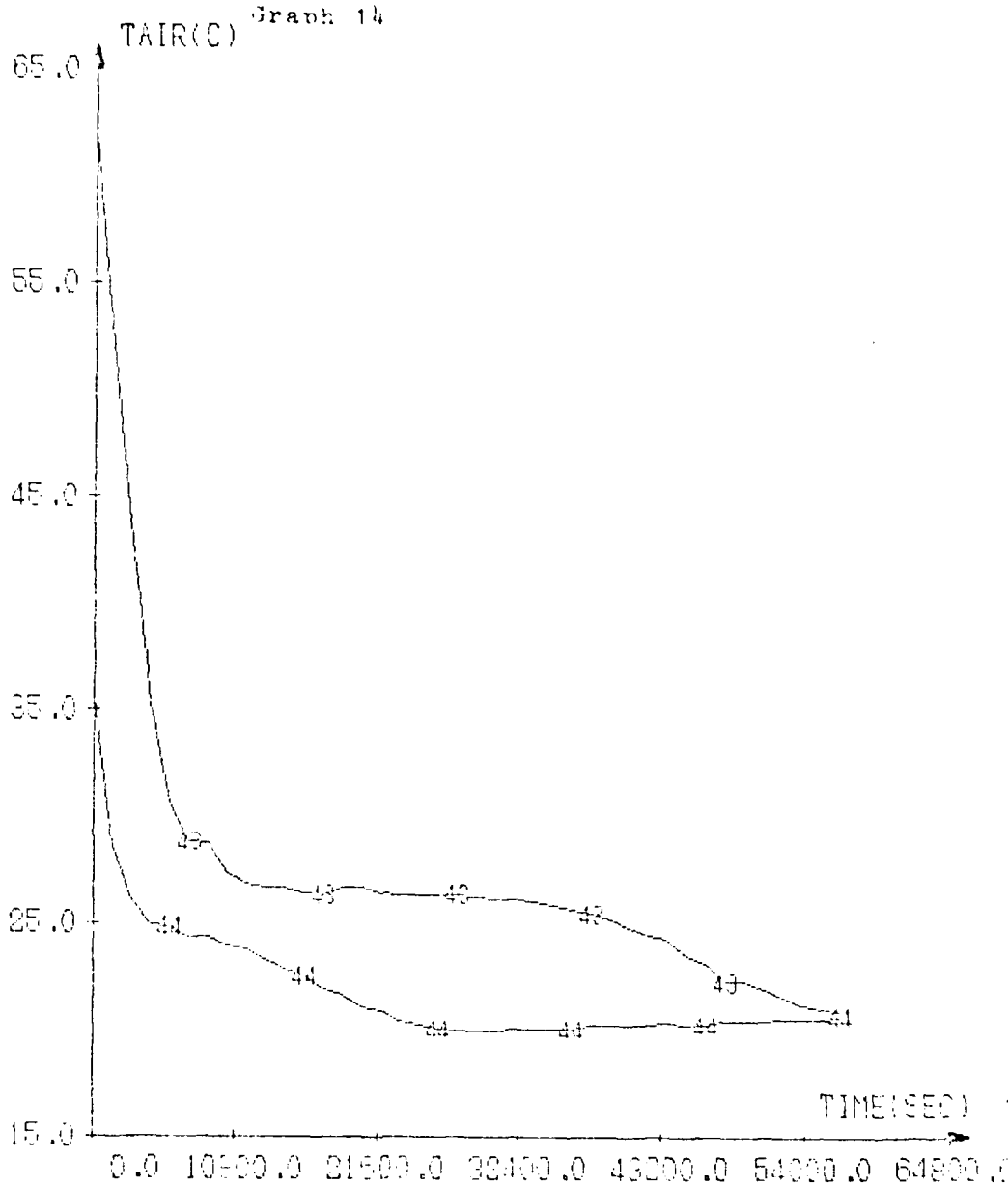

TEMPERATURE AS FUNCTION OF TIME
AIR EXPRESSWAYJET SORTIE(43)
DATE=09-04-81
AIR FLOW=0.05MG PER SECOND
TUBES CROSS FLOW WITH CACLO-6H20

THEUNISSEN P-H WHITE P ELMER J OUETSTROEY R

THEUNISSEN P-H WHITE P ELMER J QUETSTROEY R

Graph 15

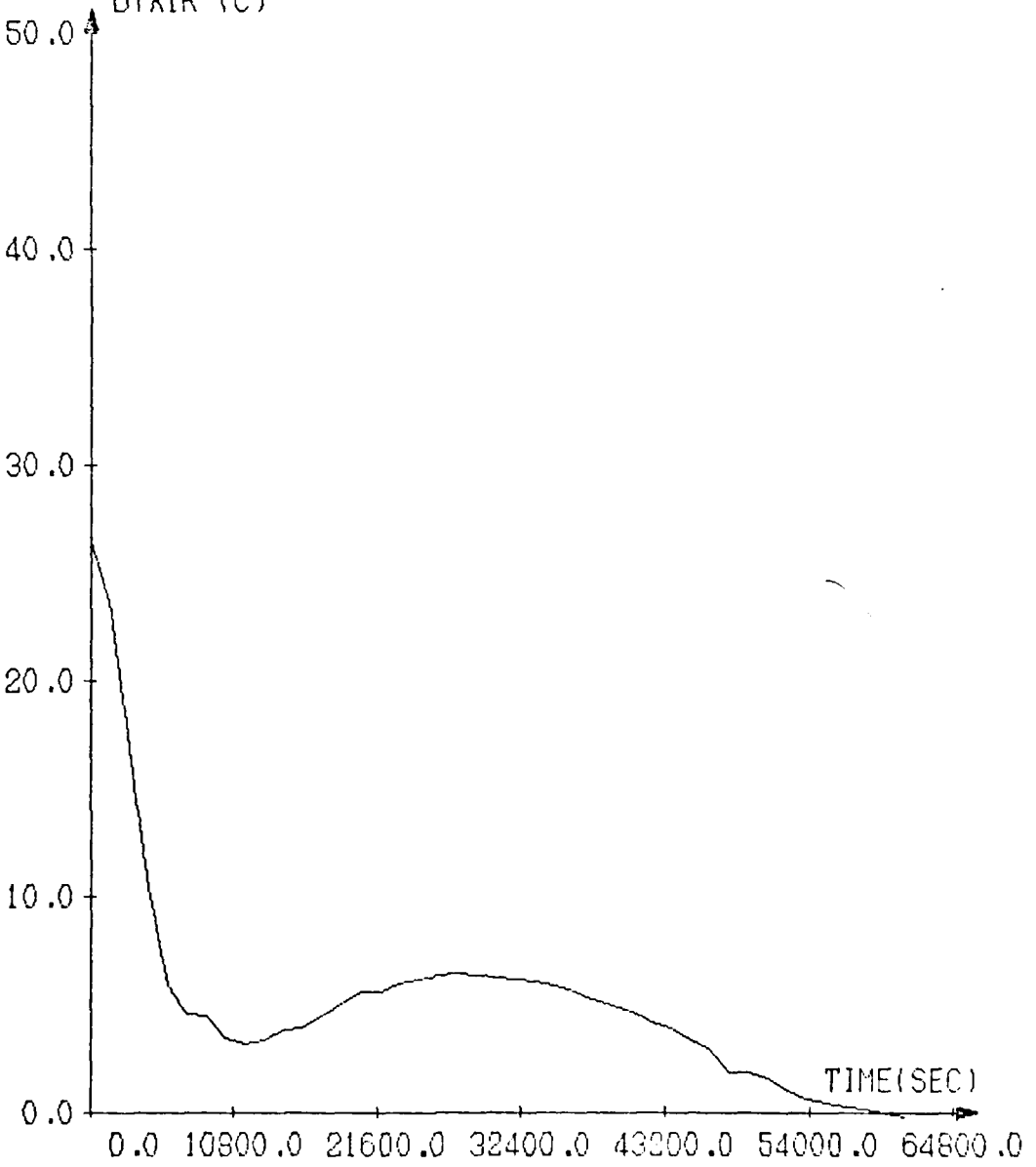

DIFFERENCE BETWEEN OUTLET AND INLET
AIR TEMPERATURES (DTAIR)
DATE=09-04-81
AIR FLOW=0.05KG PER SECOND
TUBES CROSS FLOW ,DISCHARGE, CACL2-6H2O

Graph 16

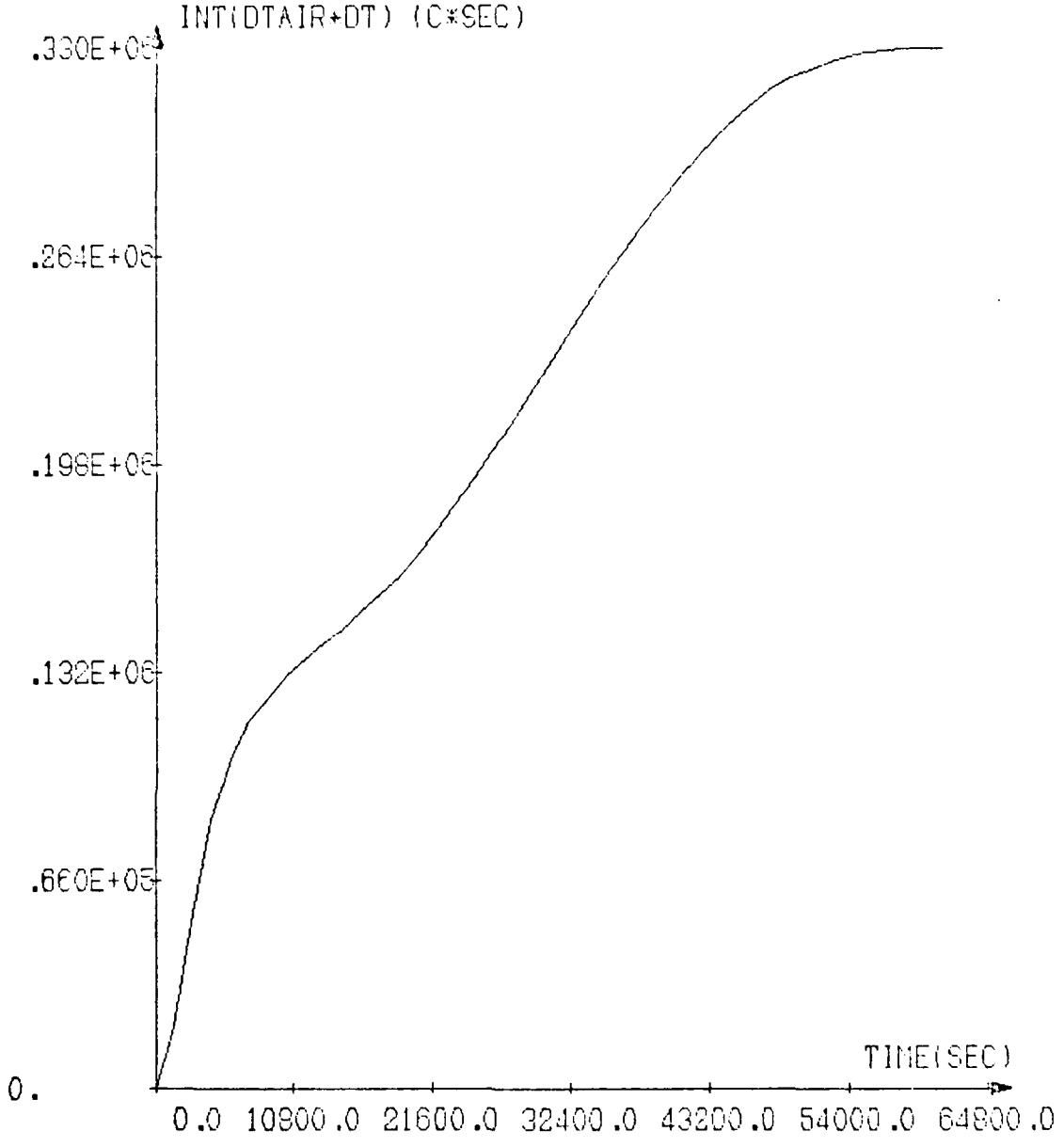

THEUNISSEN P-H WHITE P ELMER J OUETSTROEY R

TIME INTEGRATION OF DIFFERENCE BETWEEN INLET AND OUTLET AIR TEMPERATURES((INT(DTAIR*DT)) VERSUS TI

DATE=09-04-81

AIR FLOW=0.05KG PER SECOND

TUBES CROSS FLOW .DISCHARGE. CACL2-6H2O

Graph 17

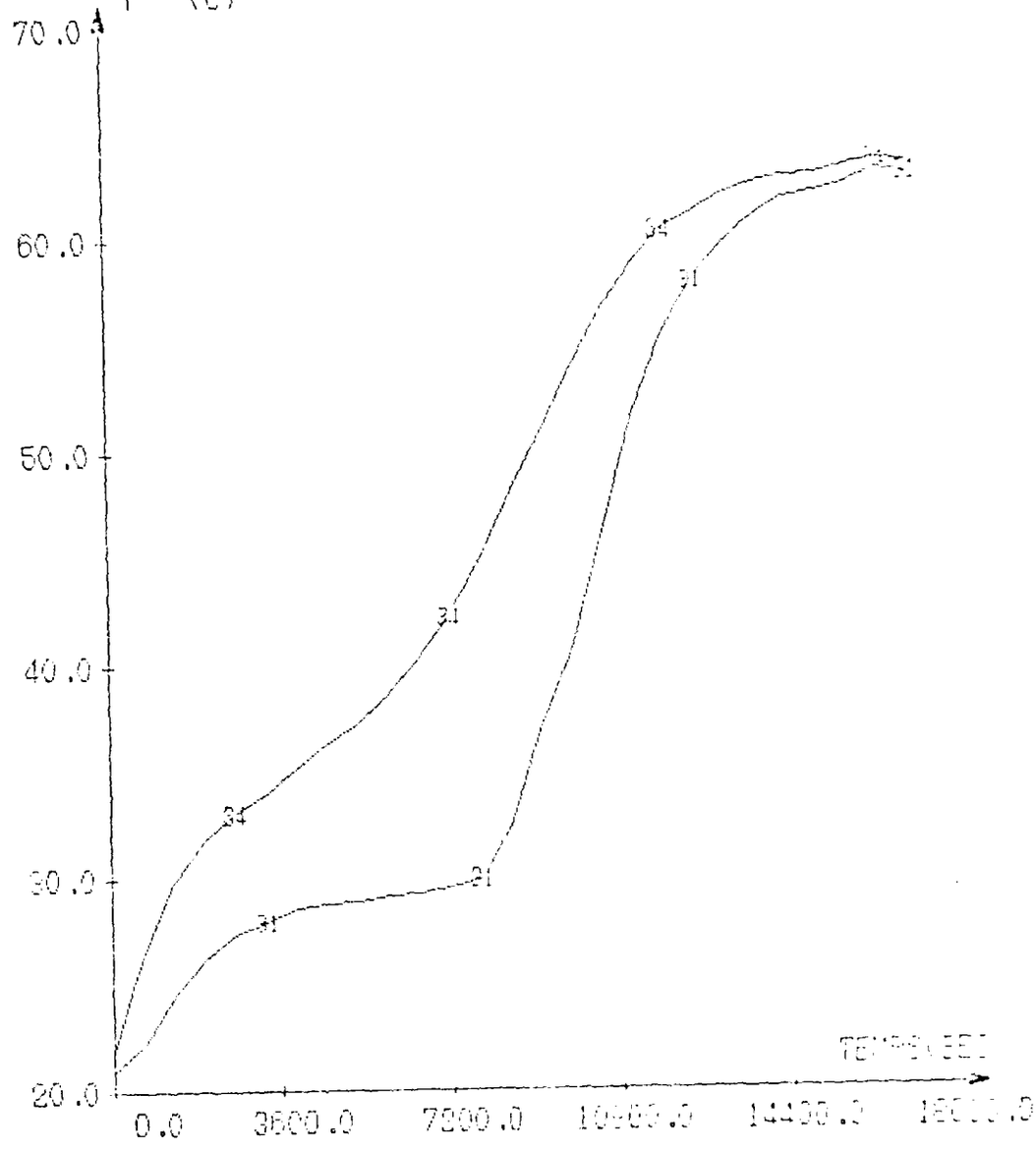

THEUNISSEN P-H WHITE P ELMER J QUITTSTROEY R

TEMPERATURE EN FONCTION EN TEMPS

SECTION MILIEU AIR (31) (35/31)

DATE 9-04-81

DEBIT AIR .05 KG/SEC

TUBES CROSS FLOW CACLO-EHCO

Graph 16

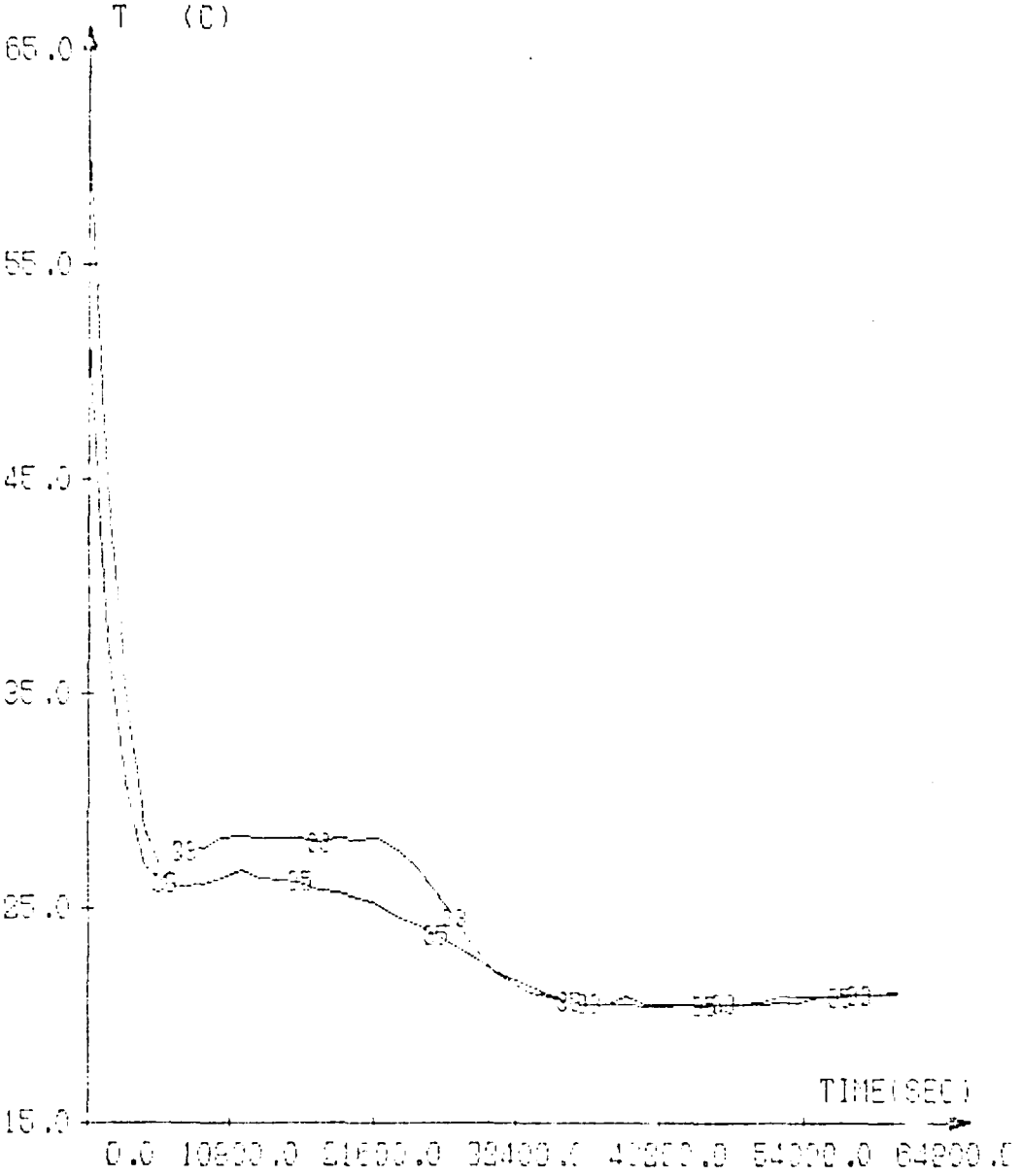

TEMPERATURE EN FONCTION DU TEMPS

SECTION MILIEU AIR(35) MCP(32)

DATE=06-04-81

AIR FLOW=0.05PG PER SECOND

TUBES CROSS FLOW WITH CACLO-6H20

THERMISSEN P-H WHITE P ELMER J CHETSTRUEY R

THEUNISSEN P-H WHITE P ELMER J OULTSTROEY R

Graph 19

TMCP(C)

65.0
55.0
45.0
35.0
25.0
15.0

TIME(SEC)

0.0 10800.0 21600.0 32400.0 43200.0 54000.0 64800.0

TEMPERATURE EN FONCTION DU TEMPS

MCP SECTION ENTREE(10,11,12,13)

DATE=09-04-81

AIR FLOW=0.05MG PER SECOND

TUBES CROSS FLOW WITH CACLS-SHSD

THEUNISSEN P-H WHITE P ELMER J OUETSTROEY R

Graph 20

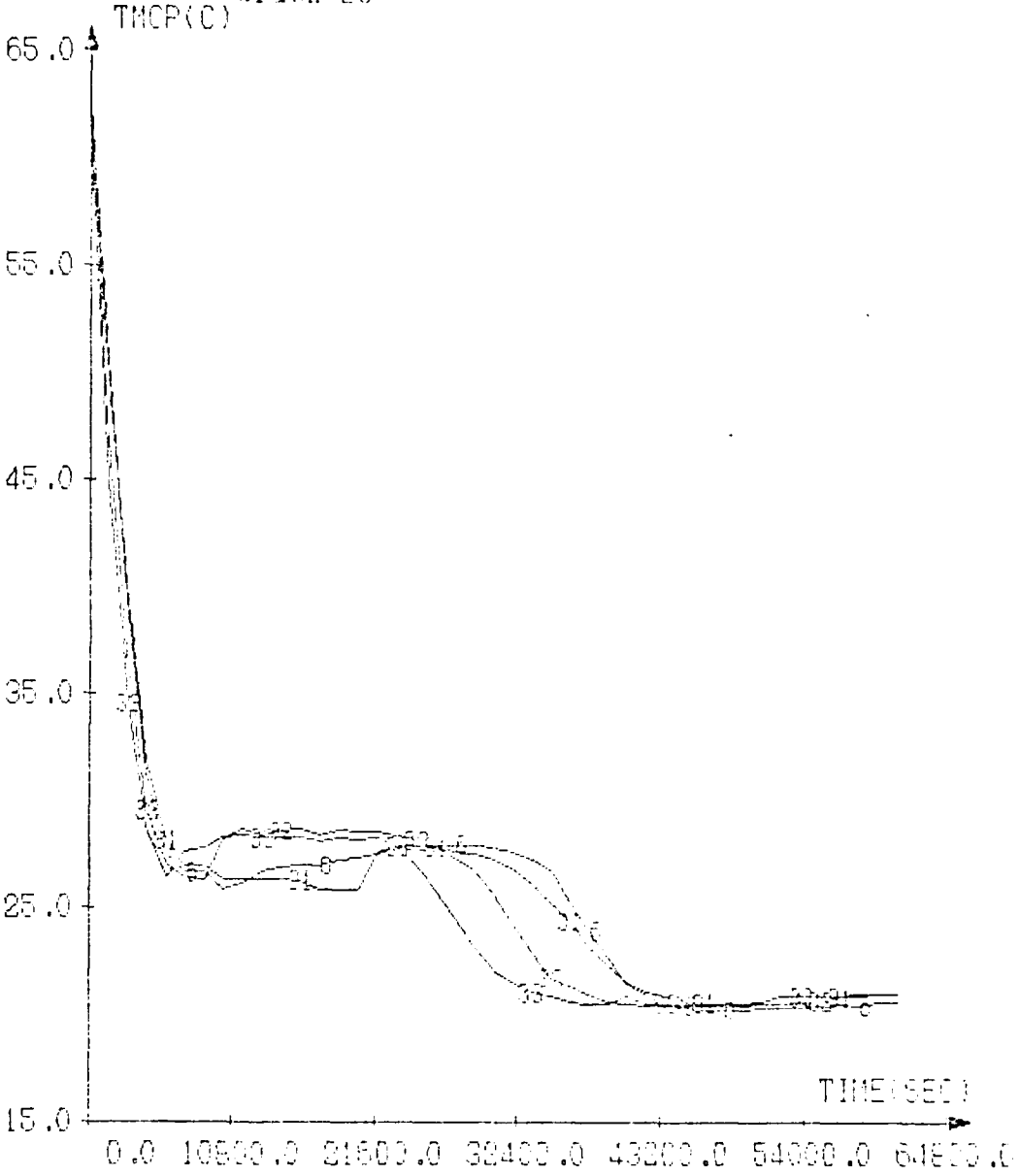

TEMPERATURE EN FONCTION DU TEMPS

MCP SECTION MILIEU(31,32,33,6)

DATE=09-04-81

AIR FLOW=0.05KG PER SECOND

TUBES CROSS FLOW WITH CACLO-6H2O

Graph 21

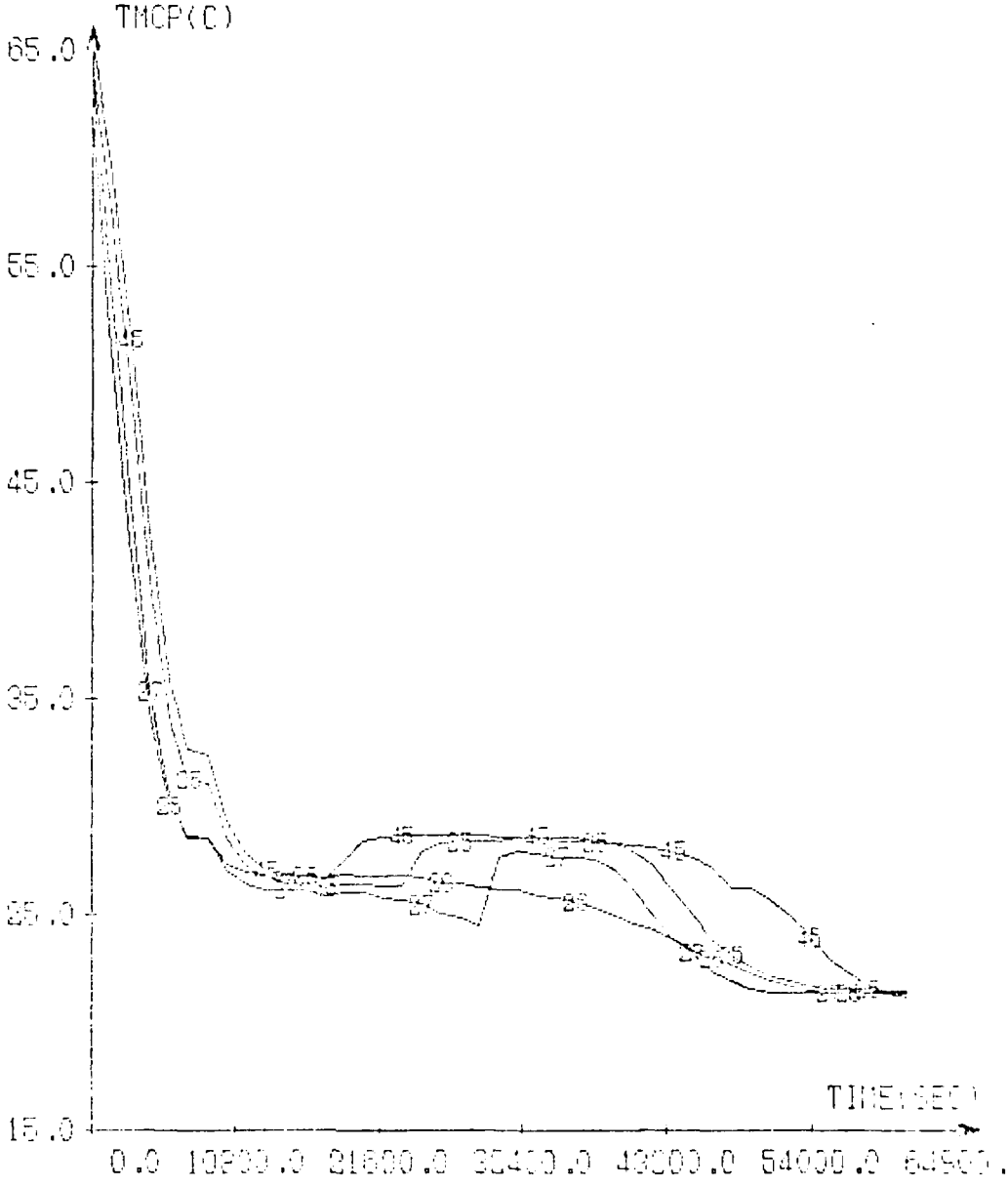

TEMPERATURE EN FONCTION DU TEMPS

MCP SECTION SORTIE(28.88.87.48)

DATE=08-04-81

AIR FLOW=0.05KG PER SECOND

TUBES CROSS FLOW WITH CACL2-EAU

THERMISSEN P-H MAITE P ELMER J QUETSTROEY R

B. Packed Bed:

Graphs 22 through 27 show the inlet and outlet temperautres, their difference, and the integral of that difference as a function of time, in the same fashion as the graphs for the charge and discharge for the tube cross flow. Here the numerical values of the integrals are closer to each other in the charge and discharge, at 4.72 X 10^5 and 4.48 X 10^5, respectively.

Graphs 28 and 29 show the air and PCM temperatures at the top, middle, and bottom of the accumulators, and Graphs 30,31, and 32 show the PCM temperatures at cross-sections at the inlet, middle, and outlet of the accumulator. It is evident that the temperature is very uniform across the cross-sections, and, as mentioned before, this is a marked advantage of the packed bed. In the discharge of the packed bed there is again the problem of supercooling (Graphs 33-35), but by having the encapsulation small, and thus making the exit from supercooling occur in a more dispersed fashion, the effect is smoothed out in the air outlet temperature readings. Also, the air temperature is made more uniform about the cross-section as the bed is traversed(Graphs 36-38), during the charge of the unit.

THEUNISSEN P-H WHITE P ELMER J OUETSTROEY R

Graph 22

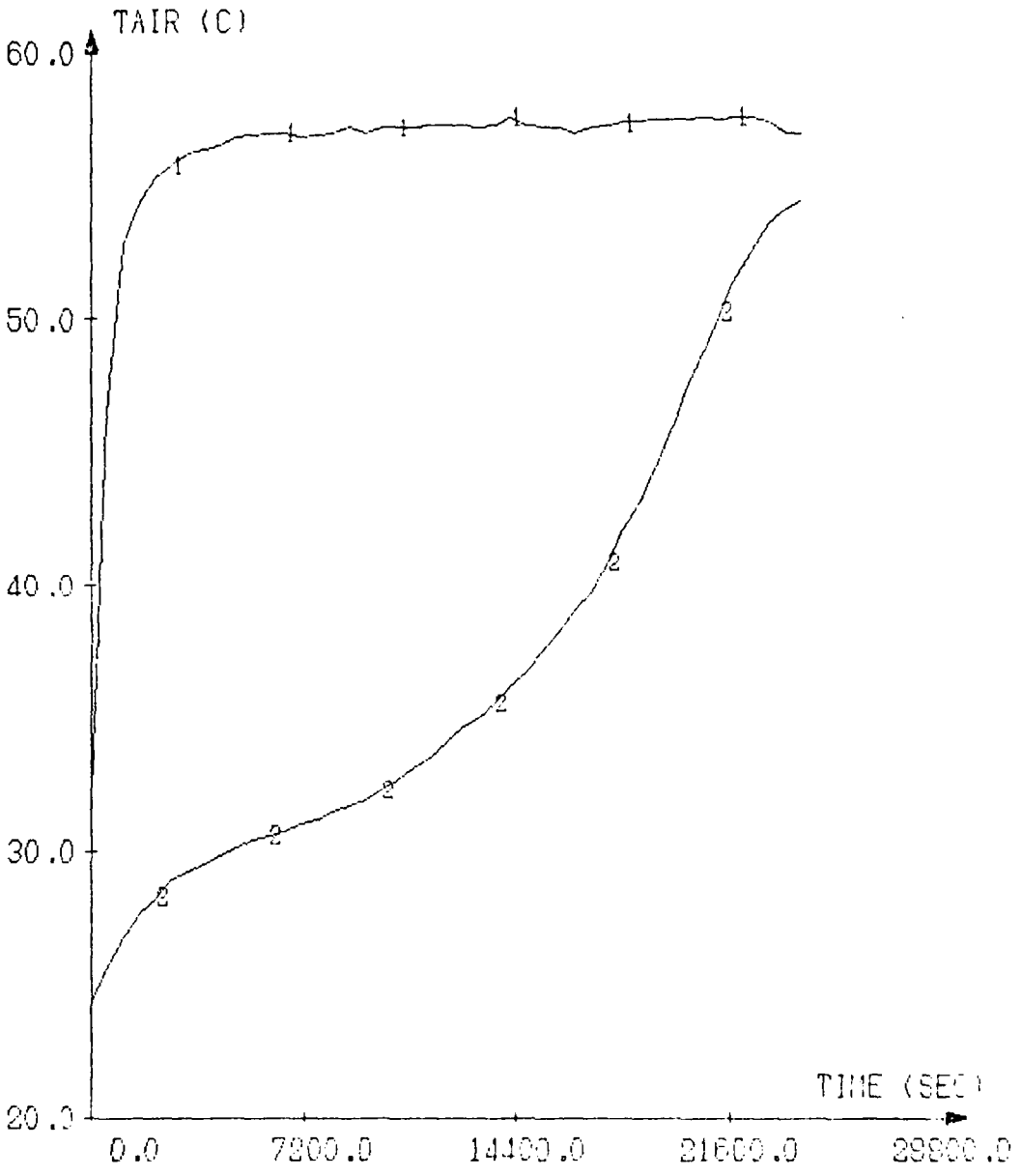

TEMPERATURE AS A FUNCTION OF TIME
AIR ENTREE ET SORTIE-CHARGE DE L ACC.
DATE=14-5-81
AIR FLOW RATE=.07 KG PER SECOND
PACKED BED WITH CACL2-6H2O

Graph 23

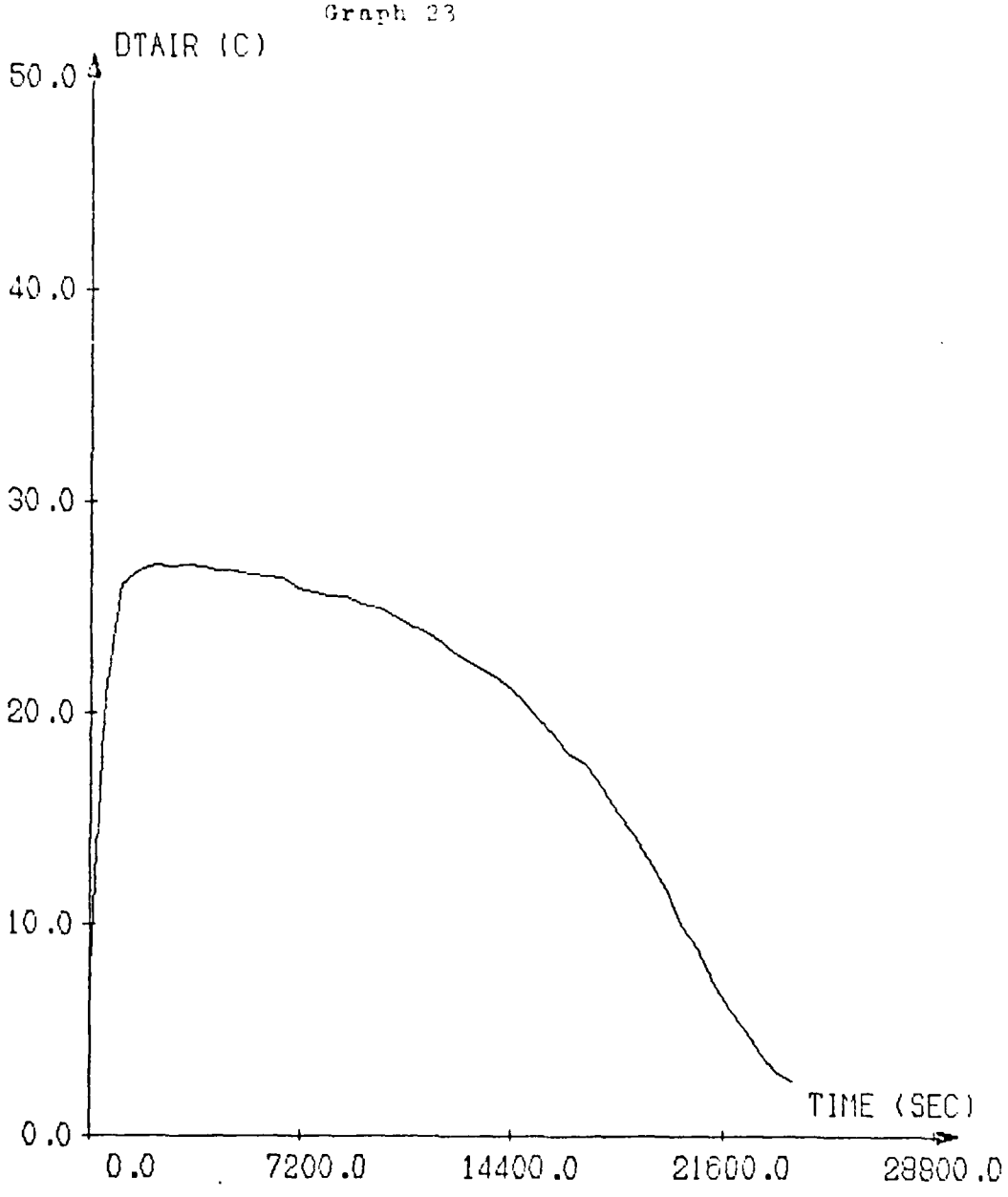

DIFFERENCE BETWEEN INLET AND OUTLET
AIR TEMPEARATURES (DTAIR)
DATE=14-5-81
AIR FLOW RATE=.07 KG PER SECOND
PACKED BED. CHARGING MODE. CACL2-6H20

THEUNISSEN P-H WHITE P ELMER J QUETSTROEY R

THEUNISSEN P-H WHITE P ELMER J QUETSTROEY R

Graph 24

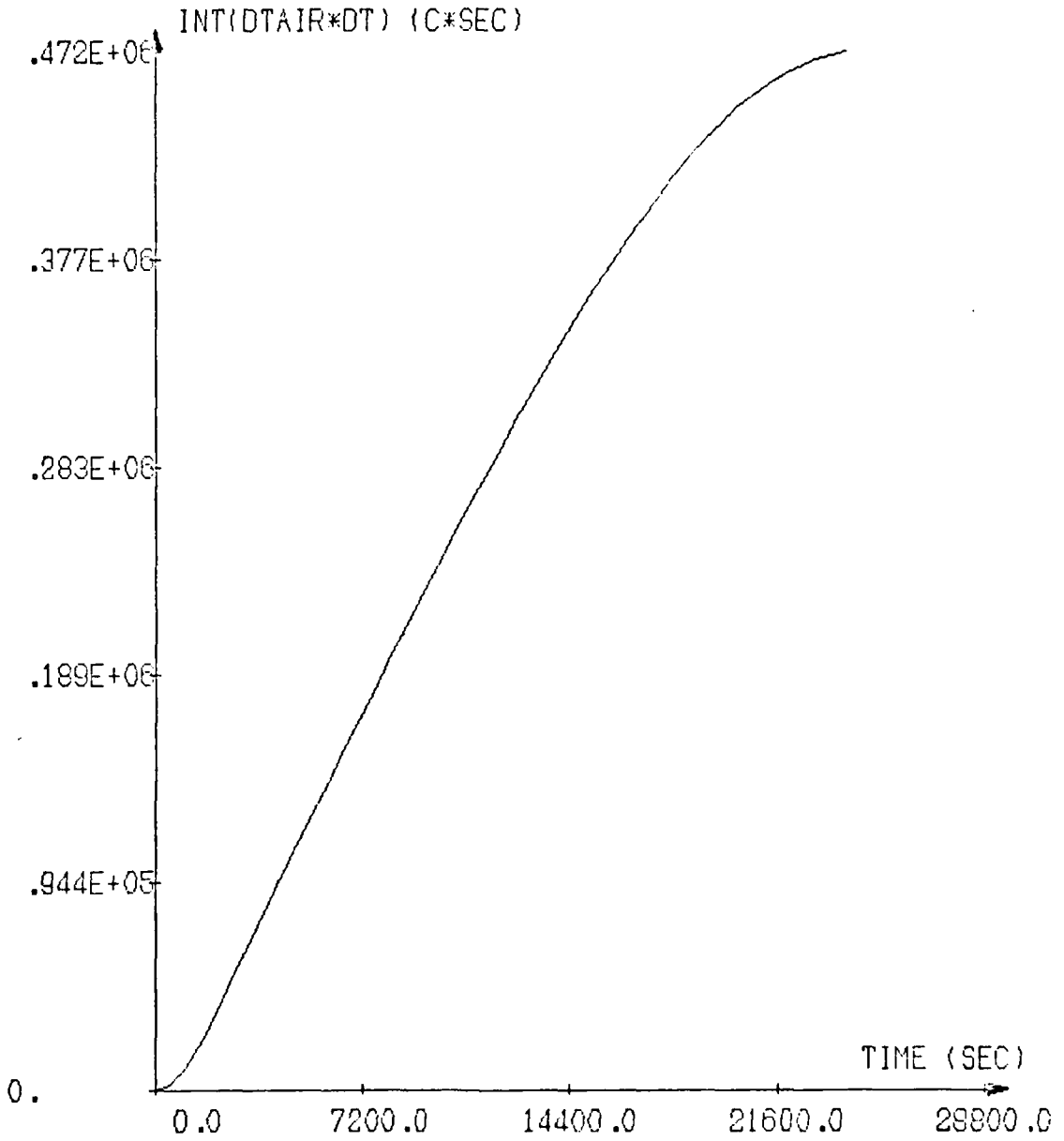

TIME INTEGRATION OF DIFFERENCE BETWEEN INLET AN OUTLET TEMPERATURES (INT(DTAIR*DT)) VERSUS TIME

DATE=14-5-81

AIR FLOW RATE=.07 KG PER SECOND

PACKED BED, CHARGING MODE, CACL2-6H20

THEUNISSEN P-H WHITE P ELMER J QUETSTRODEY R

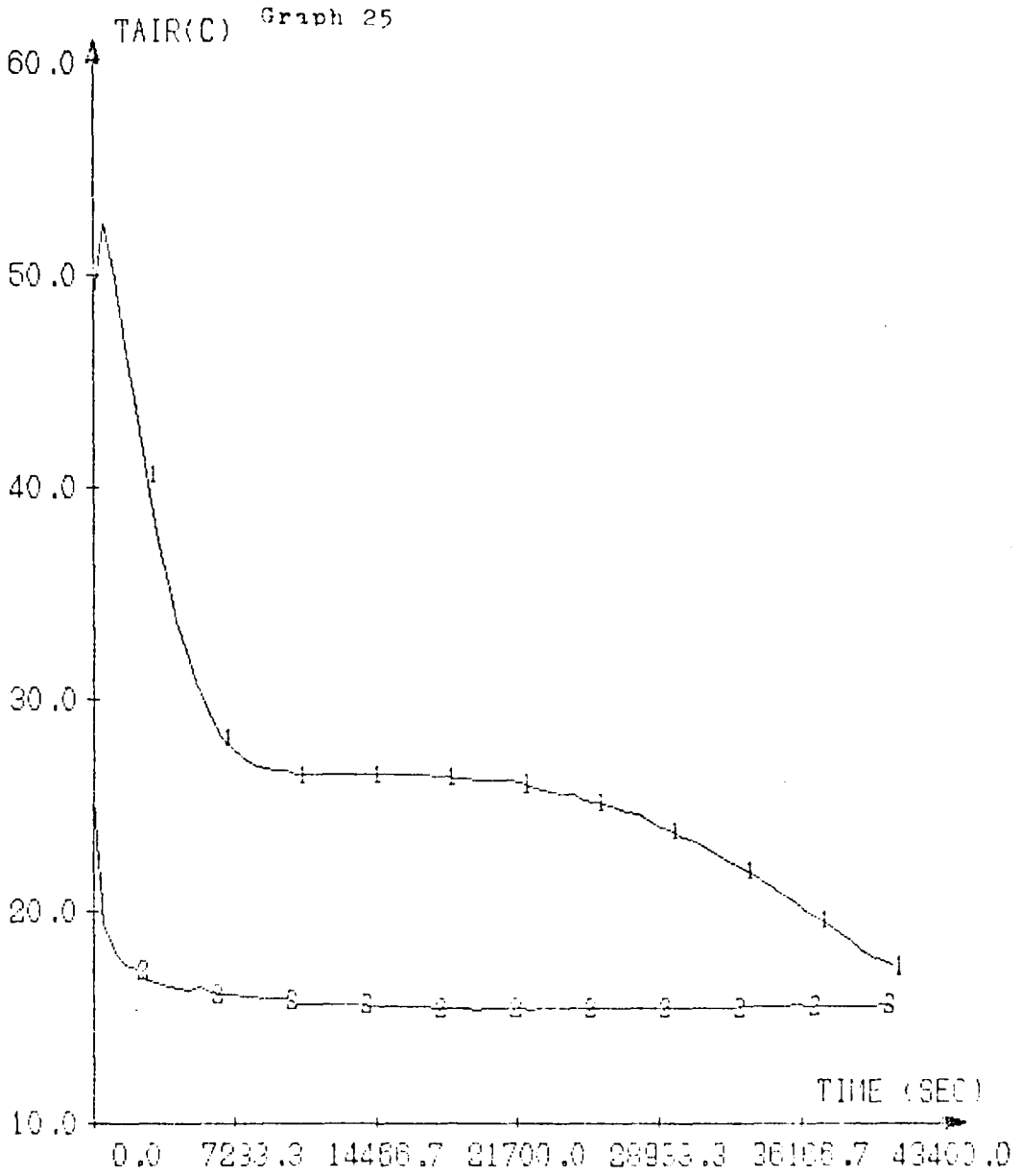

Graph 25

TEMPERATURE AS A FUNCTION OF TIME

AIR ENTREE(2) ET SORTIE(1)

DATE 81-5-15

MASS FLOW RATE .07 KG/SEC

PACKED BED DISCHARGE CACL2-CH3O

THEUNISSEN P-H WHITE P ELMER J QUETSTROEY R

Graph 26

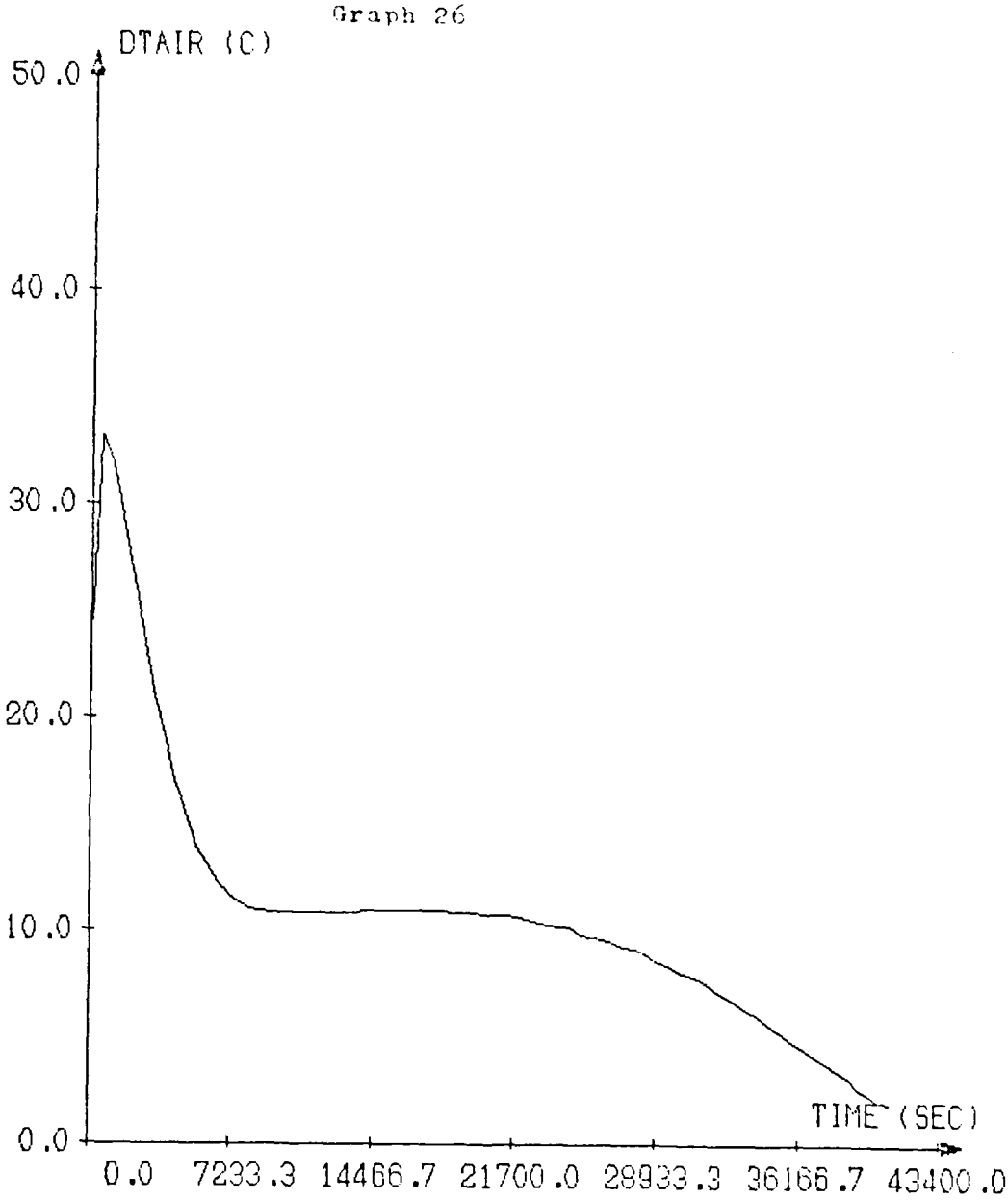

DIFFERENCE BETWEEN OUTLET AND INLET
AIR TEMPERATURES (DTAIR)
DATE 81-5-15
MASS FLOW RATE .07 KG/SEC
PACKED BED DISCHARGE CACL2-6H2O

THEUNISSEN P-H WHITE P ELMER J QUETSTROEY R

Graph 27

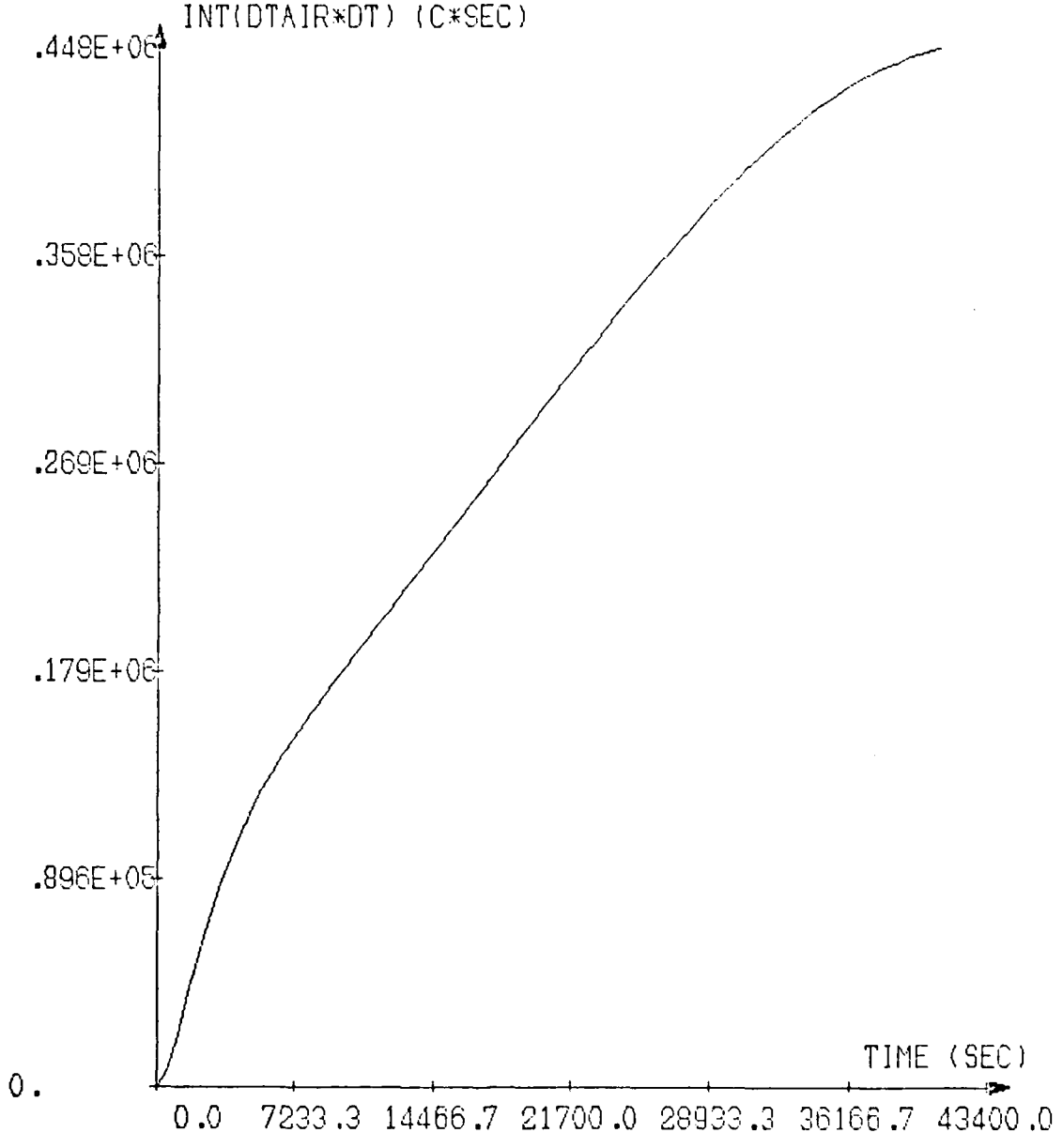

TIME INTEGRATION OF DIFFERENCE BETWEEN INLET AND OUTLET TEMPERATUREST(INT(DTAIR*DT)) VERSUS TIME

DATE 81-5-15

MASS FLOW RATE .07 KG/SEC

PACKED BED DISCHARGE CACL2-6H2O

THEUNISSEN P-H WHITE P ELMER J OUETSTROEY R

Graph 28

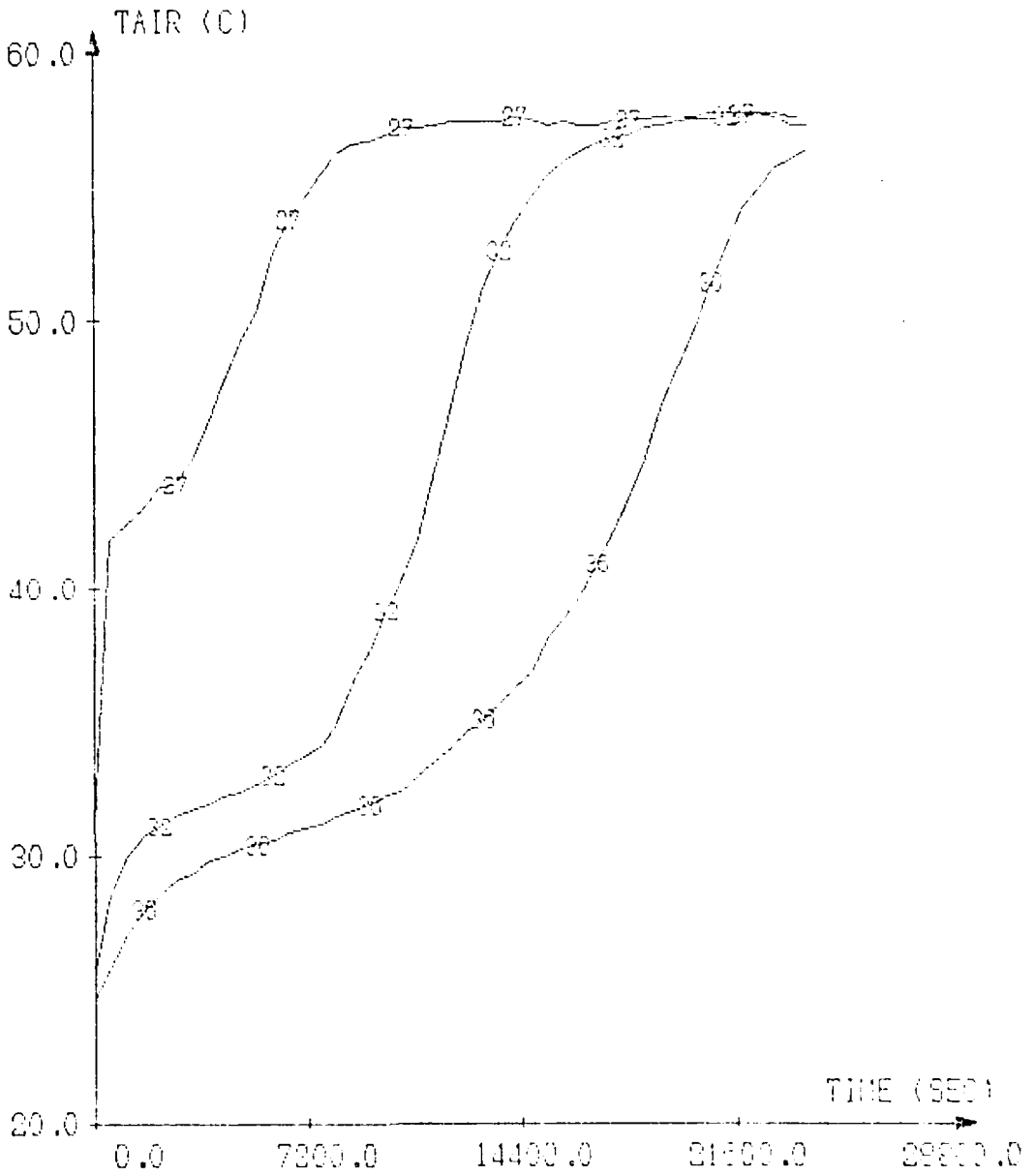

TEMPERATURE AS A FUNCTION OF TIME

AIR DIFFERENT POINTS 27,32,36,

DATE=14-5-81

AIR FLOW RATE=.07 KG PER SECOND

PACKED BED WITH CACL2-6H2O

Graph 29

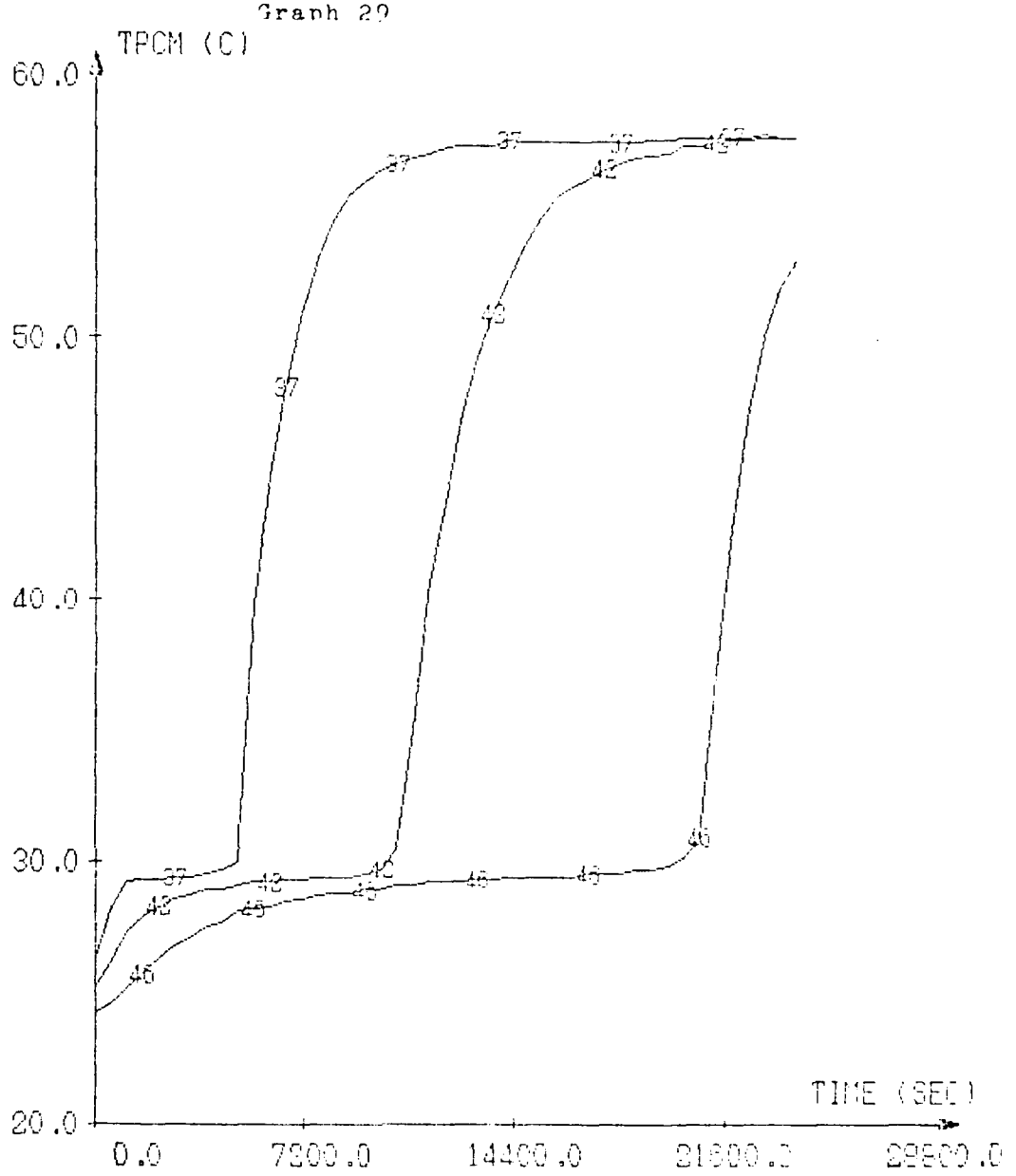

TEMPERATURE AS A FUNCTION OF TIME

PCM DIFFERENT POINTS 37,42,45

DATE=14-5-81

AIR FLOW RATE=.07 KG PER SECOND

PACKED BED WITH CACL2-6H2O

THEUNISSEN P-H WHITE P ELMER J OUETSTROEY R

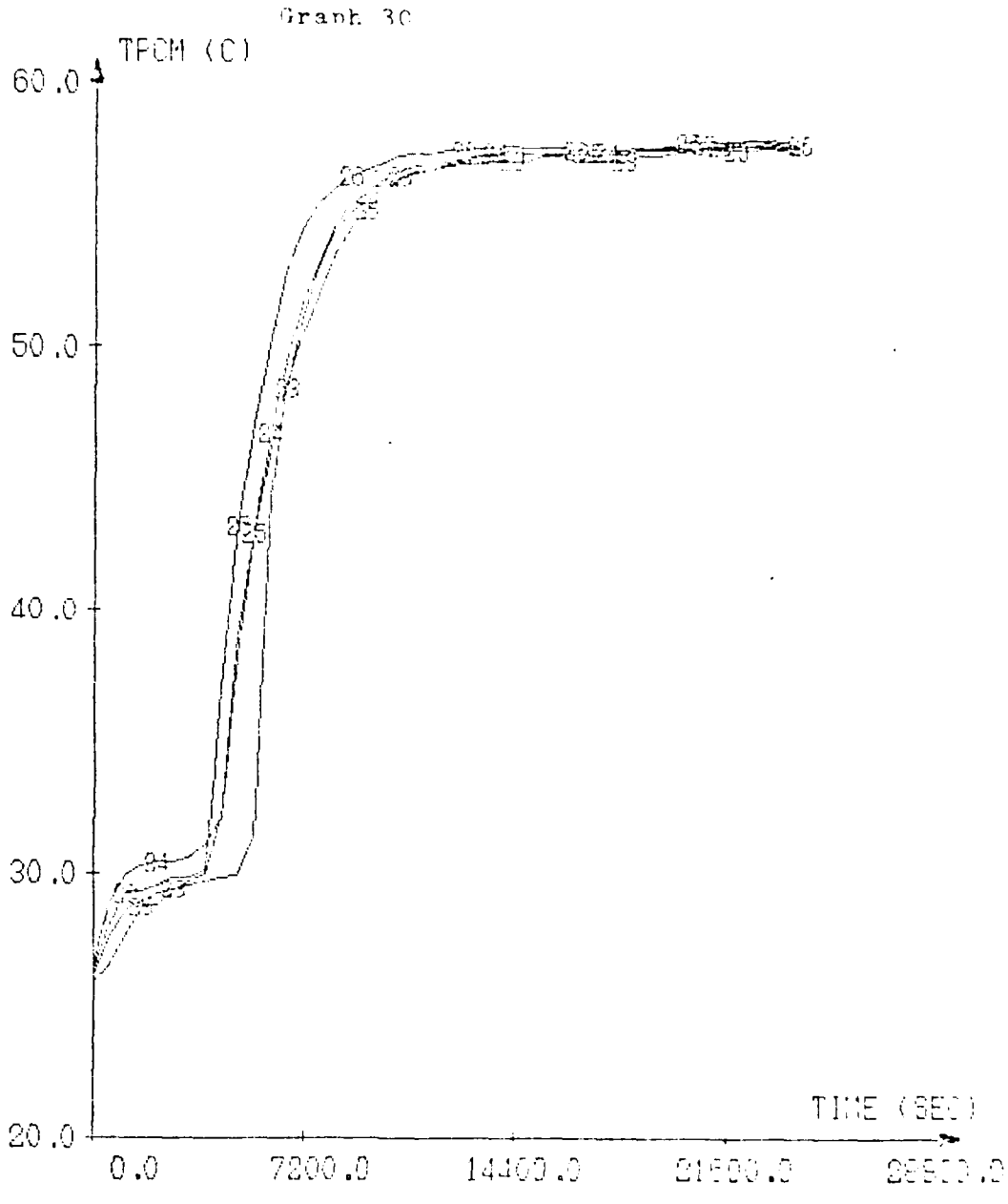

TEMPERATURE AS A FUNCTION OF TIME

PCM SECTION ENTREE(33,34,35,36)

DATE=14-5-81

AIR FLOW RATE=.07 KG PER SECOND

PACKED BED WITH CACL2-6H2O

THEUNISSEN P-H WHITE P ELMER J OUETSTROEY R

THEUNISSEN P-H WHITE P ELMER J QUEYSTROEY R

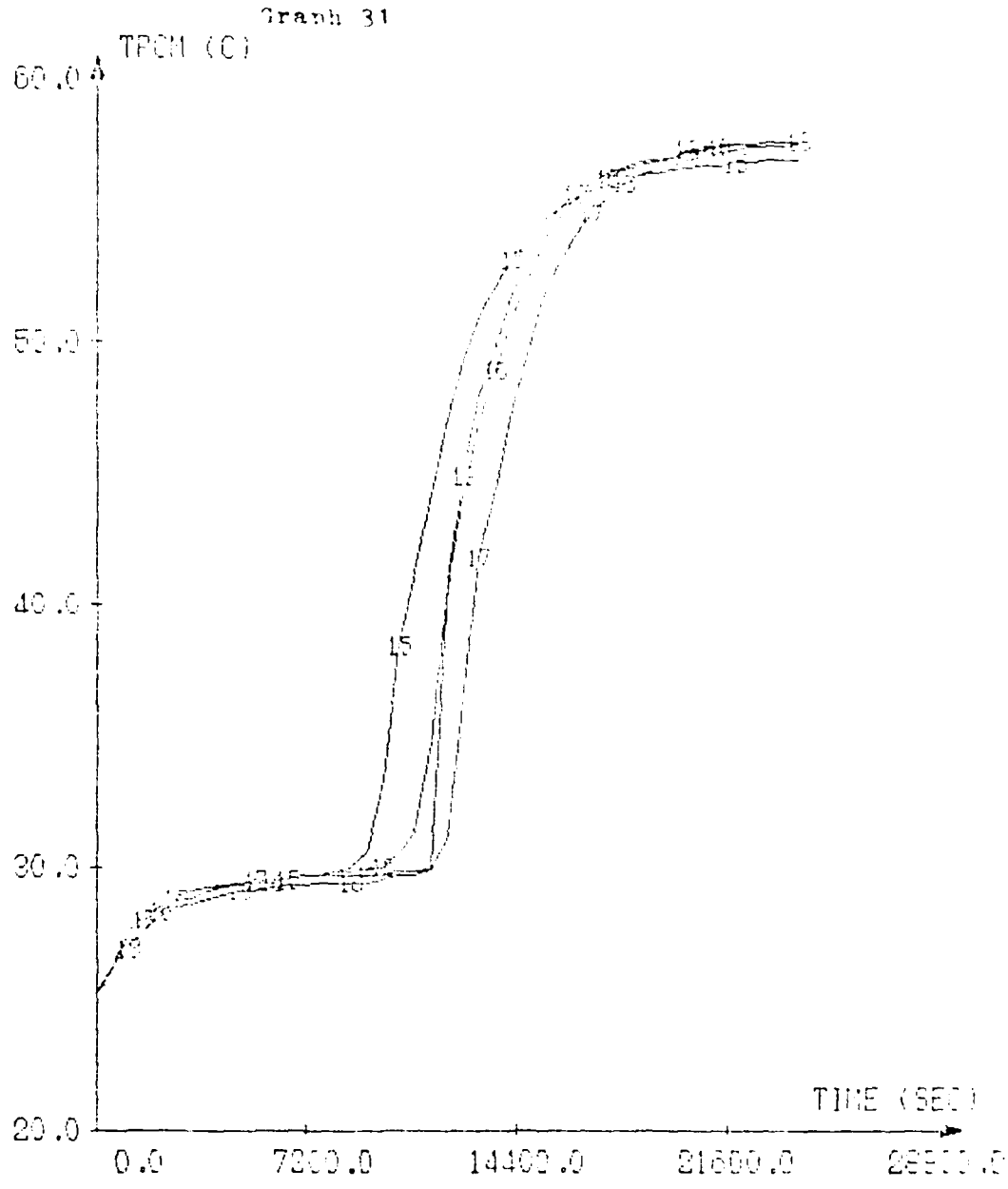

TEMPERATURE AS A FUNCTION OF TIME

PCM SECTION MILIEU-15,16,17,18

DATE=14-5-81

AIR FLOW RATE=.07 KG PER SECOND

PACKED BED WITH CACL2.6H2O

Graph 32

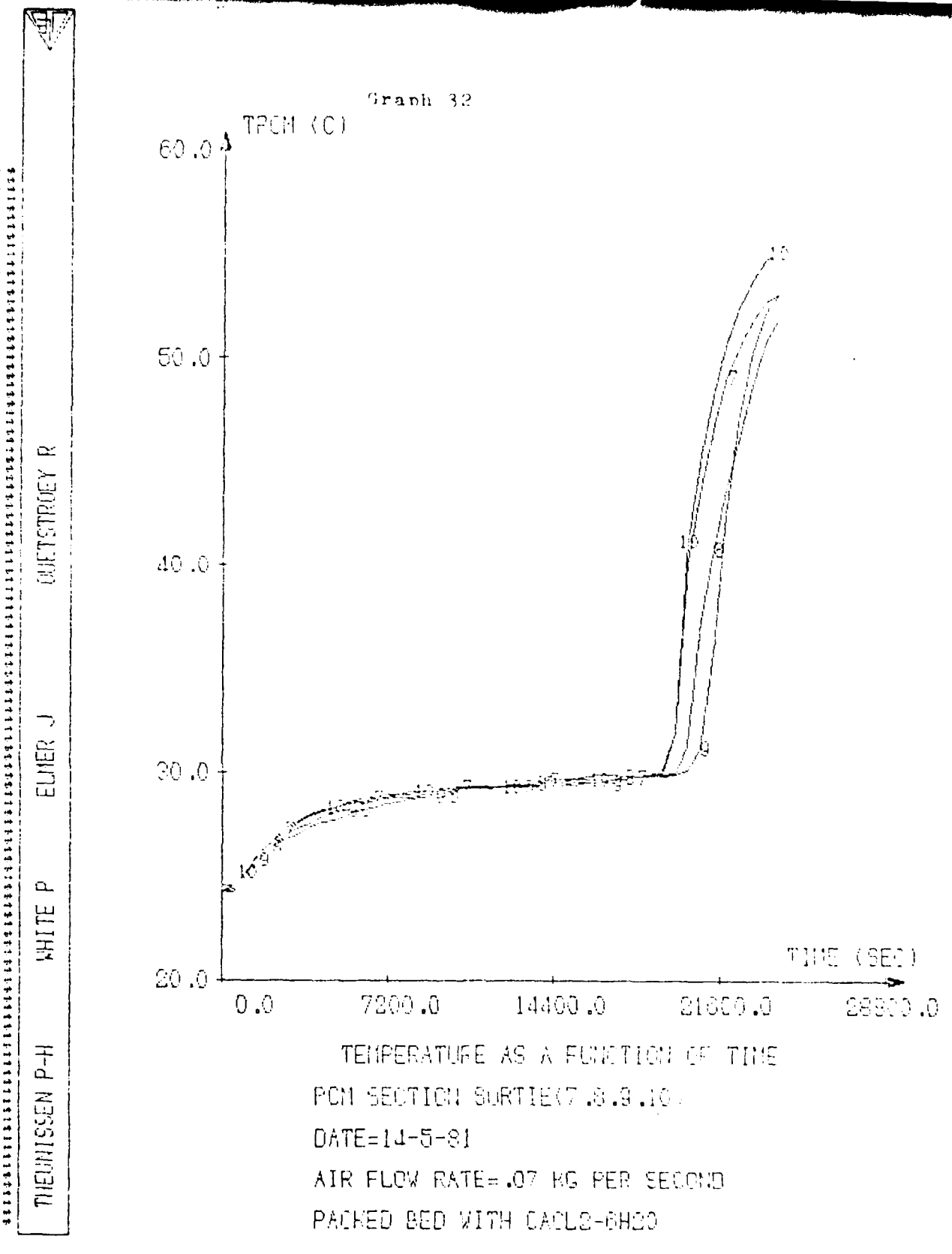

TEMPERATURE AS A FUNCTION OF TIME

PCM SECTION SURTIE(7.8.9.10)

DATE=14-5-81

AIR FLOW RATE=.07 KG PER SECOND

PACKED BED WITH CACL2-6H2O

Graph 33

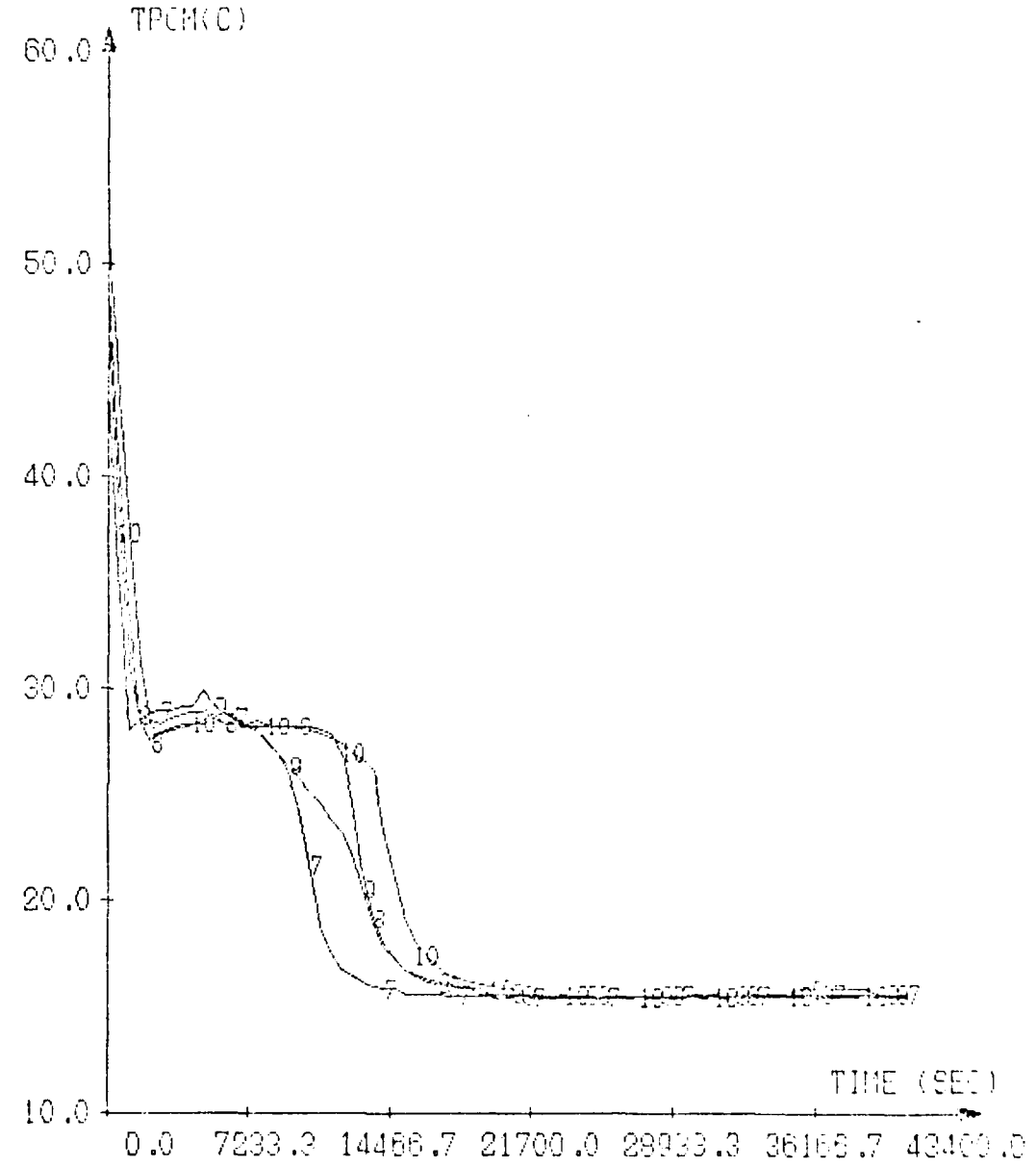

TEMPERATURE AS A FUNCTION OF TIME

PCM SECTION ENTREE(7,8,9,10)

DATE 81-5-15

MASS FLOW RATE .07 KG/SEC

PACKED BED DISCHARGE CACL2-6H2O

THEUNISSEN P-H WHITE P ELMER J QUETSTRODEY R

Graph 34

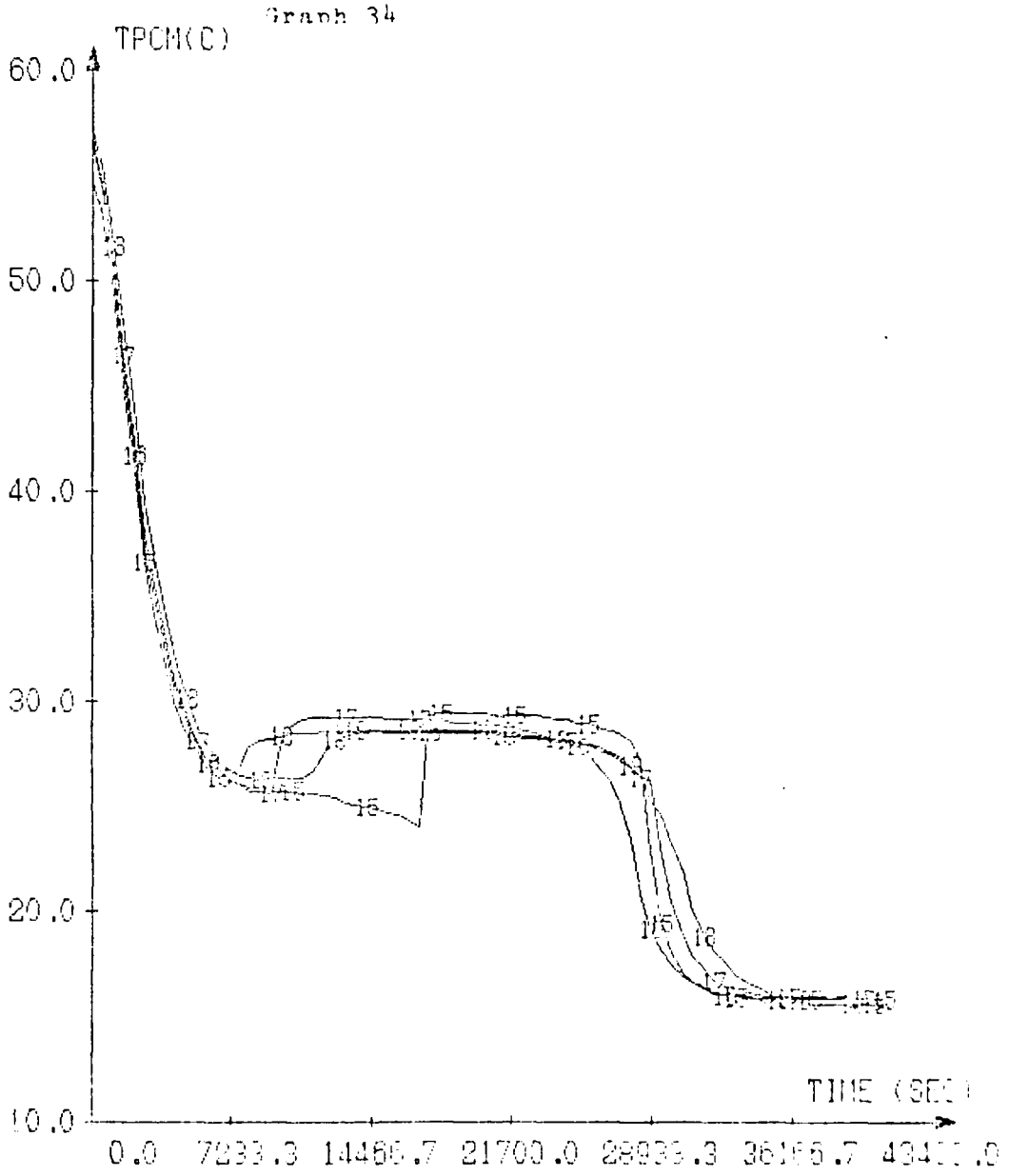

TEMPERATURE AS A FUNCTION OF TIME

PCM SECTION MILIEU(15.16.17.18)

DATE 81-5-15

MASS FLOW RATE .07 KG/SEC

PACKED BED DISCHARGE CACL2-6H2O

THEUNISSEN P-H WHITE P ELMER J QUETSTROEY R

Graph 35

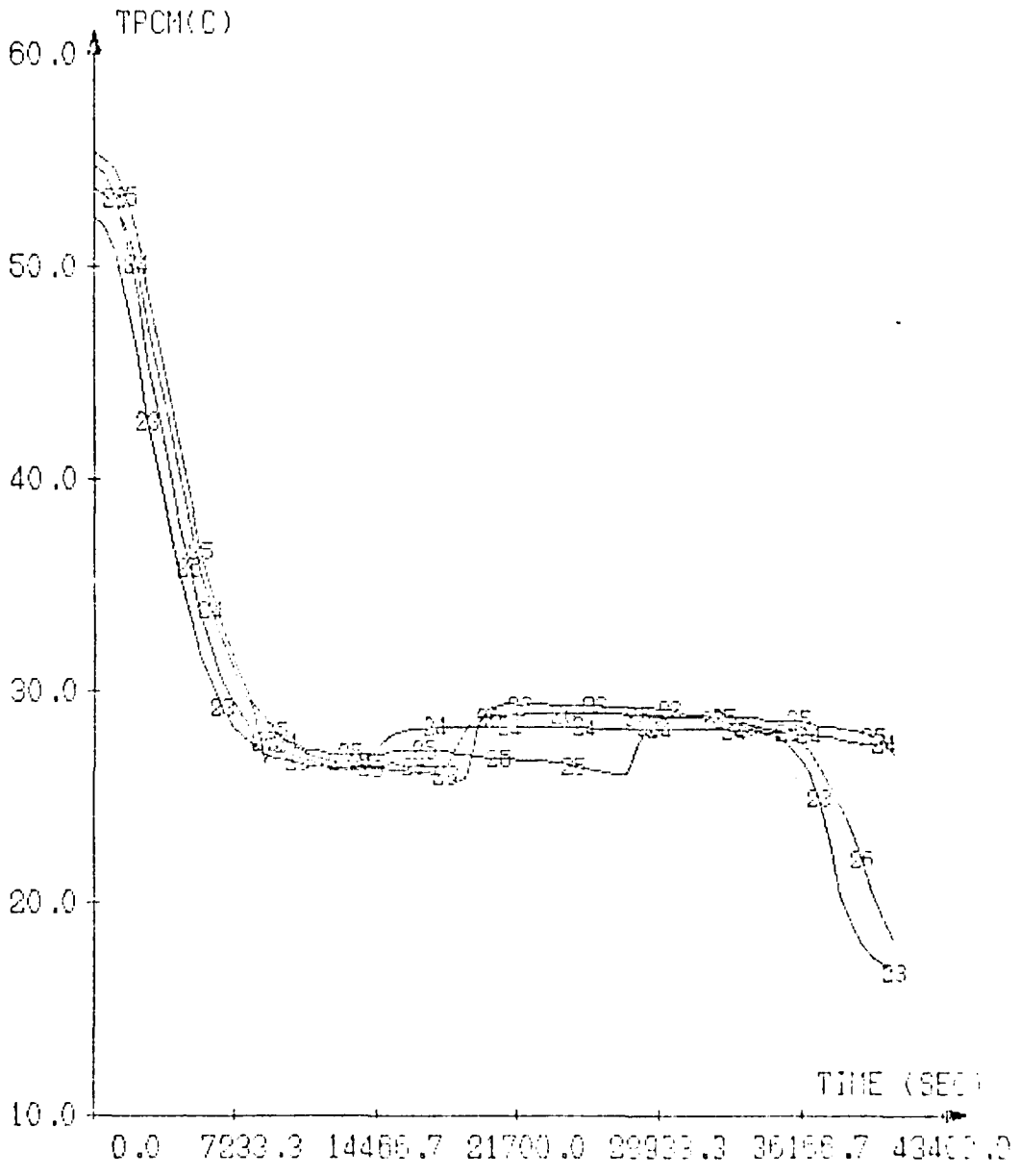

TEMPERATURE AS A FUNCTION OF TIME

PCM SECTION SORTIE(

DATE 81-5-15

MASS FLOW RATE .07 KG/SEC

PACKED BED DISCHARGE (ACLO-CH3)

THEUNISSEN P-H WHITE P ELMER J OUETSTROEY R

THEUNISSEN P-H WHITE P ELMER J OUETSTROEY R

Graph 36

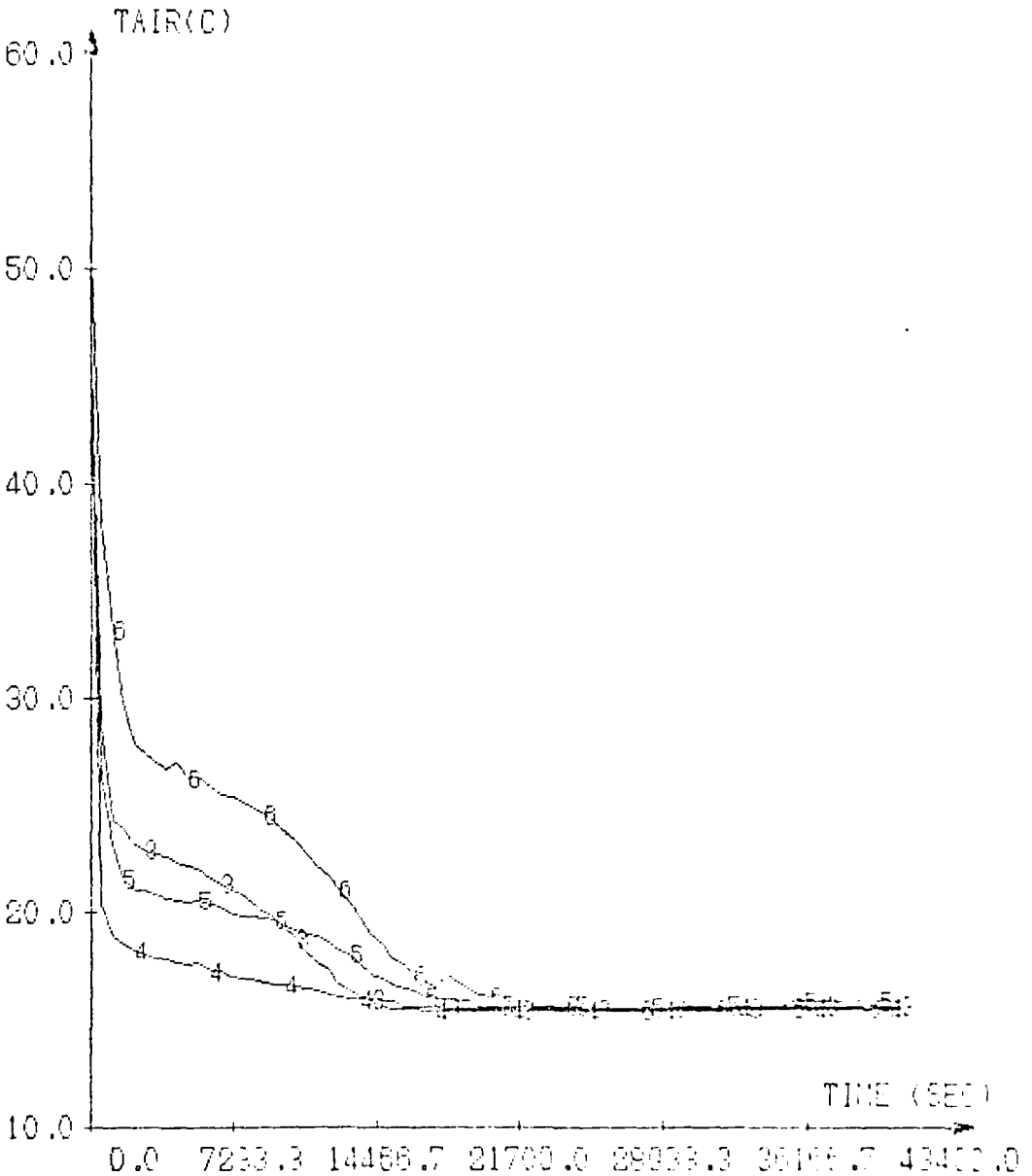

TEMPERATURE AS A FUNCTION OF TIME

AIR SECTION ENTREE(3,4,5,6)

DATE 81-5-15

MASS FLOW RATE .07 KG/SEC

PACKED BED DISCHARGE (AGLO-GAGO

Graph 37

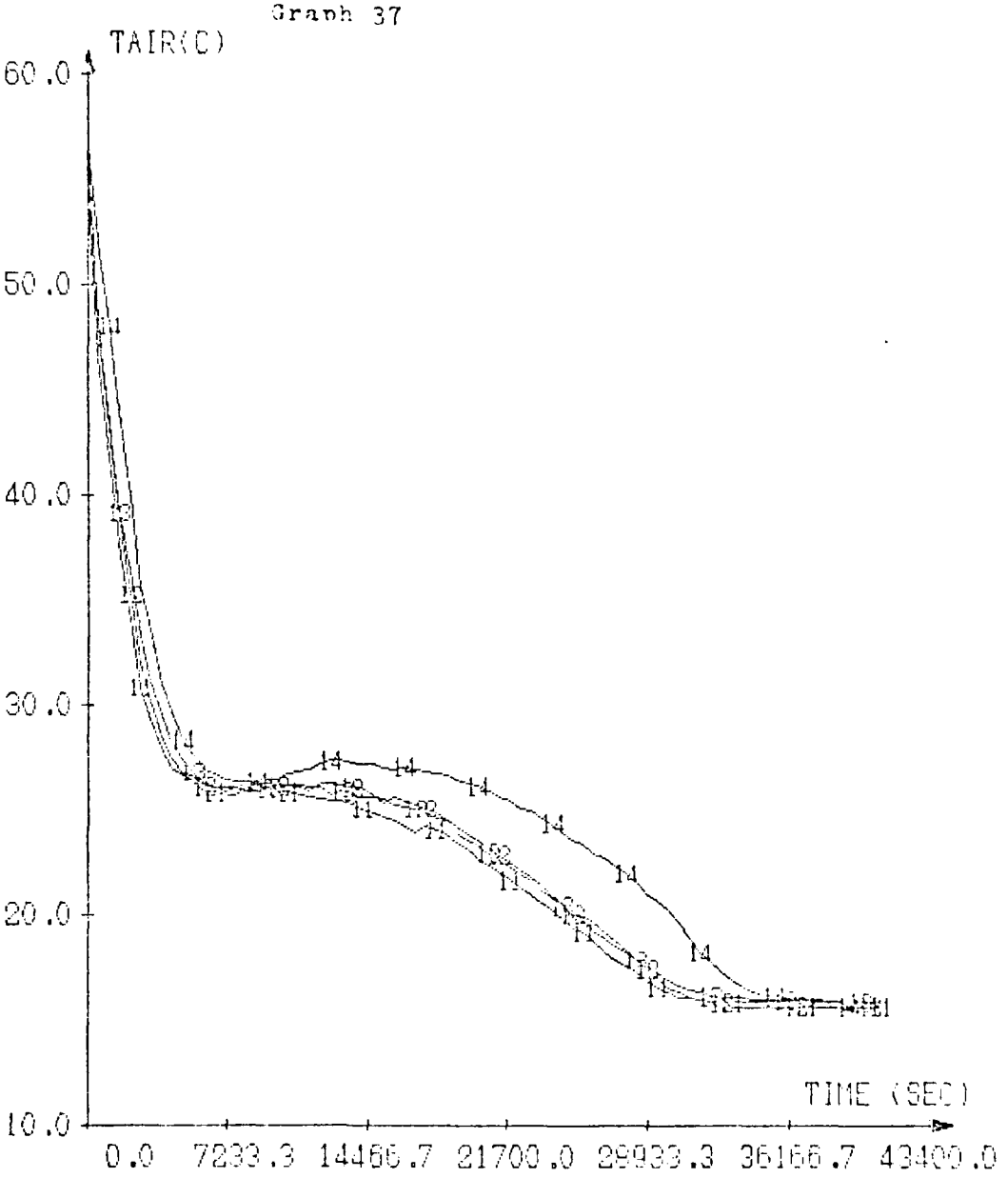

TEMPERATURE AS A FUNCTION OF TIME

AIR SECTION MILIEU(11.13.13.14)

DATE 81-5-15

MASS FLOW RATE .07 KG/SEC

PACKED BED DISCHARGE CACL2-6H2O

THEUNISSEN P-H WHITE P ELMER J QUETSTROEY R

Graph 38

TEMPERATURE AS A FUNCTION OF TIME

AIR SECTION SORTIE(19,20,21,22)

DATE 81-5-15

MASS FLOW RATE .07 KG/SEC

PACKED BED DISCHARGE CACL2-6H2O

THEUNISSEN P-H KNITE P ELMER J QUIETSTROEY R

C. Tube Parallel Flow:

Here again the inlet and outlet air temperatures in the center of the accumulator, their difference, and the integral of the difference are shown on Graphs 3 to 4 . This can be compared with confidence to the data for the packed bed charge, since we are confident of the mass flow rates. We determint the average rate of energy storage as follows:

Packed Bed: $\dot{m}C_{p,air}\left(\int_0^t \Delta T\, dt\right)/t_{charge}$

= .07 kg/sec X 1008 Joule/Kg-°C X472,000 °C-sec /23000 sec

= 1450 joule/sec

Tube Parallel flow

.095 Kg/sec X 1008 Joule/Kg-°C

X 883000°C-sec / 70000 sec

= 1200 joule/sec

Thus we can see that the packed bed stores heat at a rate 1.2 times that at which the tube parallel flow stores heat.

Further indications of the thermal performance of the tube parallel flow unit are shown in graphs 42 and 43 . These show temperature evolutions at different heights in the accumulator. Graphs 44 and 45 show the inlet and outlet air temperature distributions about the cross-section of the accumulator. These last 2 graphs show the surprising result that the air temperatures are close to each other as the accumulator is entered, and there is a larger spread among them at the exit from the accumulator. This may be due to irregular melting of the PCM about the accumulator, as well as motion of the melted PCM from one part of the accumulator to another. A complete discharge was performed on the tube parallel flow unit, and the noteworthy aspect of that test was that it took almost 48 hours for the resolidification to occur, because of an air inlet temperature of 18°C.

THERMISSEN P-H WHITE P ELMER J QUETSTROEY R

Graph 39

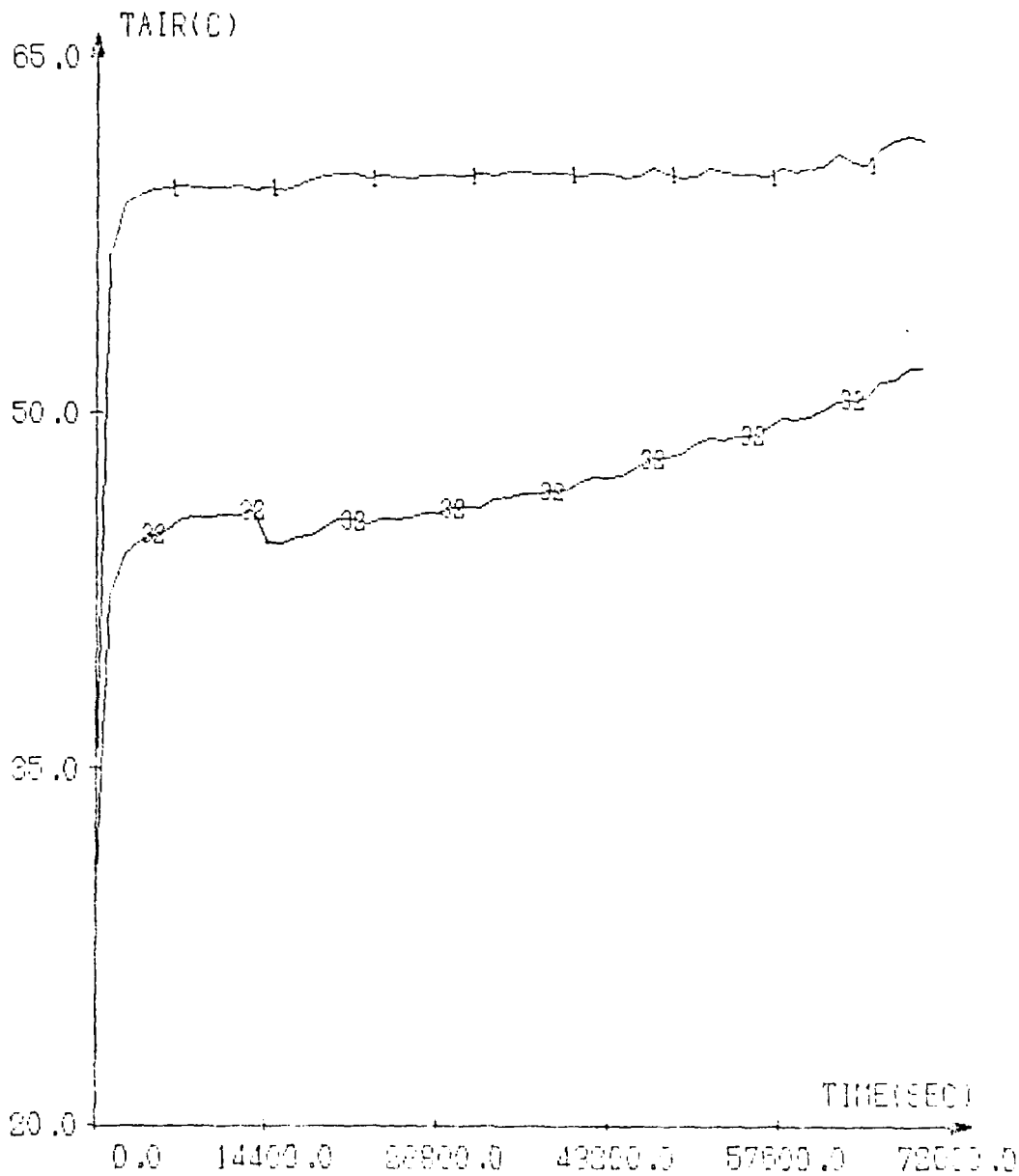

TEMPER-TURE AS A FUNCTION OF TIME

AIR.ENTRY=1.EXIT=32

DATE=5-19-81.MASS FLOW=0.095 KG/SEC

TUBE PARALLEL FLOW.CACL2-GH2O

INLET AND OUTLET AIR TEMPERATURES

THEUNISSEN P-H WHITE P ELMER J QUETSTROEY R

Graph 40

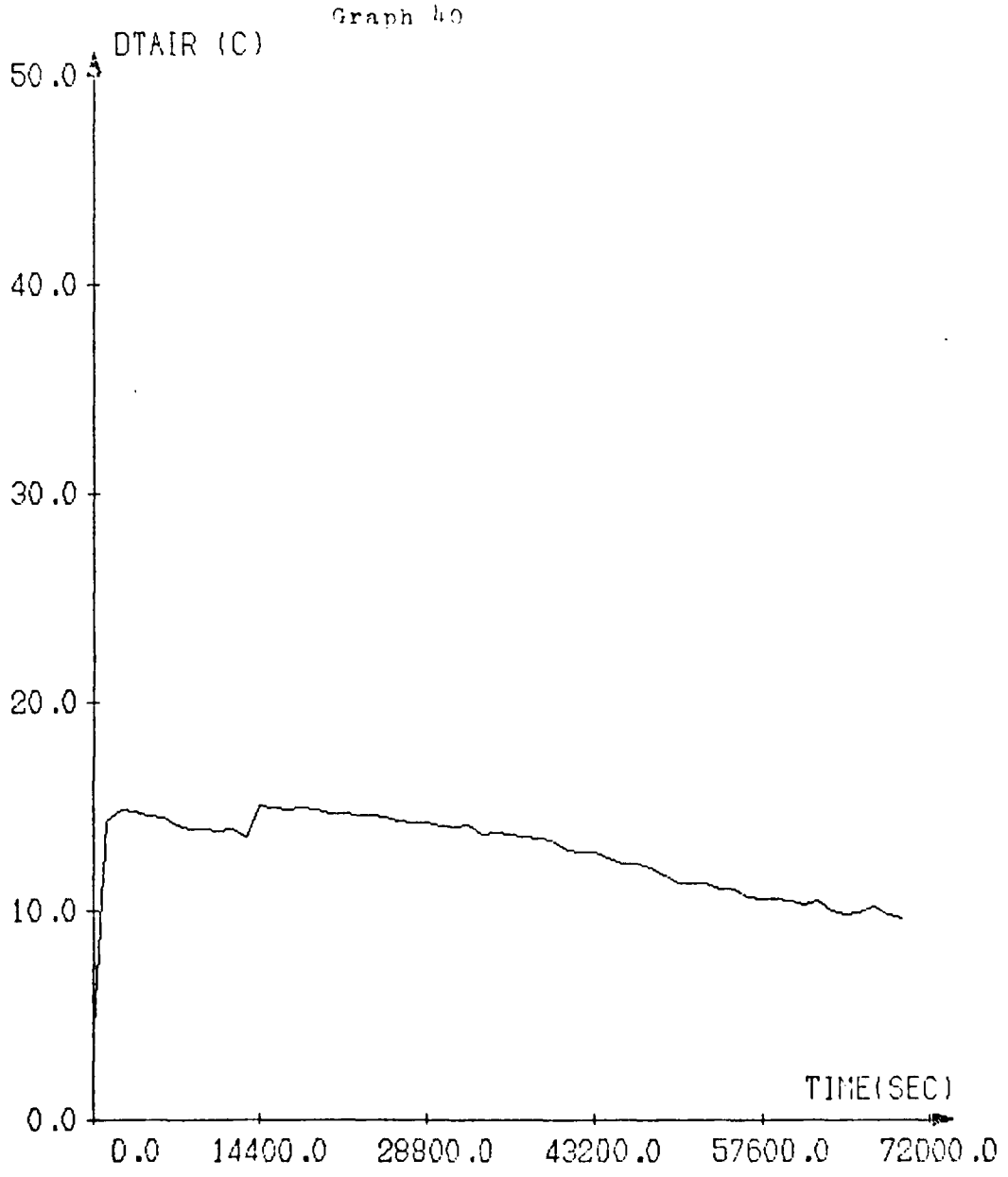

57 RECORD 9999 SEC 81/06/16 14.14.34 AIDA52

DIFFERENCE BETWEEN INLET AND OUTLET
AIR TEMPERATURES (DTAIR)
DATE=5-19-81
MASS FLOW .095 KG/SEC
TUBES PARALLEL FLOW.OCHARGE, CACL2-6H2O

Graph 41

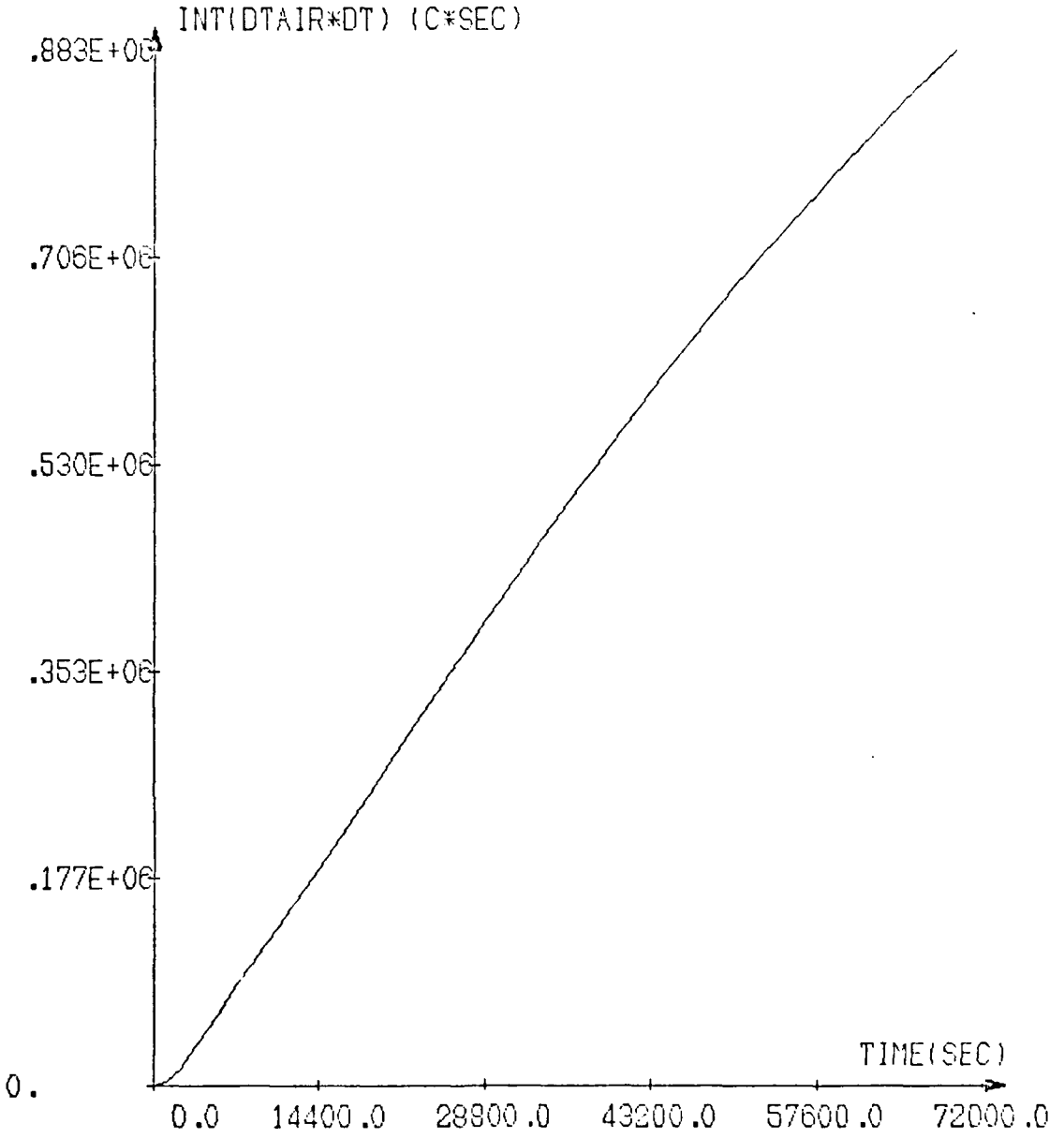

TIME INTEGRATION OF DIFFERENCE BETWEEN INLET AND OUTLET TEMPERATUREST(INT(DTAIR*DT)) VERSUS TIME

DATE=5-19-81

MASS FLOW .095 KG/SEC

TUBES PARALLEL FLOW.OCHARGE, CACL2-6H2O

THEUNISSEN P-H WHITE P ELMER J QUETSTROEY R

Graph 42

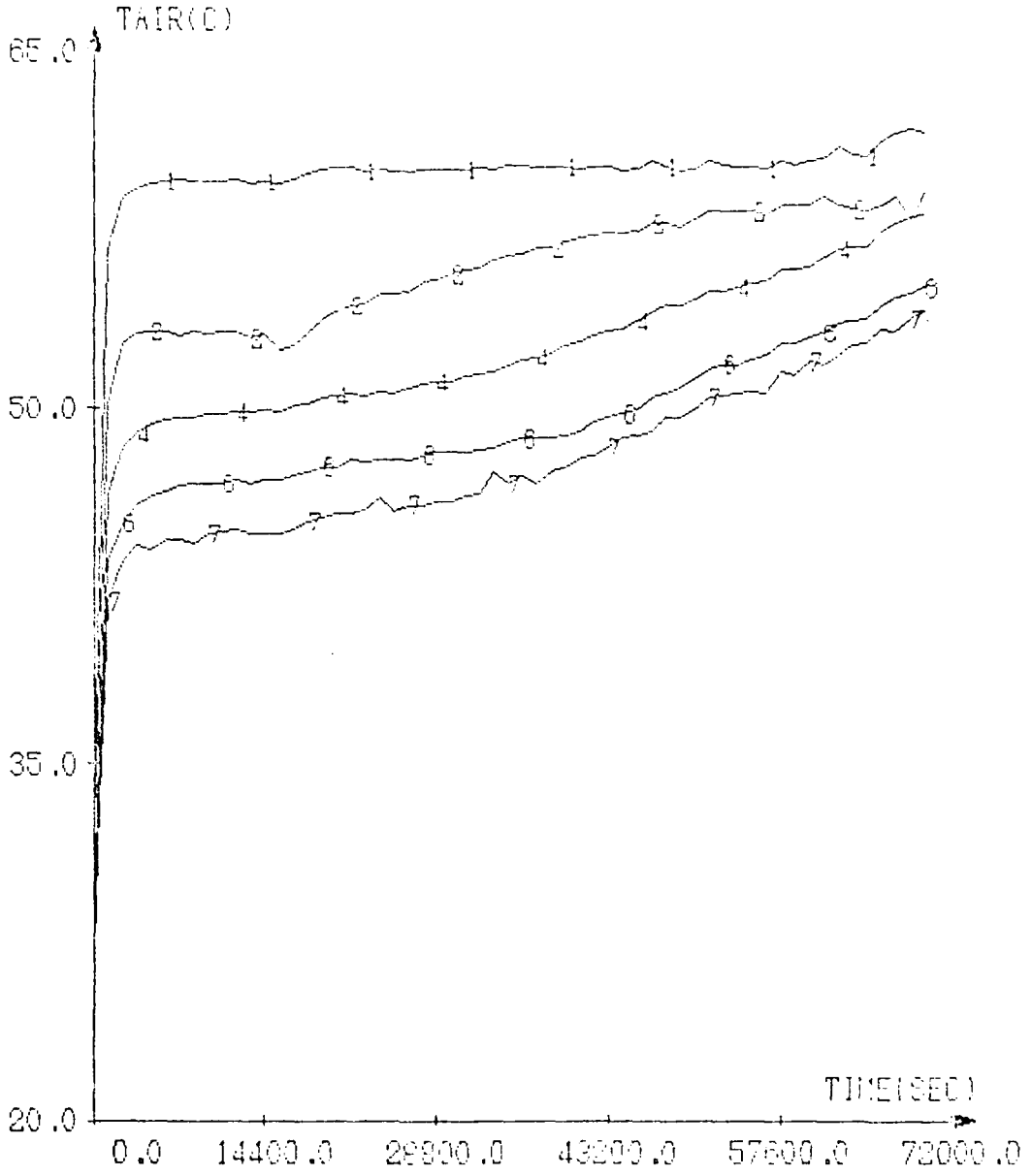

TEMPERATURE AS A FUNCTION OF TIME

AIR AT CENTER .1=0 .2=135 .4=405 .6=810 .7=945 MM FROM TOP

DATE=5-19-81 .MASS FLOW= .95 KG/SEC

TUBE PARALLEL FLOW .CACL2-EH20

TUBE IN CENTER OF BANK OF 37 TUBES

THERMISSEN P-H WHITE P ELMER J QUETSTROEY R

THEUNISSEN P-H WHITE P ELMER J OUETSTROEY R

Graph 43

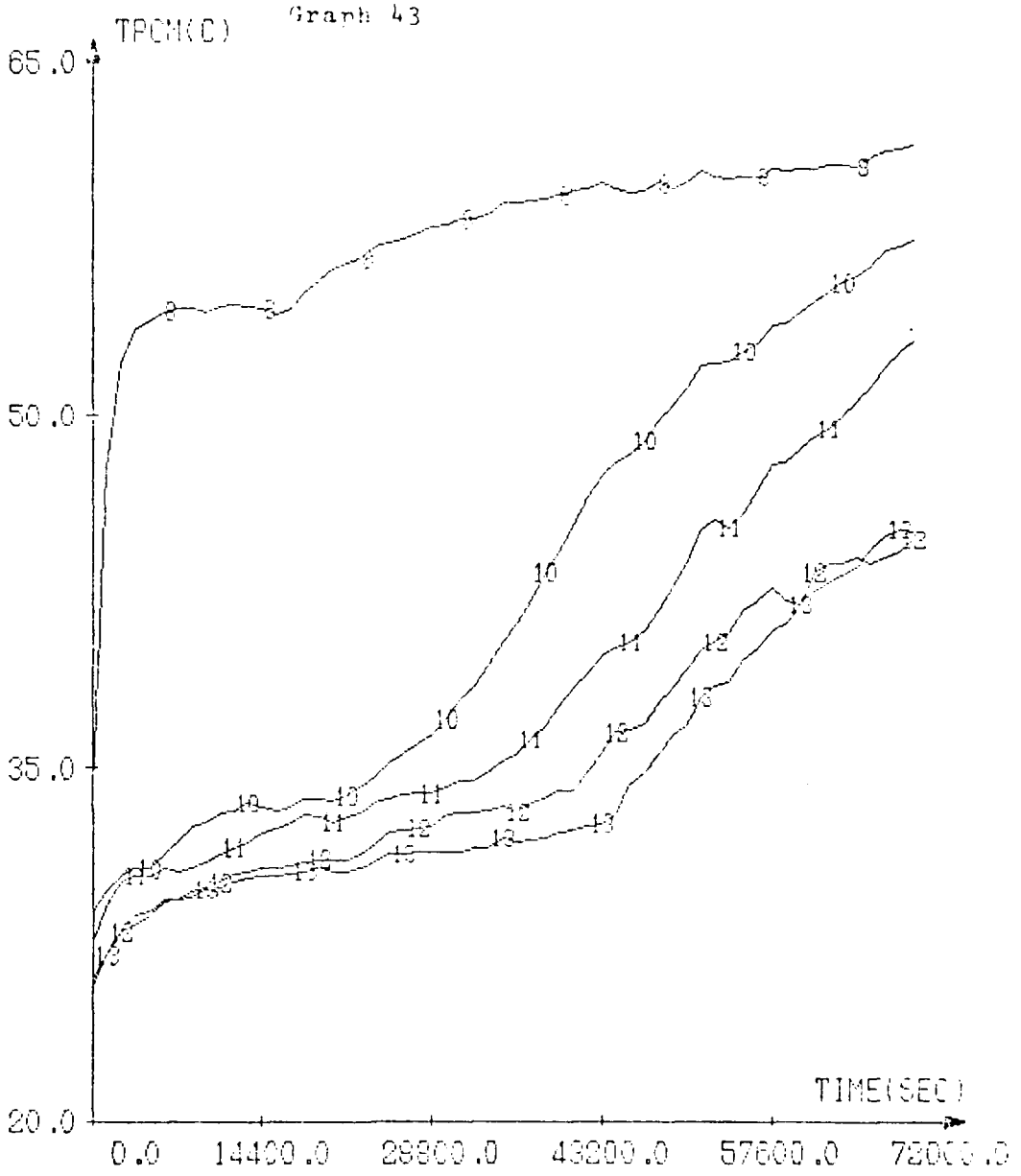

TEMPERATURE AS A FUNCTION OF TIME

PCM AT CENTER.8=0.10=270.11=405.12=675.13=810. NM FROM

DATE=5-19-81.MASS FLOW=.95 KG/SEC

TUBE PARALLEL FLOW.CACL2-6H2O

TEMPERATURE MEASURED ADJACENT TO CENTER TUBE

Graph 44

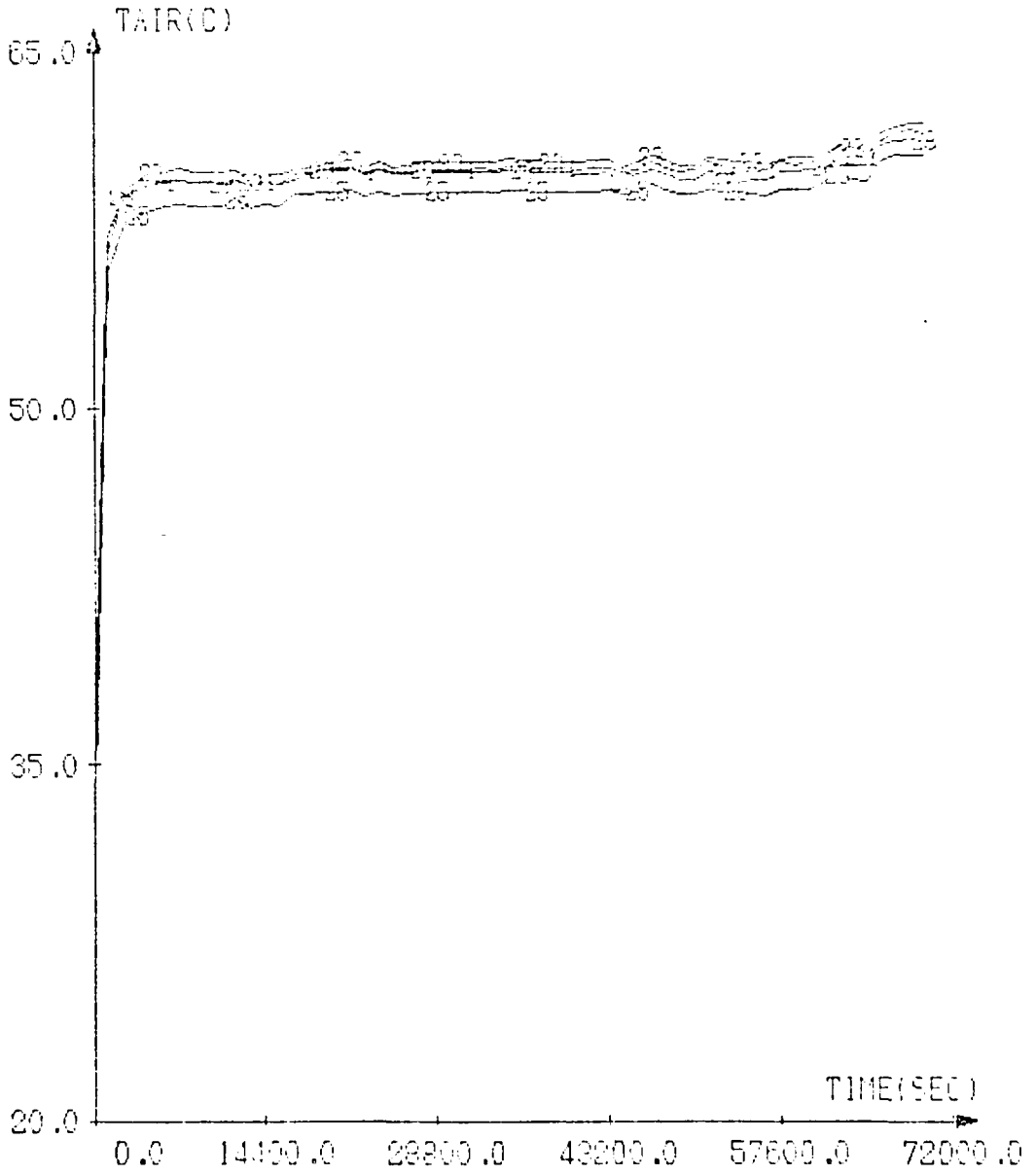

TEMPERATURE AS A FUNCTION OF TIME

AIR TOP TEMPERATURE IN DIFFERENT TUBES

DATE=5-19-81 MASS FLOW=0.035 KG/SEC

TUBE PARALLEL FLOW CACL2-6H2O

SEE DIAGRAM FOR LOCATIONS

THE UNIVERSITY OF TENNESSEE P-H WHITE P ELMER J QUETSTROEY R

THEUNISSEN P-H WHITE P ELMER J OUETSTROEY R

Graph 45

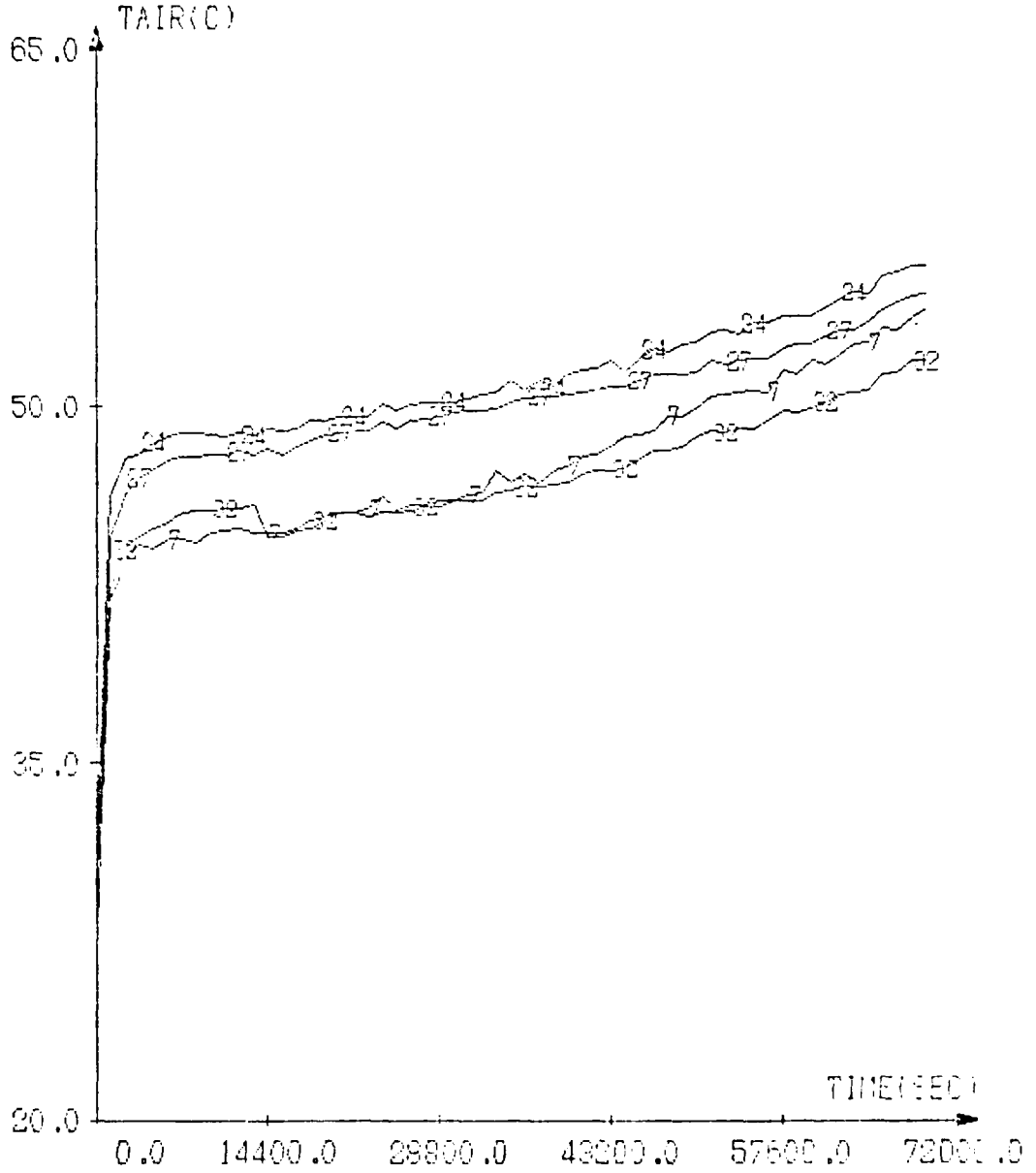

TEMPERATURE AS A FUNCTION OF TIME
AIR EXIT TEMPERATURE AT DIFFERENT POINTS
DATE=5-19-81 MASS FLOW=0.065 KG/SEC
TUBE PARALLEL FLOW CACLS-6H20
SEE DIAGRAM FOR LOCATIONS

VIII: Comparison of Numerical and Experimental Results

Graphs 46 and 47 show the numerical curves and the experimental points for the packed bed unit. Graph 46 shows that for the charge, the numerical simulation proceeds faster than the experimental data. Again for the discharge, in Graph 47, the numerical curves proceed more abruptly than experiment. This difference between the numerical and experimental results is probably due to the resistance to heat transfer of the PCM in the solid phase. Such a resistance, neglected in the numerical simulation, would indeed result in a slower rate of discharging and charging. Thus if this added resistance were taken into account, the experimental and numerical results would be in better agreement.

Graph 46

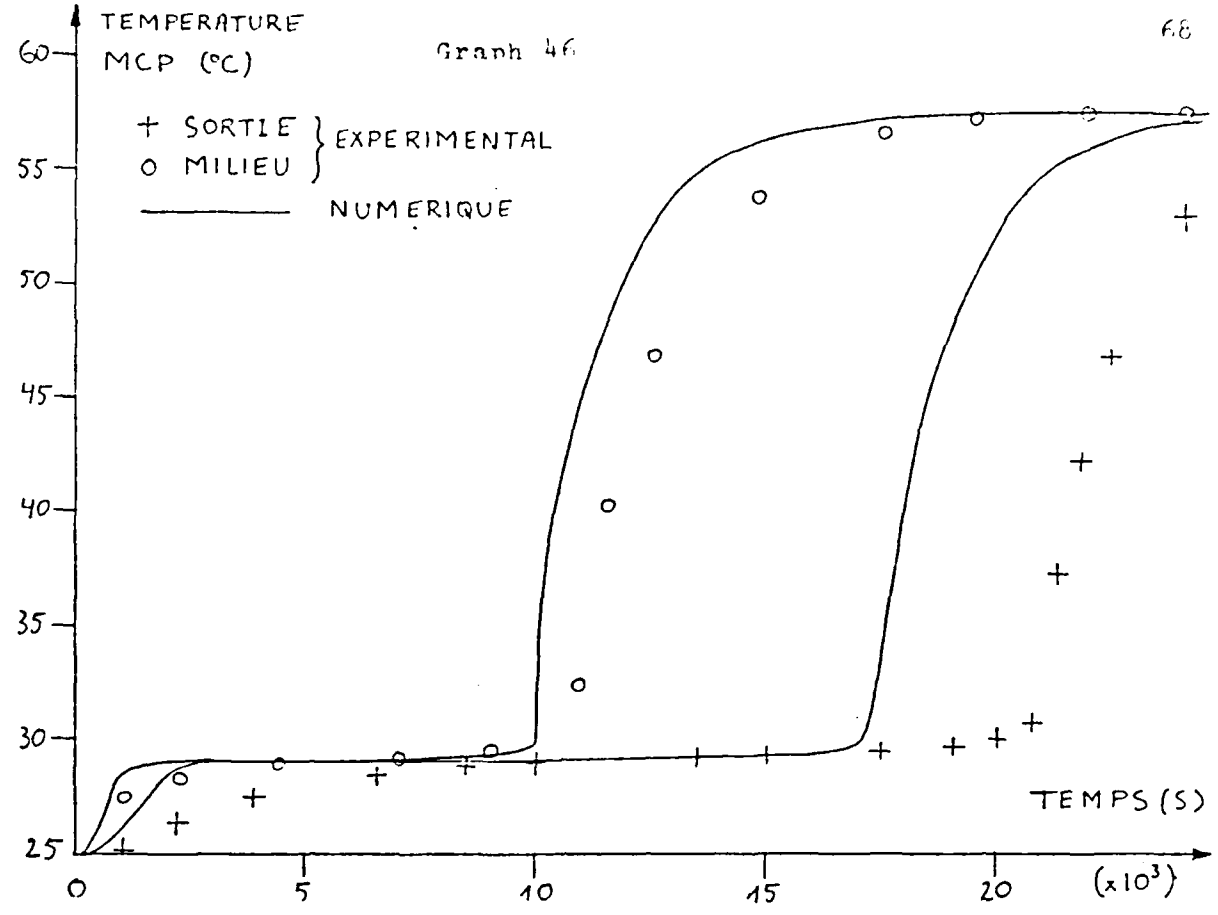
TEMPERATURE
MCP (°C)
+ SORTIE
o MILIEU
EXPERIMENTAL
NUMERIQUE
60
55
50
45
40
35
30
25
0
5
10
15
20
(x10³)
TEMPS (S)

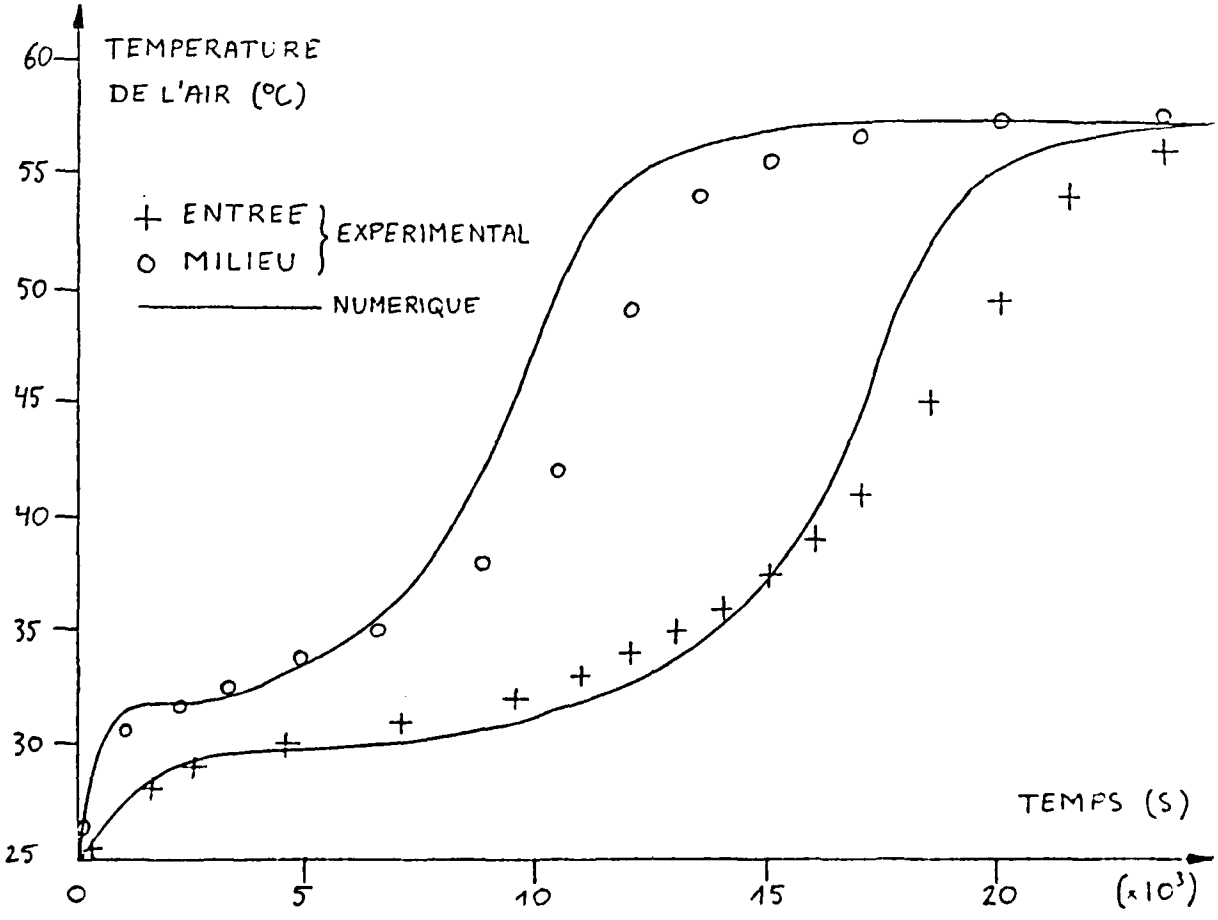
TEMPERATURE
DE L'AIR (°C)
+ ENTREE
o MILIEU
EXPERIMENTAL
NUMERIQUE
60
55
50
45
40
35
30
25
0
5
10
15
20
(x10³)
TEMPS (S)

Graph 47

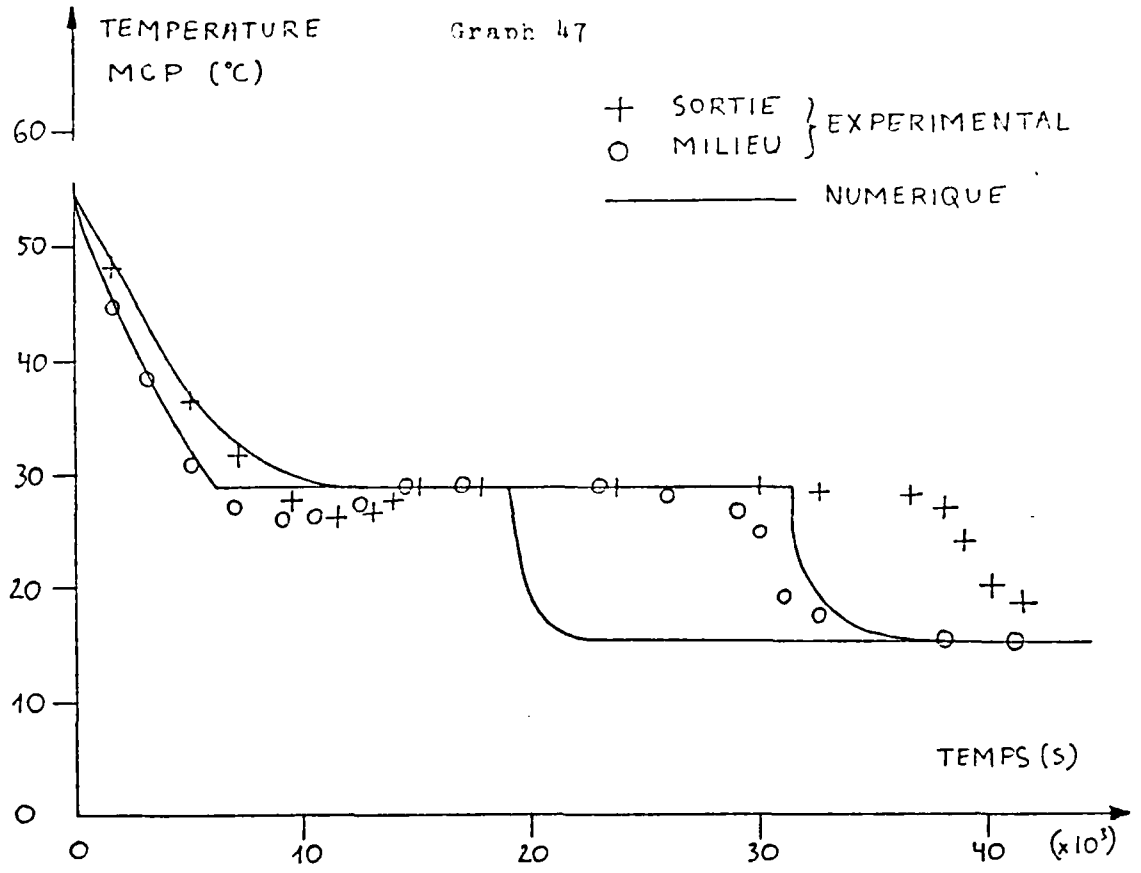
TEMPERATURE
MCP (°C)
+ SORTIE
o MILIEU
EXPERIMENTAL
NUMERIQUE
60
50
40
30
20
10
0
TEMPS (S)
0
10
20
30
40
(x10³)

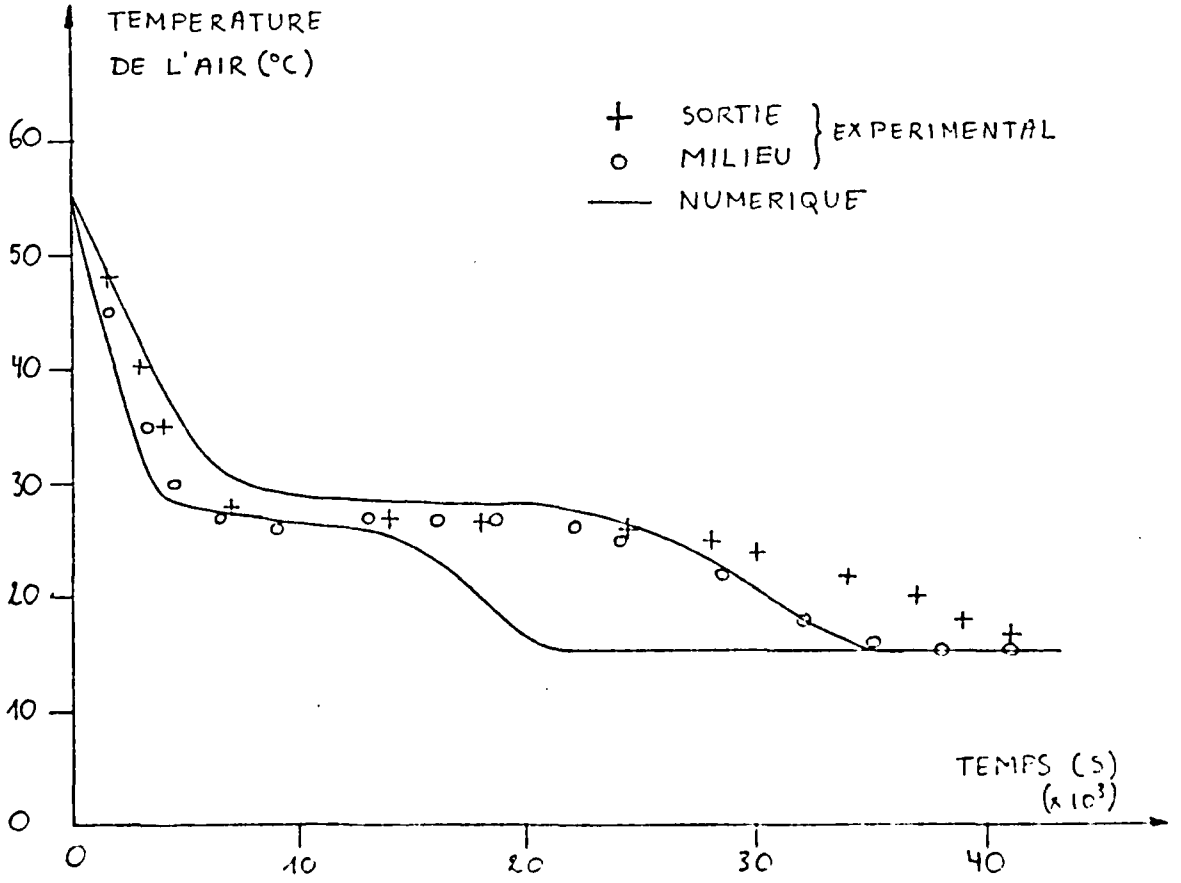
TEMPERATURE
DE L'AIR (°C)
+ SORTIE
o MILIEU
EXPERIMENTAL
NUMERIQUE
60
50
40
30
20
10
0
TEMPS (S)
(x10³)
0
10
20
30
40

IX: Efficiency Considerations

The mechanical energy required to store the heat in each accumulator can be written as $\Delta P \times \dot{V}$ = Power = $\dot{W}$. This says that the power required to maintain a volume flow of $\dot{V}$ across a pressure difference of ΔP, is equal to the product of the two. Looking at this in terms of work, it can be said that W is the amount of work done in moving a volume of fluid V across a pressure drop ΔP. Thus we have the amount of work required for our accumulators by measuring the pressure drop accross them.

The thermal energy transfer is $\dot{m}C_{p,\,air}\Delta T$, where ΔT is the difference between the inlet and outlet air temperatures, and $\dot{m}$ is the mass flow rate. We then find $\dot{Q} = \rho\dot{v}C_p \Delta T$. Now if we want a measure of the amount of heat transferred in relation to the amount of work required to transfer that heat, we can devide $\dot{Q}$ by $\dot{W}$. This is simply $C_p\Delta T/\Delta P$. This then is readily available data from the experiments, and it has been found that in every case it is on the order of 50 to 100. This high apparent efficiency though must be considered to be divided first by 2, since there is a charge and a discharge of the accumulator in any application where the heat is used. Then it must again be divided by 3, for the overall efficiency of the electric system. This brings it down by almost an order of magnitude, to 8 to 16 already., down from 50 to 100.

Together with this idea of efficiency, a criterion for stopping the charge or discharge should be developed. That is, the $\dot{W}$ remains more or less constant during the charge and discharge while $\dot{Q}$ decreases with time due to ΔT decreasing with time. Thus the efficiency is decreasing throughout the experiment and after a certain point, oil or electricity could be used more advantageously than by pumping low temperature air in and out of a storage unit.

X: CONCLUSIONS AND RECOMMONDATIONS

The experimental study shows that from a heat transfer standpoint the packed bed is the best method of encapsulation. It has a negligible pressure loss, large heat exchange surface area, a self distribution of the flow and an avoidance of the problems of supercooling. On the other hand, the geometry which was worst in heat transfer characteristics, the tube parallel flow, was the only one of the three that had no PCM leakage problem, while the packed bed, though the containers were sealed with silicon rubber on the caps, did have leakage problems. Thus the problem is one of feasibility and cost of construction as well as heat transfer.

Further studies of such storage units should include an operation over a broad range of Reynolds numbers, to find the optimum range for thermo-mechanical efficiency. Also, experiments should be done which include solar collector with inlet temperature varying with time, instead of the fixed inlet temperature which was used in the past experiments.

References:

1. Telkes, Maria, "Heat of fusion systems for solar heating and cooling", Solar Engineering, September, 1977.

2. Gross, R.J., et al. "Numerical Simulation of Dual-Media Thermal Energy Storage Systems", Journal of Solar energy Engineering, Vol. 102, P. 287, November, 1980.

3. Eissenberg, David, and Wyman, Charles, "What's in Store for Phase Change?", Solar Age, May, 1980, P. 13.

4. Riordan, Michael, "Thermal Storage: A Basic Guide to the State of the Art", Solar Age, April, 1978, P. 10.

5. Telkes, Maria, "Thermal Energy Storage in Salt Hydrates", Solar Energy Materials, 2, 1980, pps. 381-393.

6. Smith, R. N. et al. "Heat Exhcanger Performance in Latent Heat Thermal Energy Storage", Journal of Solar Energy Engineering, Vol. 102, May, 1980, pps. 112-118.

7. Questois, Remi,"Numerical Study of Melting Phenomena in Phase-change material Heat Exchangers", Senior thesis, Free University of Brussels, Faculty of Engineering, 1981.

8. Theunissen, Paul-Hervé,"Studies of Heat Accumulators", internal reports of the von Karman Institute for Fluid Dynamics, Rhode-St.-Genèse, Belgium.

Appendix I
Photographs of Experimental Program

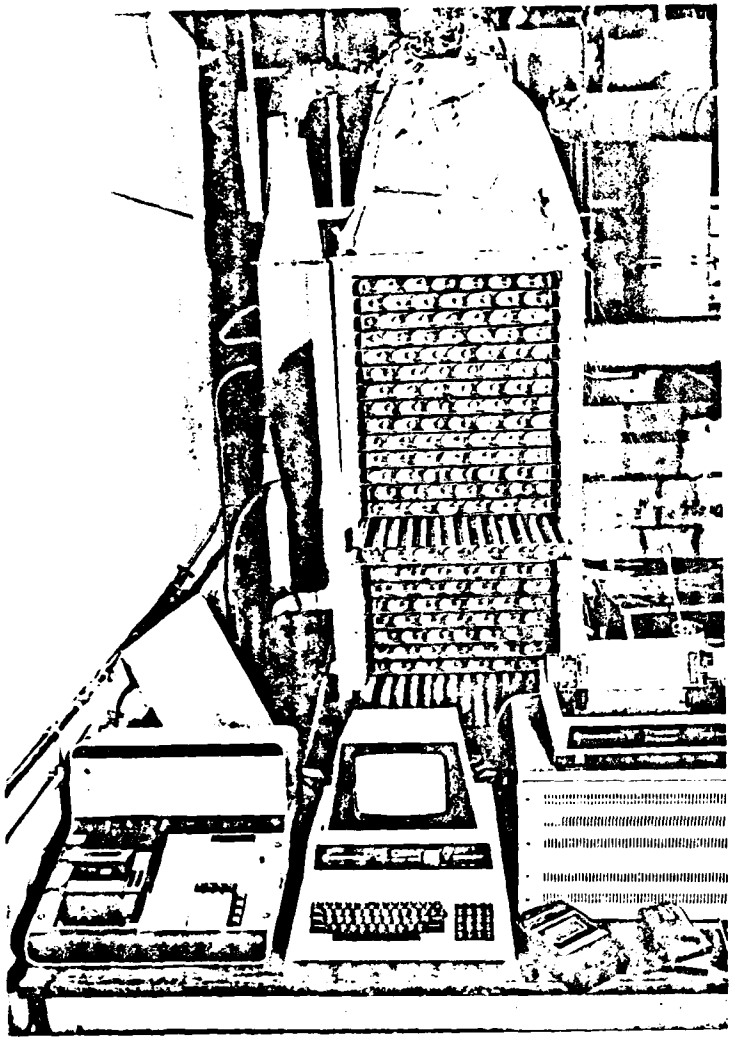

Photo 1:
Experimental System

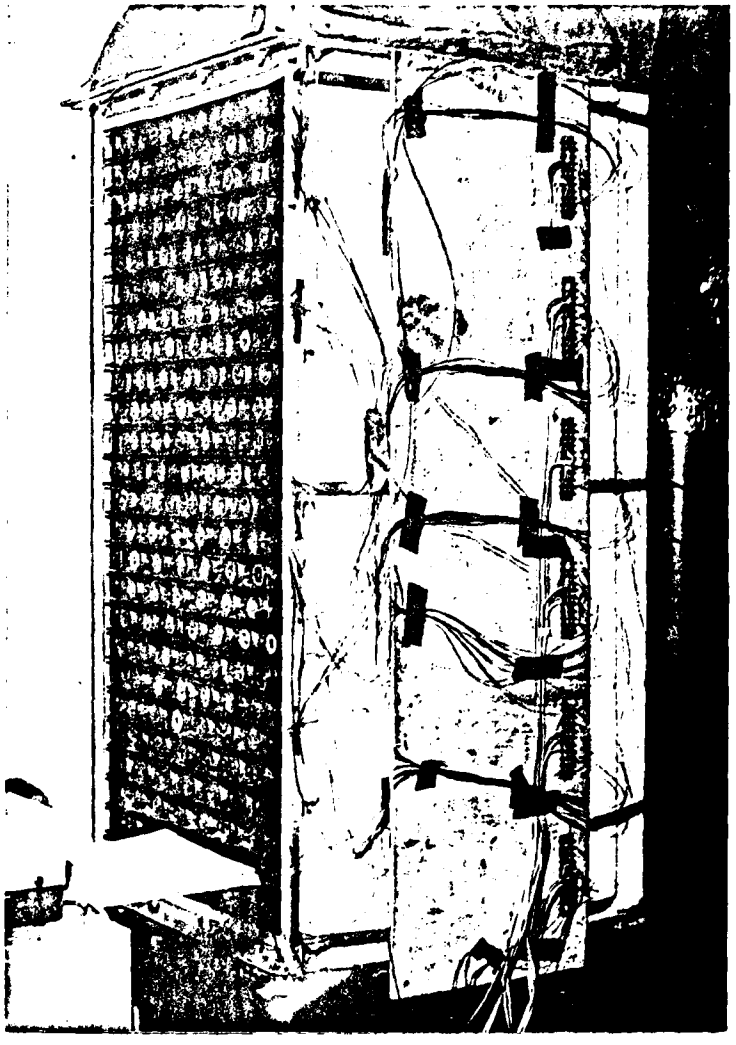

Photo 2:
Thermocouple mounting,
Tube Cross Flow Accumulator

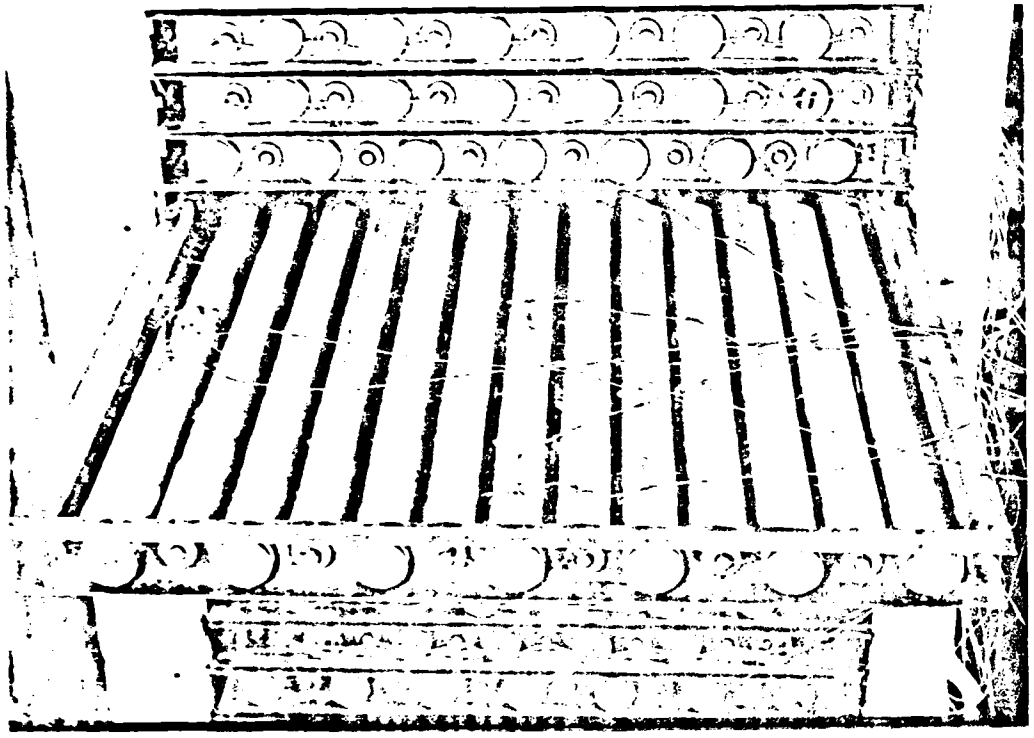

Photo 3: Detail of thermocouple mountings,
Tube Cross Flow Unit

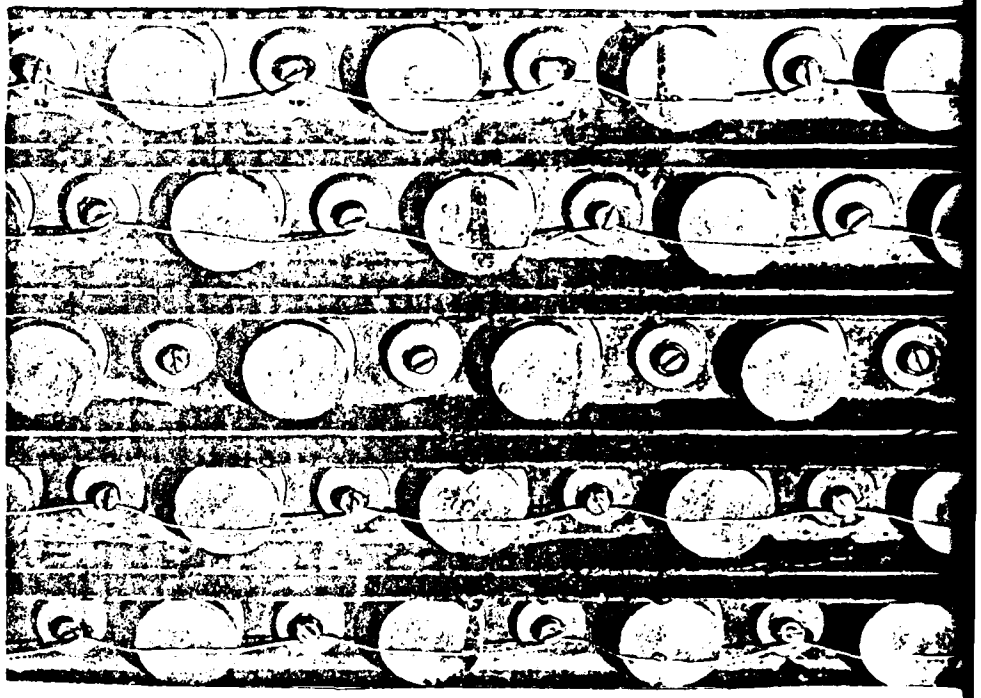

Photo 4: Evidence of leakage of PCB after 1 run
Tube Cross Flow Unit

Photo 5: Filling elements of
Packed Bed Unit

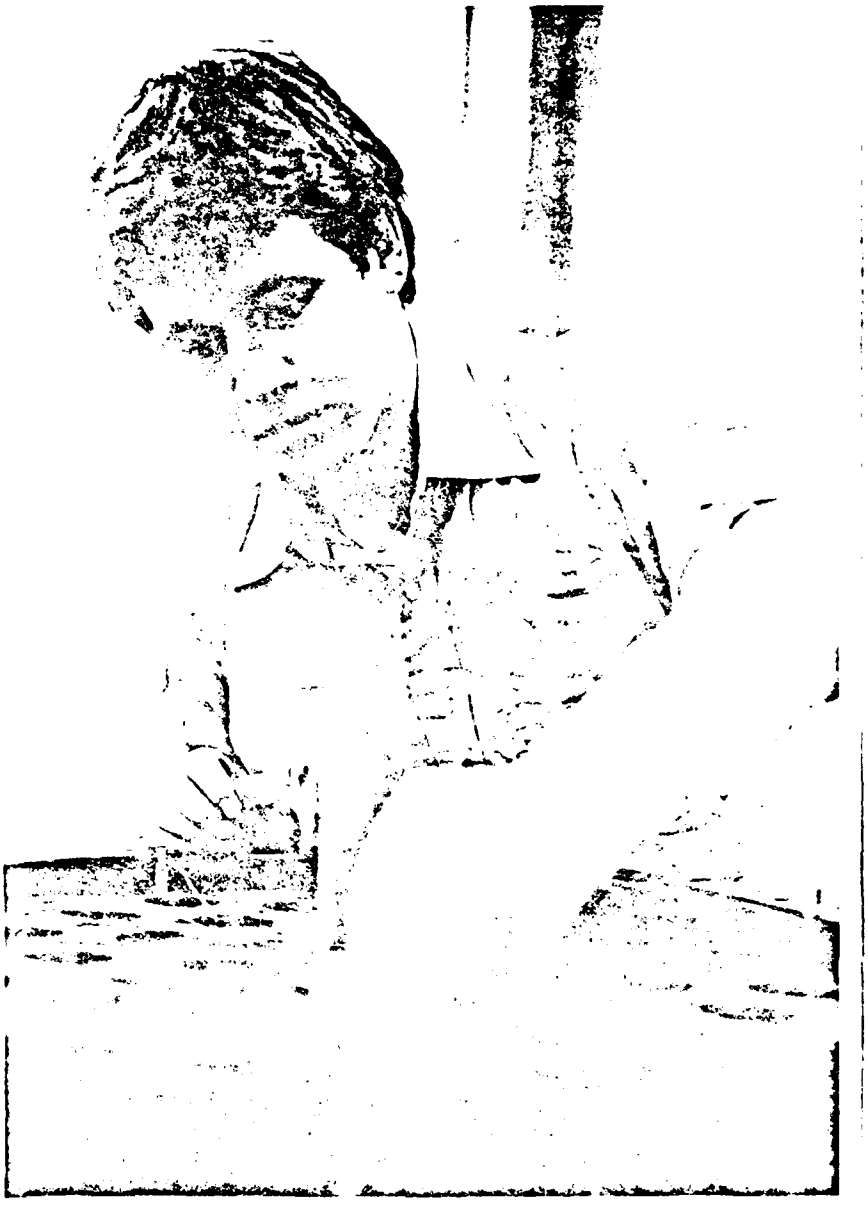

Photo 6: Adjusting thermocouples for
Tube Parallel Flow Unit

Appendix II

Diagram of S.U.N. Facility

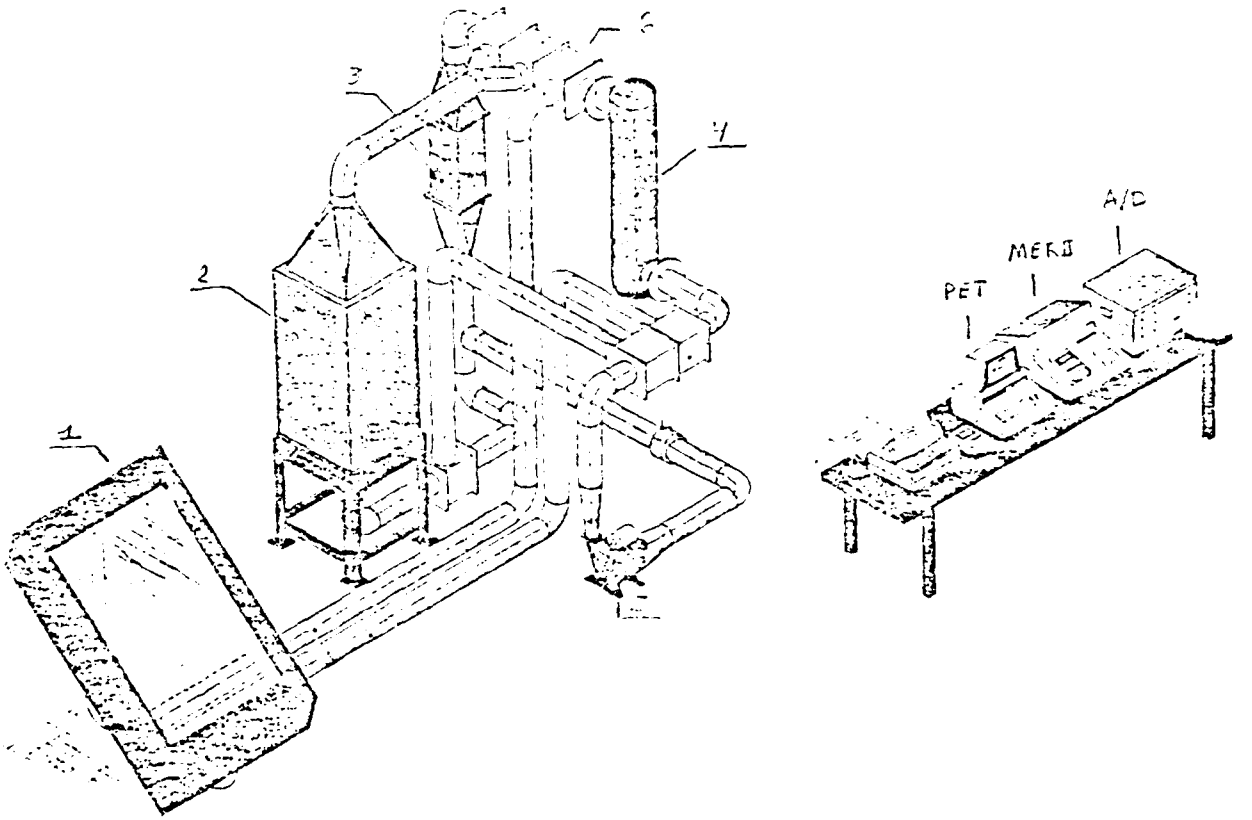

1 Solar Panel
2 Heat accumulator
3 Refrigerant for discharge experiments
4 Electric resistance heater for charging experiments
5 Air Blower
6 Pneumatic Dampers

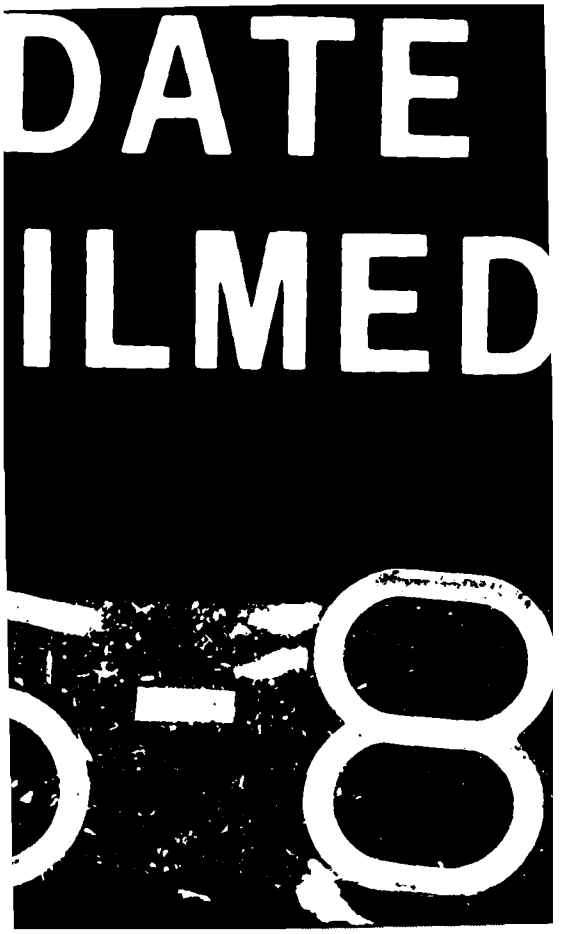
DATE
ILMED
8